

AD-751 050

ASPECTS OF MECHANICAL BEHAVIOR OF ROCK
UNDER STATIC AND CYCLIC LOADING. PART B.
MECHANICAL BEHAVIOR OF ROCK UNDER CYCLIC
LOADING

Bezalel C. Haimson, et al

Wisconsin University

Prepared for:

Advanced Research Projects Agency

March 1972

DISTRIBUTED BY:

NTIS

National Technical Information Service
U. S. DEPARTMENT OF COMMERCE
5285 Port Royal Road, Springfield Va. 22151

**BEST
AVAILABLE COPY**

ENGINEERING EXPERIMENT STATION

AD751050

MECHANICAL BEHAVIOR OF ROCK UNDER CYCLIC LOADING

Annual Report

by

B. C. Haimson

Department of Metallurgical and Mineral Engineering



Reproduced by
**NATIONAL TECHNICAL
INFORMATION SERVICE**
U.S. Department of Commerce
Springfield VA 22131

DISTRIBUTION STATEMENT A

Approved for public release
Distribution Unlimited

Mar 7, 66

Security Classification

DOCUMENT CONTROL DATA - R & D

(Security classification of this document and including annotation must be entered when the overall report is classified)

1. ORIGINATING ACTIVITY (Corporate author) Dept. of Metallurgical & Mineral Engr. University of Wisconsin Madison, Wisconsin 53706	2a. REPORT SECURITY CLASSIFICATION unclassified
3. REPORT TITLE "Mechanical Behavior of Rock Under Cyclic Loading," Part B - of "Aspects of Mechanical Behavior of Rock under Static Cyclic Loading"	3b. GROUP

4. DESCRIPTIVE NOTES (Type of report and inclusive dates) Annual Report (Jan. 29, 1970 - Feb. 28, 1972)
5. AUTHOR(S) (First name, middle initial, last name) Bezalel C. Haimson

6. REPORT DATE March, 1972	7a. TOTAL NO. OF PAGES 92	7b. NO. OF REFS 20
8a. CONTRACT OR GRANT NO. H0210004	8b. ORIGINATOR'S REPORT NUMBER(S)	
b. PROJECT NO. 1579, Amendment 2	8c. OTHER REPORT NO(S) (Any other not here that may be assigned this report)	
c.	d.	

10. DISTRIBUTION STATEMENT Distribution of this document is unlimited.		
--	--	--

11. SUPPLEMENTARY NOTES Details of illustrations in this document may be better studied on microfiche	12. SPONSORING MILITARY ACTIVITY ARPA
---	---

13. ABSTRACT S-N curves were obtained for a marble and a limestone in uniaxial compression and for two marbles in tension. No major differences were found between the effects of cyclic compression and cyclic tension. Rock is weakened by cyclic loading, whether under compression or tension, if the upper level of applied stress is above a certain threshold within the inelastic range of the rock stress-strain characteristics. As the upper peak of the cyclic load is raised, the number of cycles to failure decreases. Failed rock exhibits considerable fatigue strength. Both the axial and lateral strains undergo cyclic creep; the volumetric strain experiences cyclic compression dilatancy. The static complete stress-axial strain curve appears to define the limit of cyclic creep prior to failure. The study of internal structure changes in rock subjected to uniaxial compression (acoustic emission, optical diffraction, photomicrography) revealed that cyclic fatigue is the result of a microfracturing process, consisting of grain boundary loosening in the first cycles, intragranular cracking in the following, succeeded by crack extension, coalescence, widening, fracture. Consideration of cyclic loading effects due to phenomena like earthquakes, drilling, blasting, should be incorporated in any design of underground or surface rock structures.	
---	--

DD FORM 1 NOV 65 1473

I
-

Mar 7, 66

Security Classification

14. KEY WORDS	LINK A		LINK B		LINK C	
	ROLE	WT	ROLE	WT	ROLE	WT
Rock Mechanics Fatigue Cyclic Loading in Rock S-N curves Complete stress-strain curve						

II

ASPECTS OF MECHANICAL BEHAVIOR OF ROCK UNDER
STATIC AND CYCLIC LOADING

PART B: MECHANICAL BEHAVIOR OF ROCK UNDER CYCLIC LOADING

ANNUAL TECHNICAL PROGRESS REPORT
MARCH 1972

by

B. C. Haimson (Co-Principal Investigator with
R. W. Heins)

Department of Metallurgical and Mineral Engineering
and the
Engineering Experiment Station
College of Engineering
The University of Wisconsin
Madison, Wisconsin 53706

ARPA Order No. 1579, Amendment 2
Program Code No. 1F10
Contract No. H0210004

Contract Period: January 29, 1971 through February 28, 1972

Total Amount of Contract: \$47,985

Sponsored by: ARPA

Disclaimer:

The views and conclusions contained in this document are those of the author and should not be interpreted as necessarily representing the official policies, either expressed or implied, of the Advanced Research Projects Agency or the U.S. Government.

PREFACE

This report covers the first year accomplishments in the research program entitled "Mechanical Behavior of Rock Under Cyclic Loading," B. C. Haimson - Principal Co-Investigator. The program is Part B of the project entitled, "Aspects of Mechanical Behavior of Rock Under Static and Cyclic Loading" (Contract H0210004). The report on Part A of the project is published in a separate volume.

ACKNOWLEDGEMENTS

The reported research was supported by ARPA, and monitored by Mr. Egons S. Podnieks of the Twin Cities Mining Research Center, U.S. Bureau of Mines. His cooperation and that of Dr. S. Peng are gratefully acknowledged. In its initial stages the project had been sponsored by the Wisconsin Alumni Research Foundation.

The graduate research assistants who performed most of the reported experimental work were Chin Man Kim and Thomas Tharp.

The optical diffraction analysis was performed by Mr. R. Wipf under Professor H. Pincus' guidance in the Department of Geological Sciences, University of Wisconsin, Milwaukee.

TABLE OF CONTENTS

	<u>Page</u>
PREFACE	2
ACKNOWLEDGEMENTS	3
LIST OF FIGURES	6
SUMMARY	10
INTRODUCTION	12
PREVIOUS WORK - A LITERATURE SURVEY	13
LABORATORY EQUIPMENT AND EXPERIMENTAL PROCEDURES	16
Rock Types	16
Specimen Preparation	16
Apparatus	17
a. Cyclic Uniaxial Compression	17
b. Cyclic Tension	19
Experimental Program	22
a. Cyclic Uniaxial Compression	22
b. Cyclic Tension	26
EXPERIMENTAL RESULTS	28
A - UNIAXIAL COMPRESSION	
Monotonic Loading	28
Cyclic Loading	28
a. Stress Controlled Tests with Constant Lower Peak Stress	28
I. S-N Curves	28
II. Stress-Strain Behavior	32
III. Strain-Time Behavior	34
IV. Lateral Strain and Volumetric Changes	41
V. Microseismic Activity	47
VI. Photography, Optical Diffraction and Photomicrography	48

TABLE OF CONTENTS (contd)

	<u>Page</u>
b. Stress Controlled Tests with Constant Mean Stress	69
c. Strain Controlled Tests with Constant Lower Peak Strain	71
d. Cyclic Loading of Failed Rock	71
 B - TENSION	 79
Monotonic Loading	79
Cyclic Loading	79
 CONCLUSIONS AND PRACTICAL APPLICATIONS	 88
Mechanical Behavior	88
Internal Structure Changes	89
 FUTURE WORK	 90
 REFERENCES	 91

LIST OF FIGURES

Figure 1a. Loading system, electronic controls and data acquisition instrumentation.

Figure 1b. Loading jig with specimen, cantilever set and swivel head.

Figure 2. Acoustic emission system - block diagram.

Figure 3. Set-Up for uniaxial tensile cyclic testing.

Figure 4. Cyclic fatigue program.

Figure 5. Typical programmed and readout curves in stress-controlled cyclic tests.

Figure 6. Typical programmed and readout curves in strain-controlled cyclic tests (shown in Indiana limestone behavior).

Figure 7. S-N curve for White Tennessee marble subjected to cyclic compression with constant lower peak stress.

Figure 8. S-N curve for Indiana limestone subjected to stress cyclic compression with constant lower peak.

Figure 9. Typical stress-strain curves for Indiana limestone.

Figure 10. Strain difference between last and first stress-strain cycle peaks versus expected complete stress-strain curve - White Tennessee marble.

Figure 11. Strain difference between last and first stress-strain cycle peaks versus expected complete stress-strain curve - Indiana limestone.

Figure 12. Stress-strain curve and acoustic emission in monotonic compression (White Tennessee marble).

Figure 13. Typical recordings during cyclic loading of White Tennessee marble.

Figure 14. Stress-strain and acoustic emission in monotonic compression Indiana limestone.

LIST OF FIGURES (contd)

Figure 15. Typical recordings during cyclic loading of Indiana limestone.

Figure 16. Typical stress-lateral strain recording in cyclic loading of White Tennessee marble.

Figure 17. Typical stress-lateral strain recording in cyclic loading of Indiana limestone.

Figure 18. Calculated typical volumetric changes in cyclically loaded White Tennessee marble.

Figure 19. Calculated typical volumetric changes in cyclically loaded Indiana limestone.

Figure 20. Typical stress-strain curve for cyclically loaded White Tennessee marble, (upper peak stress = 85%), showing the position of the specimens that were optically analyzed (Figures 21-26).

Figure 21. White Tennessee marble - optical analysis of a specimen prior to loading (See Figure 20).

Figure 22. White Tennessee marble - optical analysis of a specimen after 10 cycles of loading (See Figure 20).

Figure 23. White Tennessee marble - optical analysis of a specimen after 500 cycles of loading (See Figure 20).

Figure 24. White Tennessee marble - optical analysis of a specimen after 3,000 cycles of loading (See Figure 20).

Figure 25. White Tennessee marble - optical analysis of a specimen after 3,700 cycles of loading (See Figure 20).

Figure 26. Photograph of a White Tennessee marble specimen (2.5 X), fatigued in cyclic loading (See Figure 20).

Figure 27. Optical analysis of a previously unloaded specimen of Indiana limestone.

LIST OF FIGURES (contd)

Figure 28. Indiana limestone - optical analysis of a specimen after being cyclically loaded to well within the steady state stage (upper peak stress = 75%).

Figure 29. Indiana limestone - optical analysis of a specimen after being cyclically loaded to the accelerated tertiary stage, just before failure (upper peak stress = 75%).

Figure 30. Photograph of a fatigued Indiana limestone specimen.

Figure 31. S-N curve for White Tennessee marble subjected to cyclic compression under constant mean stress (= 50% of compressive strength).

Figure 32. Typical recordings during cyclic compression under strain-control.

Figure 33. Stress-strain curves for failed White Tennessee marble under cyclic loading (Broken line depicts the expected descending complete stress-strain curve).

Figure 34. S-N curve for failed White Tennessee marble under stress-controlled cyclic compression.

Figure 35. Stress-strain curves for failed Cherokee Georgia marble under cyclic loading (Broken line depicts expected continuation of complete stress-strain curve).

Figure 36. S-N curve for failed Cherokee Georgia marble under stress-controlled cyclic compression.

Figure 37. S-N curve for White Tennessee marble under Brazilian cyclic loading.

Figure 38. S-N curve for Pink Tennessee marble under Brazilian cyclic loading.

Figure 39. S-N curve for Pink Tennessee marble under uniaxial tension cyclic loading.

LIST OF FIGURES (contd)

Figure 40. Typical specimen of Pink Tennessee marble failed in uniaxial tension cyclic loading.

Figure 41. Acoustic emission in uniaxial tension monotonic loading - Pink Tennessee marble.

Figure 42. Acoustic emission in long life specimen of Pink Tennessee marble under uniaxial tension cyclic loading.

SUMMARY

The reported investigation is the first phase in an extensive study of the cyclic fatigue phenomenon in hard rock. This is the phenomenon of premature failure occurring in materials subjected to cyclic or repetitive loading. A thorough understanding of rock mechanical reaction to such loading could help in the design of safe rock structures and has the potential of improving rock breaking methods.

A survey of existing publications on the subject revealed that very little work had been carried out in rock fatigue. Hence, it was decided to undertake this investigation. The main objectives for the period reported were to study the mechanical behavior of two hard rock types under cyclic uniaxial compression and tension, and to assess the possible mechanism of fatigue.

S-N curves were obtained for a marble and a limestone in uniaxial compression and for two marbles in tension. No major differences were found between the effects of cyclic compression and cyclic tension. The results show that rock is weakened by cyclic loading, whether under compression or tension, if the upper level of applied stress is above a certain threshold within the inelastic range of the rock stress-strain characteristics. As the upper peak of the cyclic load is raised the number of cycles to failure decreases. Failed rock exhibits considerable fatigue strength. Both the axial and lateral strains undergo cyclic creep; the volumetric strain experiences cyclic compression dilatancy. The static complete stress-axial strain curve appears to define the limit of cyclic creep prior to failure.

The study of internal structure changes in rock subjected to uniaxial compression revealed that cyclic fatigue is the result of a microfracturing process. The acoustic emission recorded during tests indicated occurrence of microcracking from the very first cycle, followed by a decelerating rate of crack initiation, a stage of little or no emission, and finally an increasing number of crack initiation and propagation culminating in fatigue failure. The optical diffraction analysis also showed an increase in fracture abundance in the first stage of the cyclic loading, followed by a stagnation stage and continued by a renewed fracture frequency increase towards failure. The photomicrographic investigation clearly demonstrated grain boundary loosening in the first cycle, intragranular cracking in the following, succeeded by crack extension, coalescence, widening, fracture.

Several practical applications arise from the obtained results. Consideration of cyclic loading effects due to phenomena like earthquakes,

drilling, blasting, should be incorporated in any design of underground or surface rock structures. The S-N curves should be used to determine a more realistic compressive or tensile strength of the rock which could withstand both static and repetitive loadings. The results of the tests in failed rock could be extremely useful to the design of structures where rock might be deformed to beyond the limit corresponding to its compressive strength. Pillars, ribs or other structural components although 'failed' could resist cyclic loading to an extent determined by the appropriate S-N curves. The relationship found between the complete stress-strain curve and the cyclic creep provides a quick means of determining total deformation prior to fatigue failure. The behavior of the volumetric strain during cycling could also have important implication in design.

Generally, the major effects of fatigue loading in uniaxial compression and tension have been determined. However, more work is needed in other rock types and under different loading conditions like triaxial compression and tension-compression.

INTRODUCTION

Rock formations as well as rock structures are continually subjected to both static and dynamic loads. Static loads result from such sources as tectonic forces and the weight of the overlying rock. Dynamic loads are continually propagated through natural vibrations of the earth crust, and intermittently applied by major earthquakes, rock blasting, drilling, traffic, etc. The mechanical behavior of rock under static loading has been thoroughly investigated. However, rock reaction to the cyclic, pulsating stresses resulting from dynamic loads has been generally neglected with the exception of a few rather limited studies. It is a known fact that cyclic loading often causes a material to fail prematurely at a stress level lower than its determined strength under monotonic conditions. This phenomenon is commonly termed 'fatigue'. Tunnel walls, excavation roofs and ribs, bridge abutments, dam and road foundations are only a few of rock structures that can be weakened by repetitive loading. Better understanding of cyclic fatigue may assist the engineer in preparing a more rational design that will eliminate premature failures. On the other hand, knowledge of fatigue characteristics may help improve rock breaking methods, e.g., drilling and blasting. It is, therefore, imperative that the effect of pulsating stresses on rock is fundamentally studied with the ultimate goal of deriving practical applications. This has also been the general objective of the present project.

The specific objectives were:

1. investigate the mechanical behavior of two hard rock types under cyclic uniaxial compression and tension, with respect to strength and deformation.
2. attempt to understand the mechanism of fatigue through macro and micro-observations, seismic detection and optical diffraction.

The objectives have been carried out and detailed descriptions of the methods used, results obtained and analysis are given in the following sections.

PREVIOUS WORK - A LITERATURE SURVEY

During the last one hundred years a considerable amount of research has been done in the mechanical behavior of materials under cyclic loading. Metals, in the form of test specimens and structural components, have been the most thoroughly investigated. Non-metallic brittle materials, such as concrete and ceramics have also been systematically studied. Soils have lately been carefully tested in cyclic loading. Rock, however, has remained an unknown as far as its mechanical response to repetitive stresses. Very few researchers have attempted to understand rock reaction to cyclic loading and these rather limited attempts will be described in the following paragraphs.

The first traceable work in English on the fatigue characteristics of rock is that by Grover, et. al. (1). Specimens of Columbus limestone were tested in cyclic axial compression, torsion and bending at frequencies of 20-30 cps. To quote the article, the study "had been limited to relatively few tests on one particular type of rock and, therefore, was preliminary and inconclusive." Indeed, Grover, et. al. did not notice any fatigue effect in the limestone tested. However, they based their results in compression on only six tests and in bending on merely two tests!

Grover's speculations as to the absence of cyclic loading effect in rocks discouraged, apparently, any further research in the subject, since it was not until 1963 that another technical paper on repetitive loading appeared. Burdine (2) had conducted a rather thorough investigation in the mechanical reaction of Berea sandstone to cyclic loading and published the first evidence of fatigue effect in rock by plotting S-N curves under different loading conditions and showing that repetitive loading can weaken the compressive strength by as much as 26%. He worked with frequencies of 15, 45, 55 cps but found no significant difference between them as far as the fatigue effect is concerned. Tests were run up to 10^6 cycles in uniaxial and triaxial compression on dry and wet specimens. The results showed a decrease in cyclic loading effect as the confining pressure increased, and increase in the effect with the increase in rock pore pressure. Rock cycled to a maximum compression lower than the assumed fatigue limit showed a strain hardening and coaxing effect. In general, this was a good introductory work which only called for further studies in different rock types, under various loading conditions.

The next significant studies of rock fatigue were carried out independently by Hardy and Haimson and their groups. Hardy and Chugh (3) reported low-cycle (10,000 cycles), low frequency (1/4 cps) compression cyclic tests results in three hard rock types. They found a definite fatigue effect

within the limited range of the tests. The effect was more pronounced in granite than in sandstone.

Haimson and Kim (4) presented results of their work in cyclic compression of Tennessee and Georgia marbles tested at 1-4 cps to simulate earthquake and blasting major pulses. They used a maximum of 10^6 cycles to determine S-N curves for both intact and failed rock. They studied the stress-strain and strain-time behavior and found similarities between creep and fatigue behavior. Most of their work was sponsored by the present ARPA contract and is reported in detail in this report.

Outside of the United States, rock fatigue has been studied in Japan, France, the Soviet Union, and possibly other countries. Nishimatsu and Heroesewojo (5) tested andesite specimens under cyclic compression at 5 cps and a maximum of 10^6 cycles. No strain hardening was discovered in survived specimens. Using a statistical approach the authors found a relationship for the probability of survival. Two fatigue processes were observed: one of intragranular fracture and one of intergranular cracking.

Saint-Leu and Sirjeys (6) performed compression cyclic tests in Carrara marble and Sidobre granite. The cyclic frequency was extremely low, being controlled by a loading rate kept at 60 psi/sec. From measured strain, they concluded that the major permanent deformation occurred in the first cycle, gradually decreasing with time. Volumetric measurements showed an increasing dilatancy with the increase in upper peak stresses. They observed contrasting cyclic changes in elastic parameters between the two rocks. They made an interesting suggestion as to the fatigue limit of rock being determined by the stress level at which the volumetric change is zero under static loading (the onset of dilatancy).

Shreiner and Pavlova (7) used a repeated dynamic indentation method to cyclically load a dolomite, a marble and Solnhofen limestone. The impact type loading had a dramatic effect on rock strength. The ratio of the fatigue limit to strength was about 1/25! The brittier the rock the more affected it was by repetitive loading.

In addition to the few existing publications on rock fatigue, a large number of published results in cyclic loading of concrete, ceramics and soil are of interest, since these materials do resemble, at least partially, behavior of actual rock.

An excellent review paper (8) and two typical articles (9,10) on concrete experiments are listed in the References at the end of this report. The fatigue limit of concrete was found to be 50-55% of the ultimate

strength in both compression and tension. The secant modulus decreased with repeated loads, the tangent modulus of each cycle decreased slightly in the lower part of the curve and increased slightly in the upper portion. Strain hardening was found to exist in concrete. Frequency differences between 1-75 cps did not appear to affect fatigue strength. Rest periods appeared to increase the endurance of concrete. Permanent deformation was longest in the first cycles and the rate of permanent strain increase decreased with the number of cycles.

A representative sample of work performed in ceramics is given in a report by Sedlacek and Halden (11). Specimens of an alumina were tested in tension both statically and cyclically at 4 cps. Results showed that the brittle material was affected by the fatigue loading, its life decreasing with increasing maximum stress. The fatigue resistance was an inverse function of the stress range. A level of stress was found below which no material deterioration was observed even after 350,000 cycles.

The mechanical behavior of soils under cyclic loading has been thoroughly investigated especially in the last decade (12, 13). Soil characteristics are quite different from those of rock. However, the reason for mentioning these studies here is to emphasize that soil mechanics engineers have long since realized the importance of understanding soil reaction to cyclic loading as a means of controlling the effect of earthquakes on foundations.

The survey of the available literature on cyclic fatigue in rock, other brittle materials and soils shows beyond any doubt that repetitive loading has different mechanical effects than simple static or dynamic stresses. Determining these effects in rock and understanding their mechanism were the major goals of the present investigation.

LABORATORY EQUIPMENT AND EXPERIMENTAL PROCEDURE

Rock Types

The bulk of the cyclic uniaxial compression tests was conducted in White Tennessee marble and Indiana limestone. In addition, Cherokee Georgia marble was used for cyclic testing of badly failed rock.

The cyclic indirect tension tests were run in White Tennessee marble and a brownish variety of the Pink Tennessee marble. When it was decided to retest the rocks under cyclic uniaxial tension White Tennessee marble could not be purchased anymore and only the Pink Tennessee marble was used in spite of its more inferior properties.

Following is a brief description of the rocks used:

Tennessee marble is a fine to coarse crystalline limestone found in the Knoxville Belt region of Tennessee. It is almost pure calcite and had been subjected to folding, jointing and faulting. It is traversed by frequent stylolites which do not appear to affect its mechanical behavior. Bedding is sometimes visible due to the depositional orientation of fossil fragments, but the coarse elastic texture of the rock makes it quite isotropic mechanically. The brownish pink variety used in the present tests owes its color to manganese and hematite. It is generally a more coarsely grained rock than the white variety, with unusually large individual crystals responsible for some of the observed scatter in results. Both rocks are very dense having negligible viscosity and permeability.

Indiana limestone is a light gray limestone composed almost entirely of carbonate. It is very finely grained, with no apparent bedding planes. It is very porous (>15%), and pore size can vary from minuscule to 1/32 inch diameter. It is not necessarily isotropic and all specimens for a particular series of tests should be cored from the same block, drilling in one direction only.

Cherokee Georgia marble is rather similar in appearance to White Tennessee marble, except that it possesses larger size crystals. Although much weaker in compression than the Tennessee marble it has an almost identical ascending curve, but a much less abrupt descending curve in a complete stress-strain plot.

Specimen Preparation

Specimens for uniaxial tests were approximately 1.0 inch in diameter

and 2.5 inches long. Brazilian specimens were 2.1 inch in diameter and .5 inch thick. All specimens were first cored out of large blocks (usually 15 inches x 15 inches x 7 inches) by diamond barrel drilling in one direction only. The ends of the specimens were ground flat and parallel within better than 0.001 inches. Special attention was paid to specimen preparation so as not to introduce new and undesired variables in the experimental program. The prepared specimens were oven dried at 120°F for a week, and thereafter exposed for another week prior to testing to the constant temperature and humidity of the fatigue laboratory.

Apparatus

Two closed-loop servo-controlled electro-hydraulic loading machines were used. An M.B. 25,000 lbs. tester was utilized for the tension tests and an M.T.S. 100,000 lbs. machine was employed for the compression tests. Both could be programmed through a function generator to apply cyclic loading to a specimen by controlling either stress or strain rates. A digital counter gave the number of cycles per test. The load applied was sensed by a dynamic load cell mounted on the bottom part of the cross-head. The M.T.S. loading frame is shown in Figure 1a.

a. Uniaxial Compression Cyclic Testing

The cyclic compression tests were run in the M.T.S. machine. Specimens were mounted in a special jig consisting of a lower fixed platen rigidly attached to the hydraulic ram and an upper platen which was part of a swivel head mechanism (Figure 1b). The swivel head was necessary in order to prevent any possible misalignment between specimen and loading system. To control slippage of the swivel head during cyclic loading, six bolts were used to lock it, once the alignment was established, to the part of the loading jig that was rigidly attached to the load cell. Specimen installation was a slow and tedious operation but utmost care was needed to prevent premature failure in cyclic loading. The consistency of the results testify to the success of the method.

During testing, the uniaxial load, longitudinal and lateral strains, and the acoustic emission could be monitored and permanently recorded. Load was sensed by a 100,000 lbs. dynamic load cell and recorded on an X-Y plotter as a function of any of the other mentioned variables or time. Longitudinal strain was indirectly determined by end-to-end specimen displacement measurement. This was accomplished by two phosphor-bronze cantilevers mounted at opposite sides of the specimen diameter. Each cantilever was instrumented with four 350 ohms SR-4 foil strain gages connected into a four-arm Wheatstone bridge circuit to

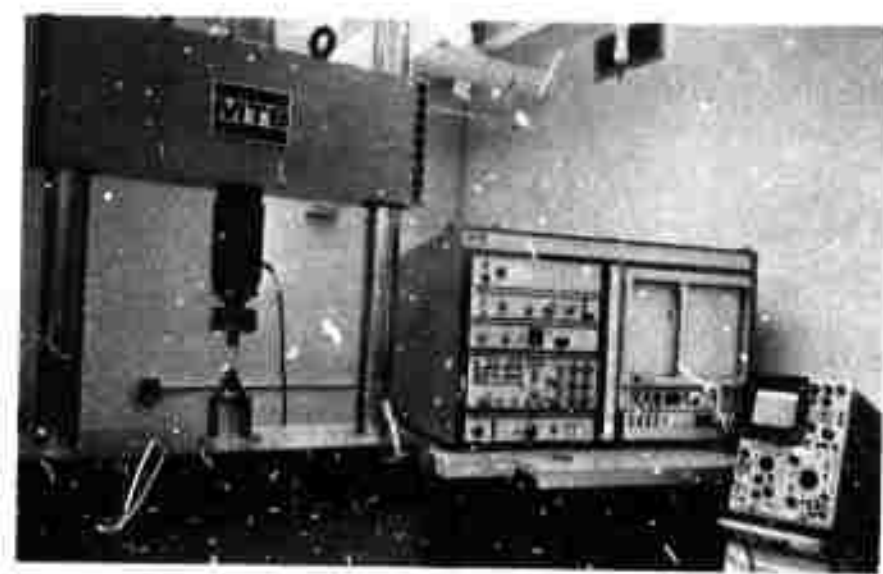


Figure 1a - Loading system, electronic controls and data acquisition instrumentation

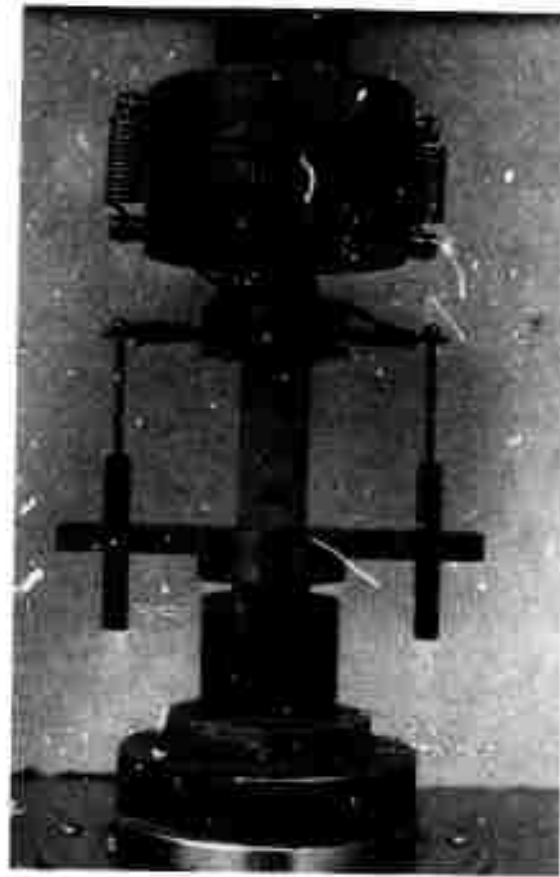


Figure 1b - Loading jig with specimen, cantilever set and swivel head.

insure satisfactory temperature compensation (Figure 2). Lateral strain was measured directly by means of two 120 ohms SR-4 strain gages bonded horizontally to the specimen at opposite sides. This arrangement is not ideal because it does not take average measurements but rather localized ones and can be affected by local microcracks or other inhomogeneities. It is, however, a simple and reliable method of lateral strain sensing.

In selected specimens the microseismic activity due to microcracking, crack extension and crack coalescence was detected and recorded by use of a Dunegan acoustic emission system (Figure 2). The sensing device was a piezo-electric transducer attached directly to the specimen side. The detected signals were preamplified, filtered so as to allow only events in the 100-300 kilocycles range to pass, amplified, counted if event amplitude was larger than one volt, converted from digital to analog, and finally recorded on either an X-Y or time base plotter.

Professor Pincus' optical bench (located at the University of Wisconsin, Milwaukee) was used for diffraction analysis of polished sections of tested specimens. The apparatus is described elsewhere (14).

b. Cyclic Tension Testing

The cyclic tension tests were run in the M.B. machine. In the indirect tension tests rock discs were mounted, with their planar sides vertical, between two fixed flat steel platens (Brazilian type loading). The diametrically applied load was sensed by a 5,000 lbs. dynamic load cell. No further instrumentation was used in these tests.

The direct uniaxial tension tests required a much more elaborate apparatus and very carefully prepared specimens. The set-up used is shown in Figure 3. Its whole purpose was to insure proper alignment between specimen and the line of load, thus preventing unnecessary bending moments which could bring about premature failure near the ends of the specimen. Steel end caps were epoxied to all specimens. To guarantee concentricity between rock and caps, all three were held firmly against a vertical glass angle bar during the curing period. The top end cap threaded into the load cell; the bottom cap screwed into a larger bolt which fit loosely into a pot filled with a commercially available "Wood's Metal." The latter has the property of melting at 160°F. A copper pipe coiled around the pot allowed steam or cold water to melt or freeze the wood's metal as needed. In the molten state, the pot enabled the specimen to hang freely from the top. As the metal froze the specimen position remained intact, alignment was assured and test results indicate that in the great majority of the tests, tensile rupture occurred near the center of the specimens.

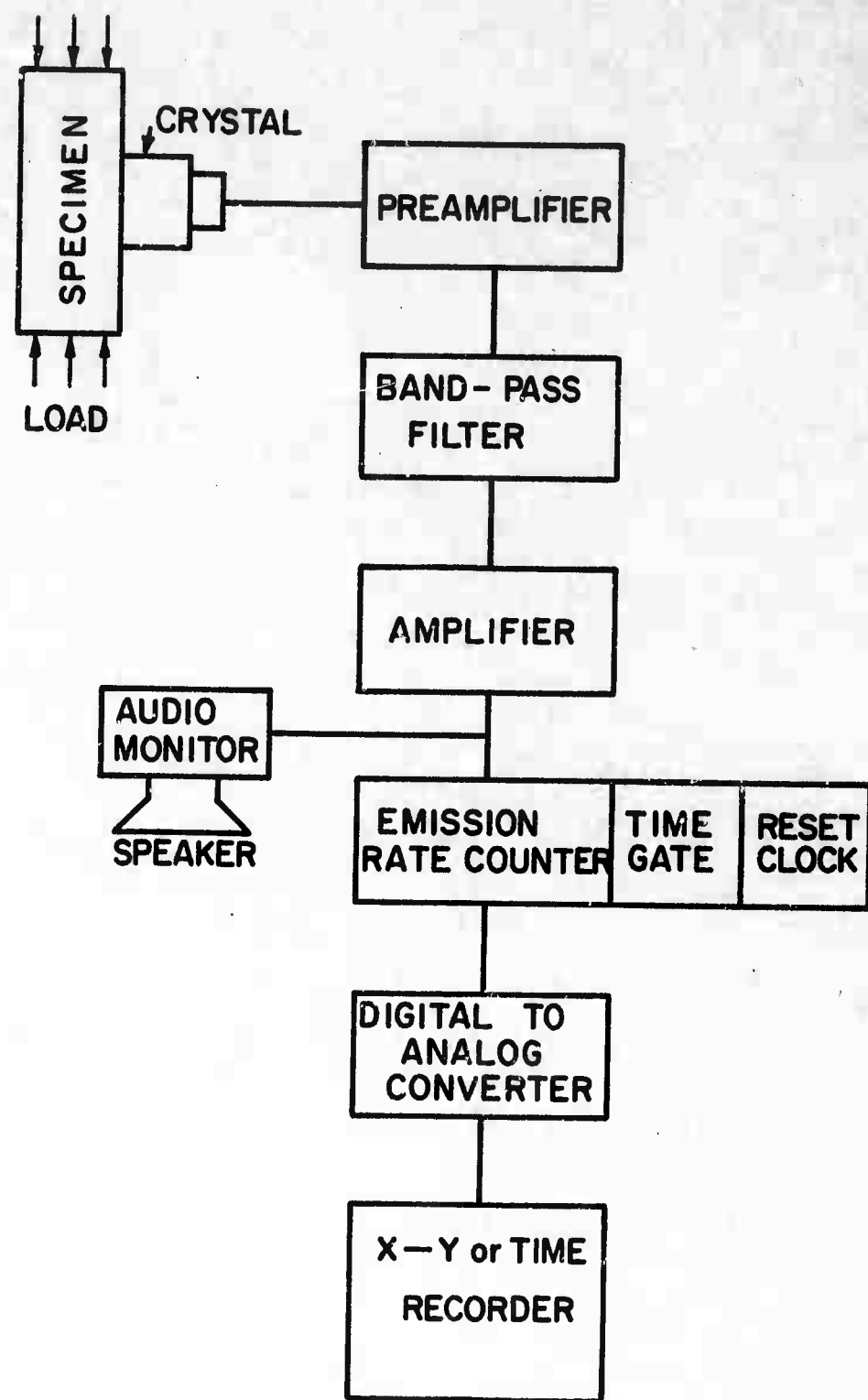


Figure 2. Acoustic emission system - block diagram

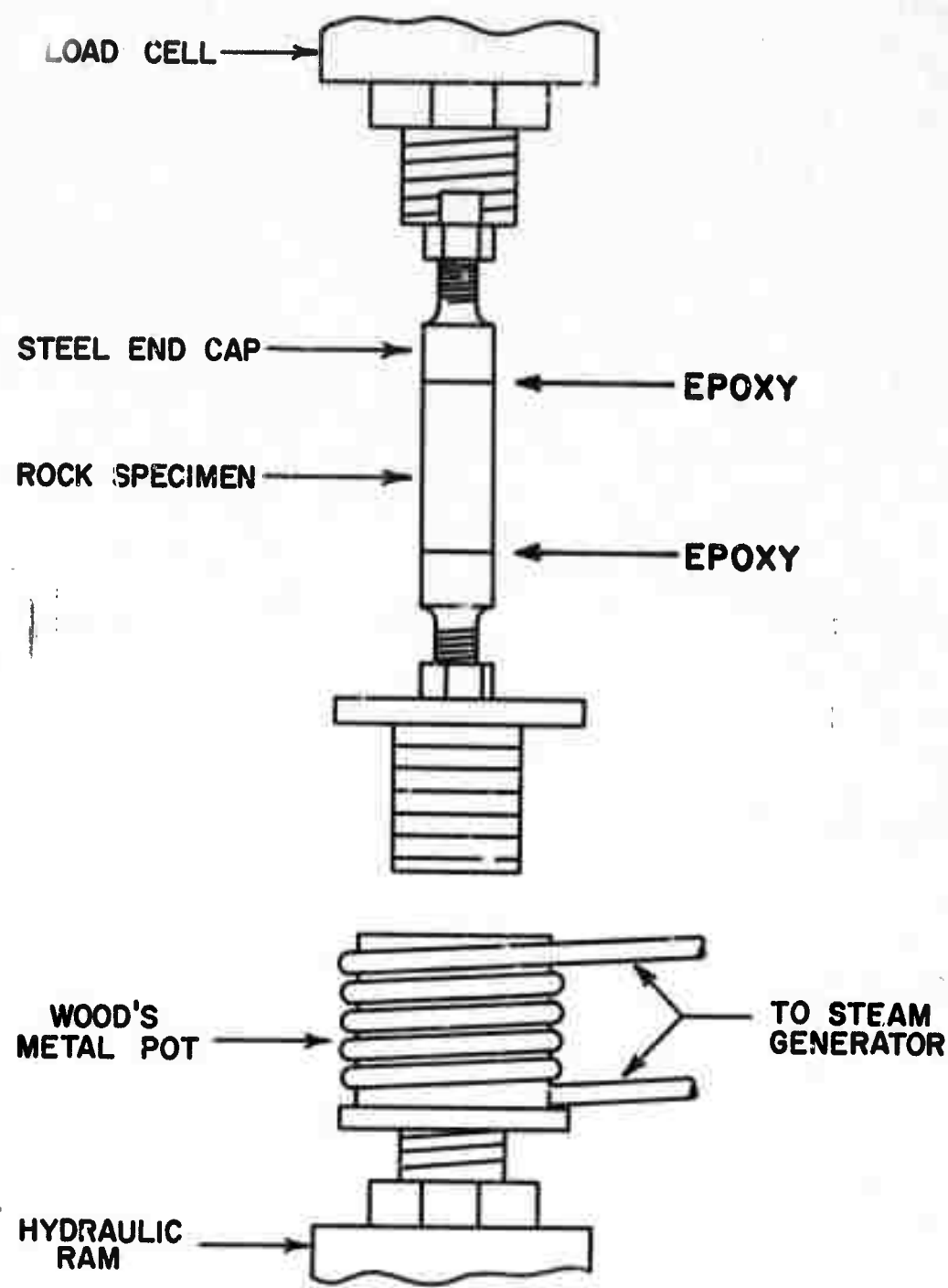


Figure 3. Set-Up for uniaxial tensile cyclic testing.

Longitudinal strain was measured by use of two 120 ohms SR-4 strain gages bonded vertically to opposite sides of the specimen. Micro-seismic activity was detected and recorded as described above.

Experimental Program

The goal of the program was two fold:

(1) Determine the mechanical behavior of rock under cyclic loading using a phenomenological approach which can provide data that is both basic and useful in practice;

(2) Study the internal mechanism that brings about cyclic loading weakening of rock (fatigue) by macroanalytical and micromechanistic methods.

Four types of cyclic loading were planned for the present investigation: uniaxial compression, tension, triaxial compression, tension-compression. Only the first two were attempted during this first year of the program. The testing program in each type of loading was to include most of the aspects mentioned in Figure 4.

a. Cyclic Uniaxial Compression

Two hard rocks (White Tennessee marble, Indiana limestone) were thoroughly tested in cyclic uniaxial compression. The major portion of the testing was stress-controlled cyclic loading between zero stress and a peak stress that was kept constant during each test but was varied from specimen to specimen. To prevent loss of contact between specimen and platens at zero load, the lower peak of the compression cycle was moved up to 150-300 psi, and was kept constant throughout this portion of the testing program. Figure 5 shows diagrammatically a typical stress-controlled test and its readouts. Both longitudinal and lateral strains were measured in selected specimens.

In a series of stress-controlled tests the mean stress rather than the lower peak stress was kept constant and the results are detailed in the next section.

Another aspect of cyclic loading was studied by controlling the strain and the strain rate. These tests were run between a minimum strain of 400 μ in/in and an upper peak that varied from test to test. Typical program diagram and readouts are shown in Figure 6.

CYCLIC FATIGUE PROGRAM

ROCK CONDITION

INTACT

FAILED

LOADING TYPES

STRESS CONTROLLED < CONST. LOWER PEAK
CONST. MEAN STRESS
STRAIN CONTROLLED

I. MECHANICAL BEHAVIOR DATA

S - N CURVES

STRESS VS.  AXIAL STRAIN
LATERAL STRAIN
VOLUMETRIC STRAIN (INDIRECT)

STRAIN VS. TIME

ACOUSTIC EMISSION VS. TIME

2. INTERNAL MECHANISM OF FATIGUE STUDY

MICROSEISMIC DETECTION

PHOTOGRAPHY

OPTICAL DIFFRACTION

PHOTOMICROGRAPHY

Figure 4. Cyclic fatigue program.

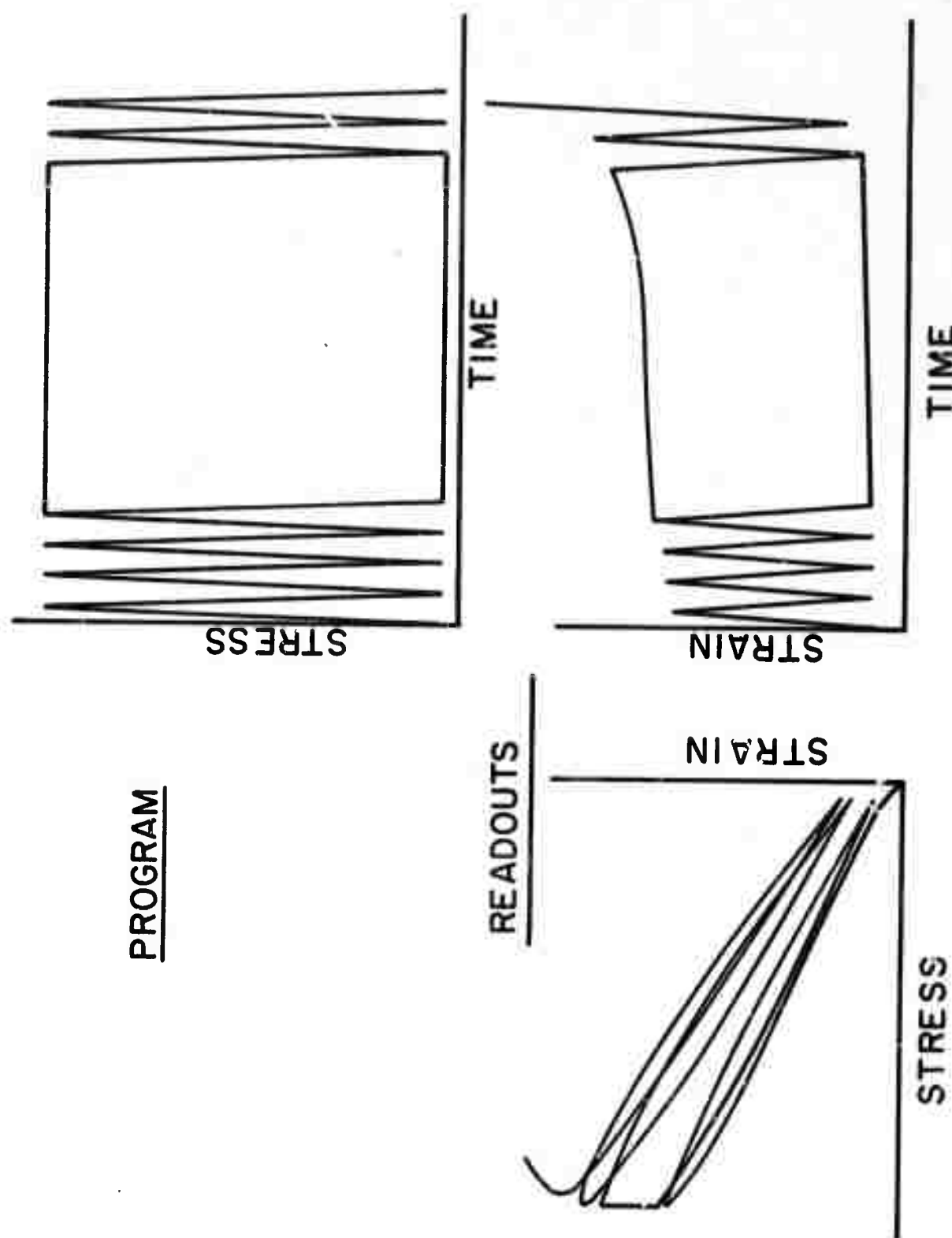


Figure 5. Typical programmed and readout curves in stress-controlled cyclic tests.

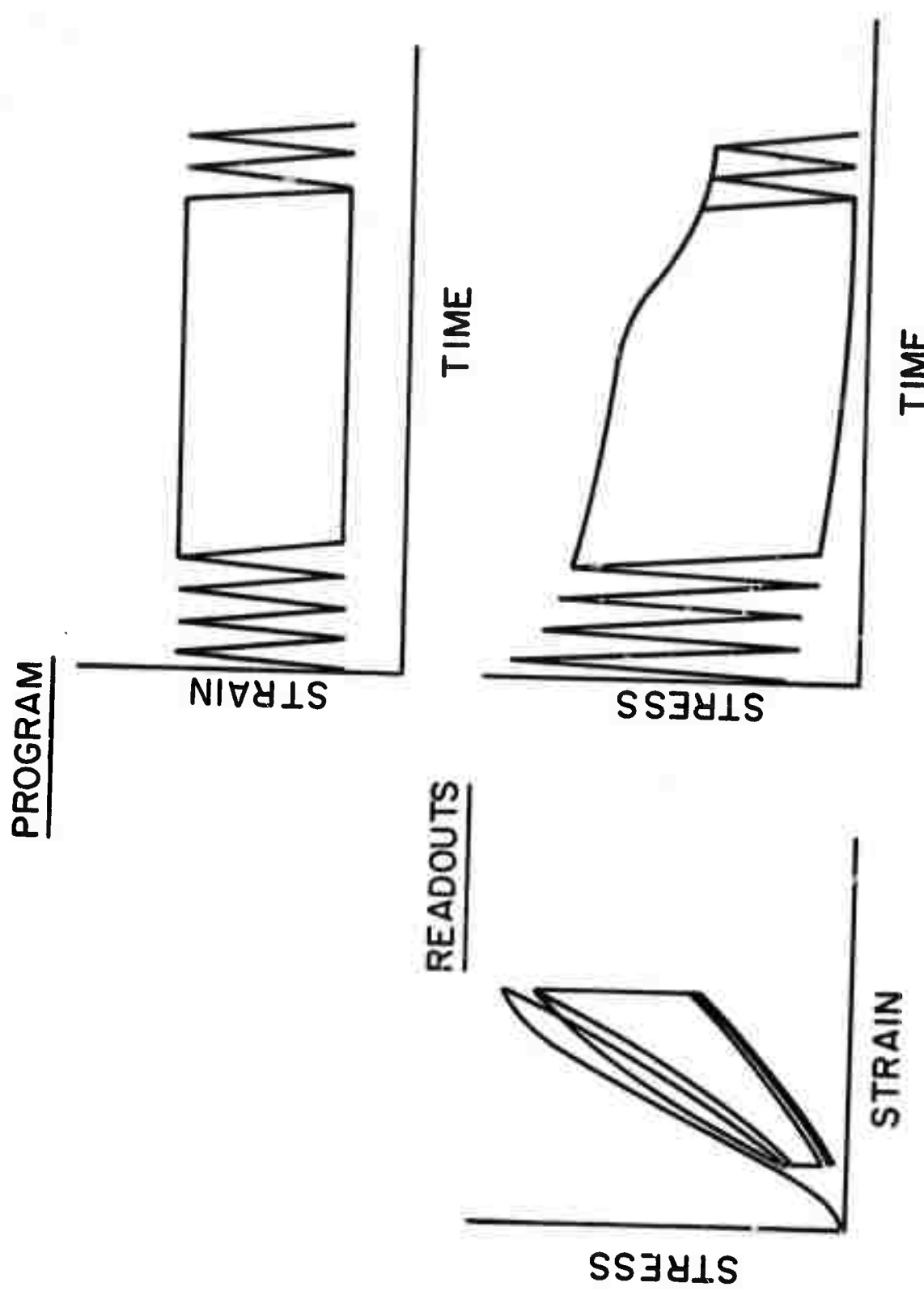


Figure 6. Typical programmed and readout curves in strain-controlled cyclic tests (shown in Indiana limestone behavior).

Stress controlled cyclic loading of failed rock was investigated in White Tennessee marble and Cherokee Georgia marble. The latter was available in a very limited quantity and was used only in this series of tests because of its convenient postfailure behavior.

The shape of the programmed pulse, whether in stress or strain control, was triangular (Figures 5 and 6), i.e., loading and unloading were applied at a constant rate during each cycle. The frequency of cycling was kept at 1-5 cycles per second (cps) to simulate major pulses in earthquakes (1-2 cps) and in rock blasting (5-10 cps). The higher frequencies were preferred because of shorter test duration, but the lower frequencies (1-2 cps) were necessary when stress-strain recordings were made due to plotter response limitations. The maximum number of cycles per test was kept at one million, a figure considered more than adequate for any repetitive type of loading applied to rock structures during their expected life.

To gain an insight into the mechanism of rock fatigue both audio and optical methods were used. Noise emission due to microcracking was recorded as described above. Photographs of vertical sections of loaded specimens were processed on the optical bench using a diffraction method. Highly polished sections were carefully observed under a Zeiss Ultraphot II-M microscope and particular areas were photomicrographed.

b. Cyclic Tension

Two hard rocks (White and Pink Tennessee marble) were tested in cyclic tension. The original plan was to bypass the formidable difficulties usually encountered in uniaxial tension testing by using an indirect method, namely the Brazilian type loading. Circular disks were diametrically compressed in stress-control, using a sinusoidal pulse (at that time constant rate loading was not available on the M.B. machine). The lower peak was held at 50 psi for all tests; the upper peak was varied from test to test. The frequency was kept at 1 cps and the maximum number of cycles per test was limited to 100,000.

Recent work on Brazilian testing (15) and the present investigators' observations casted doubt on its validity as a tensile test. Thus, it was decided to reconsider the rather inconvenient direct pull or uniaxial tension test. Using very careful specimen preparation and installation into the loading jig, tests were run in Pink Tennessee marble under stress-control between constant lower peak (50 psi) and varying upper peaks. These tests were controlled by triangular loading pulses, at 1 cps, and up to a maximum of 100,000 cycles.

Besides counting the number of cycles to failure in each test, the longitudinal strain was measured in a few specimens, and the acoustic emission from apparent internal cracking was recorded in a number of cases.

The results of this outlined program are presented in the next section.

EXPERIMENTAL RESULTS

A - UNIAXIAL COMPRESSION

Monotonic Loading

The first stage of the experimental work was the determination of the compressive strengths of the rocks used. This was done in order to find the upper limit of the maximum stresses to be applied in cyclic loading. Specimens were loaded in stress control at three different rates and the results are shown in Table 1. The results show that the compressive strength can vary considerably with the rate of loading. It is therefore imperative that whenever the compressive strength is employed it should be accompanied by the conditions under which it was determined. In the cyclic testing results reported here the compressive strength was taken as that obtained under conditions equivalent to 1 cycle/sec.

Cyclic Loading

(a) Stress-Controlled Tests with Constant Lower Peak Stress

I. S-N Curves

The first and most important objective of the stress-controlled experiments was to verify whether cyclic loading affects the compressive strength of the two tested rocks. Quantitative results are shown in Figures 7 and 8 in the form of S-N curves, where the upper peak stresses used in each test are plotted against the logarithm of the number of loading cycles required to bring about failure in compression. The immediate conclusion is that both rocks exhibited fatigue behavior, i.e., they were weakened by repetitive loading. The two S-N curves show that within the limit set for these tests (10^6 cycles) failure could occur when the applied upper peak load is as low as 77% in White Tennessee marble and 65% in Indiana limestone of the respective compressive strengths. Within the range used (1-5 cps) no apparent frequency related difference was observed as far as specimen fatigue life was concerned. Specimens that survived the maximum applied loading cycles (10^6) were loaded monotonically to failure. Their compressive strength did not appear significantly different from that of uncycled specimens. In both rocks the life expectancy of a specimen clearly increased as the maximum cyclic compressive load was decreased. However, the actual S-N relationship differed considerably from one rock to the other. In White Tennessee marble the logarithm of number of cycles to failure appears to increase linearly with the decrease

TABLE 1
COMPRESSIVE STRENGTHS AT DIFFERENT LOADING RATES

Rock	Loading Rate (psi/sec)	Equivalent Cyclic Frequency (cps)	Specimens Tested	Mean Comp. Strength (psi)	Standard Deviation psi	%
White Tennessee Marble	100	"static"	11	21,150	909	4.2
	50,000	1	12	23,285	840	3.6
	200,000	4	7	24,900	425	1.7
Indiana Limestone	100	"static"	10	9,500	173	1.8
	20,000	1	10	10,800	138	1.3
	100,000	5	6	10,630	417	3.9

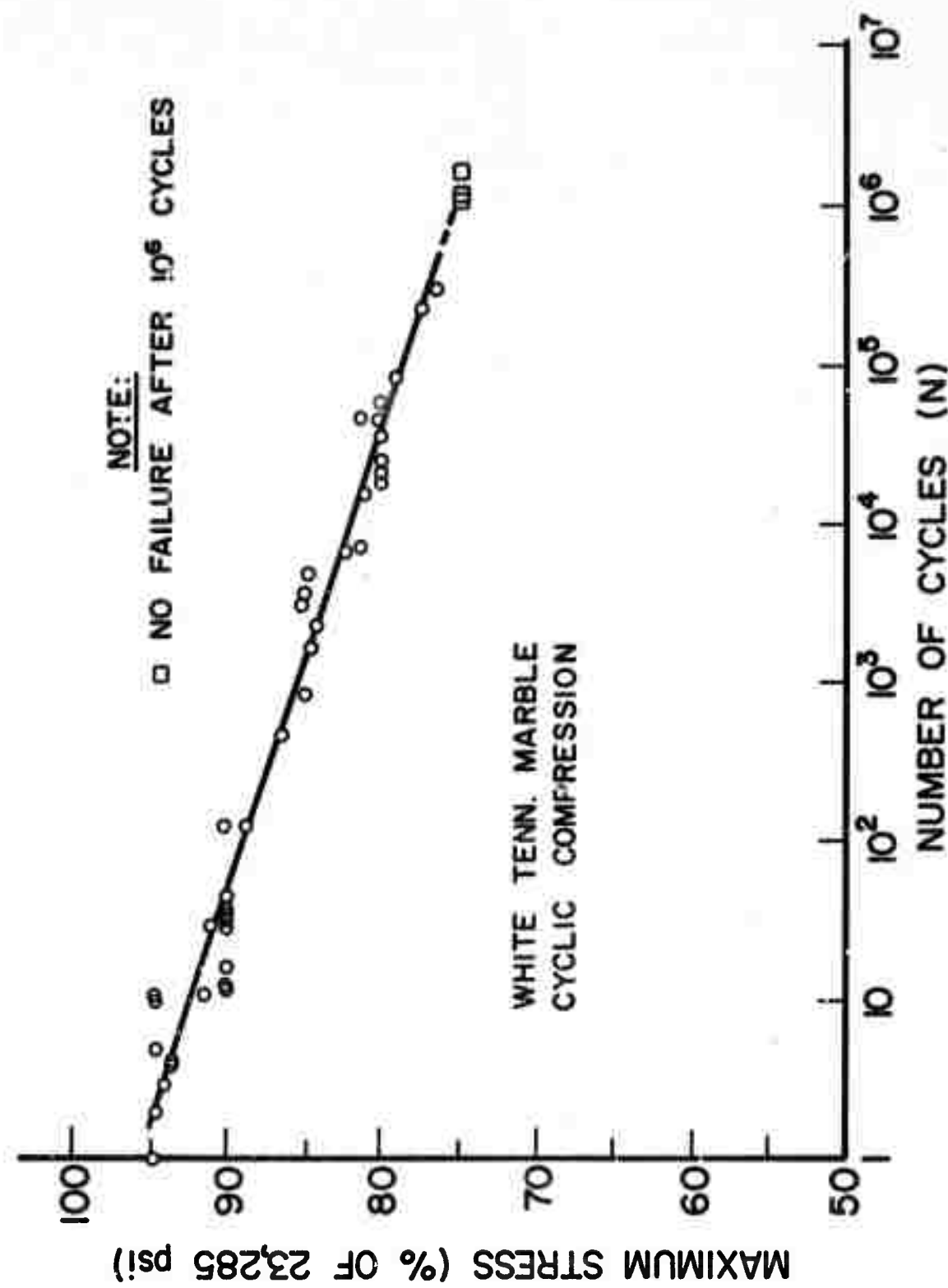


Figure 7. S-N curve for White Tennessee marble subjected to cyclic compression with constant lower peak stress.

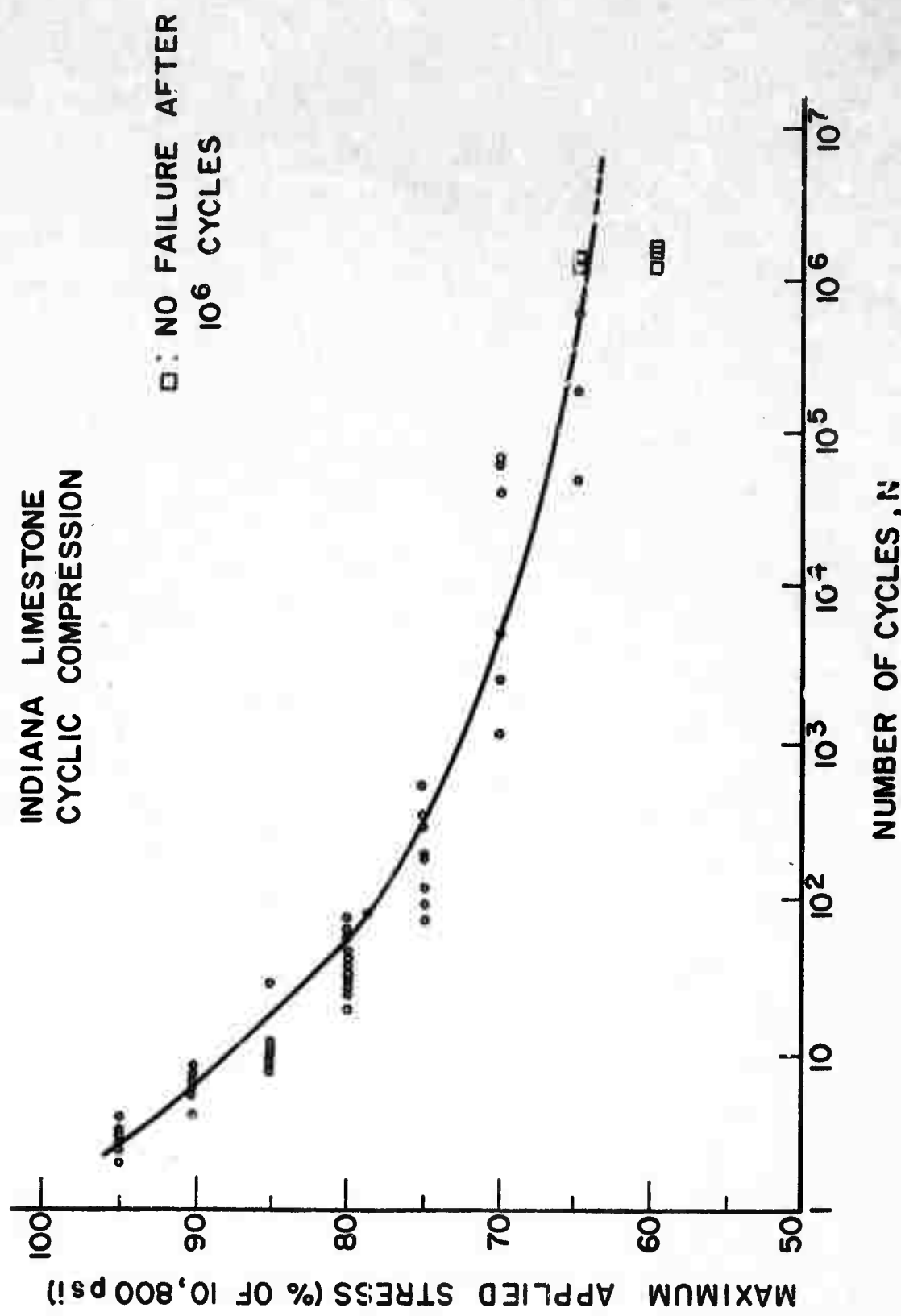


Figure 8. S-N curve for Indiana limestone subjected to stress cyclic compression with constant lower peak.

in the upper peak stress. The experimental relationship is approximately given by

$$S = 96 - 3.5 \log_{10} N \quad 1 < N < 10^6 \quad (1)$$

where S is the maximum applied stress taken as a percentage of the compressive strength. In Indiana limestone the relationship is curvilinear (Figure 8), but can be approximated as bilinear:

$$S = 100 - 12.5 \log_{10} N \quad 1 < N < 10^2$$

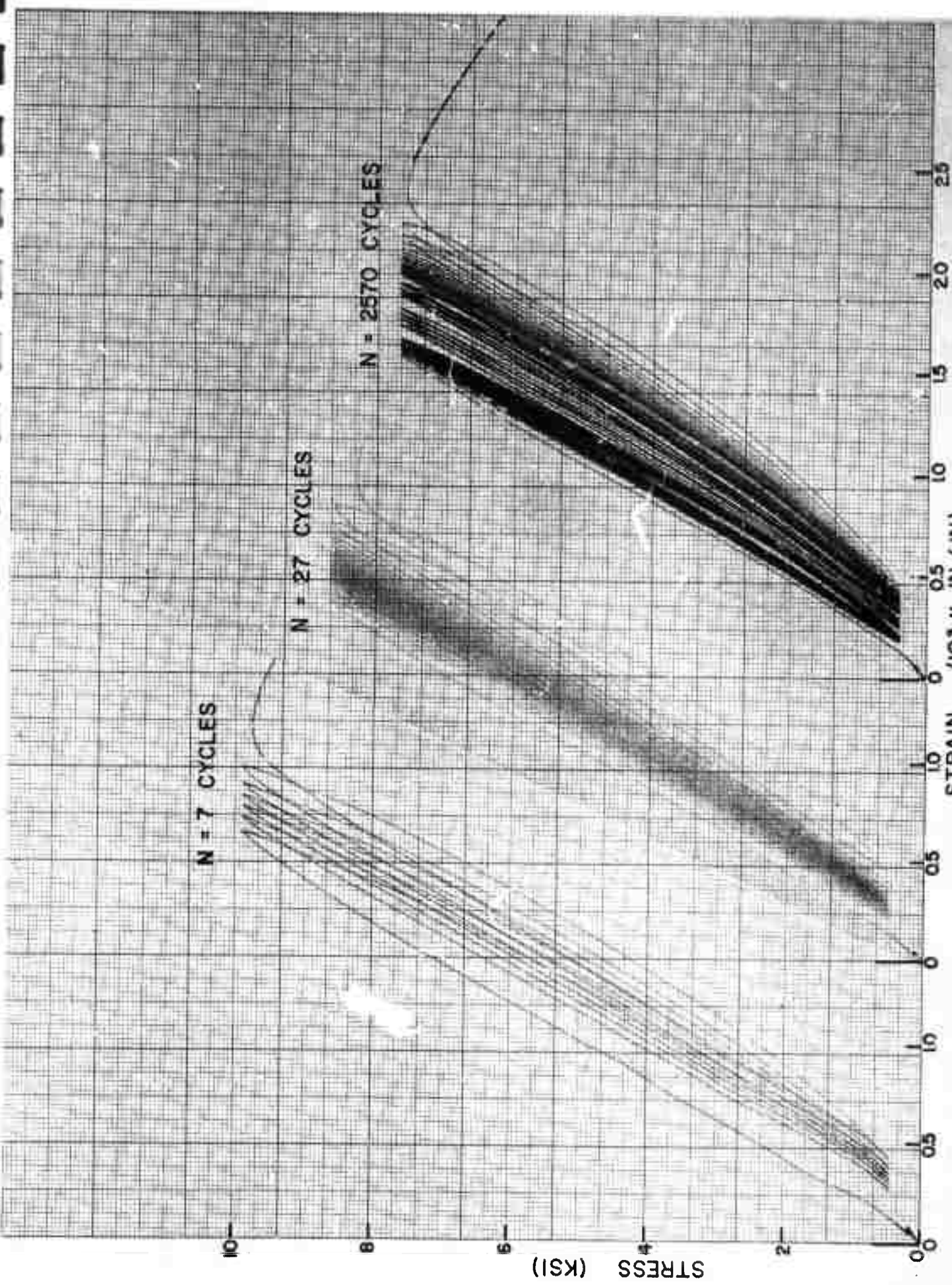
$$S = 80 - 2.7 \log_{10} N \quad 10^2 < N < 10^6 \quad (2)$$

As equations (1) and (2) show, the very porous and weaker Indiana limestone is also more affected by cyclic loading. For example, at $S = 77\%$ White Tennessee marble fatigue life was recorded as about 500,000 cycles; Indiana limestone life was only 100 cycles. As S was decreased, however, the limestone life expectancy greatly increased and appeared to asymptotically tend to some fatigue limit ($S_L \approx 60\%$) below which no number of loading cycles would fail the rock. The experimental limit of one million cycles appeared adequate since it is hardly expected that rock would be subjected to a larger number of cycles during the expected life of an engineering structure.

It is suggested that the fatigue strength at 10^6 cycles be used as the "critical compressive strength" of rock. In Tennessee marble this value will be $23,285 \times 0.75 = 17,450$ psi; in Indiana limestone, $10,800 \times 0.60 = 6480$ psi. Designs in intact rocks using these values, not only are protected against static and dynamic compression loadings but also against cyclic stresses as encountered in earthquakes, blasting, etc.

II. Cyclic Stress-Strain Behavior

Stress-strain curves were frequently recorded during the tests, Figure 9 shows three typical plots in Indiana limestone. The increase in the number of cycles to failure with the decrease in maximum applied compressive load is clearly displayed. Permanent strain appears to accumulate in the rock with the dissipation of relatively large amounts of energy. Common to all tests (in both rocks) is the phenomenon of large hysteresis in the first cycle, followed by decreasing but still large loops in the next few cycles, a narrowing of the hysteresis loops to an almost constant shape in the next group of cycles, and a reopening in the last



several cycles prior to failure. In the very short life tests (0-15 cycles) the second stage appears to be absent. The behavior of the stress-strain curve indicates internal changes in the rock during cyclic loading that eventually culminate in fatigue failure. In the first cycle a major inelastic deformation occurs probably due both to closing of some initial voids and the creation of microcracks when the loading exceeds the elastic limit of the rock. Additional irreversible changes occur in the following cycles. These, however, have an increasingly lesser impact on stress-strain behavior until an equilibrium of sorts is established. Continuous internal changes eventually bring about renewed hysteresis loops and accelerate the fatigue failure phenomenon.

The amount of strain difference between the upper peaks of the last and first stress-strain cycles, the so called cyclic creep, was measured and the averages are shown in Figures 10 and 11. The complete stress-strain curves as obtained at 4×10^{-6} /sec are also shown (curve a) together with the extrapolated curves for a loading rate equivalent to 1 cycle/second (curve c). The strain difference in both rocks seems to be bounded by the ascending and the descending portions of the extrapolated complete stress-strain curves. In no recorded test was the total cyclic creep larger than the limit set by these curves. Hence, the latter appear to define for different stress levels the limit of strain that can be applied to a rock without producing failure. This is a very important result which provides a quick estimate of the upper limit of strain in cyclic loading, and can be conceivably used in design problems. As noted in Figures 10 and 11 the cyclic creep at different stress levels defines a descending curve c which is steeper than the extrapolated curve b. The discrepancy could be due to a rate of loading effect.

In an attempt to understand the mechanism that creates the fatigue effect as demonstrated by the S-N curves and the stress-strain recordings, the variation of strain with time was investigated, the acoustic emission from fatigued specimens was detected, the volumetric changes in specimens were estimated and optical and microscopic studies were undertaken.

III. Strain-Time Behavior

Typical strain-time behavior during cyclic loading is shown in Figures 13 and 15. In both rocks, the curve shaped by the upper peak points clearly resembles that of static creep and can be divided into three stages. There is a primary stage in which the upper peak strain increases at a decelerating rate (the first 5-10 cycles). It is followed by a steady

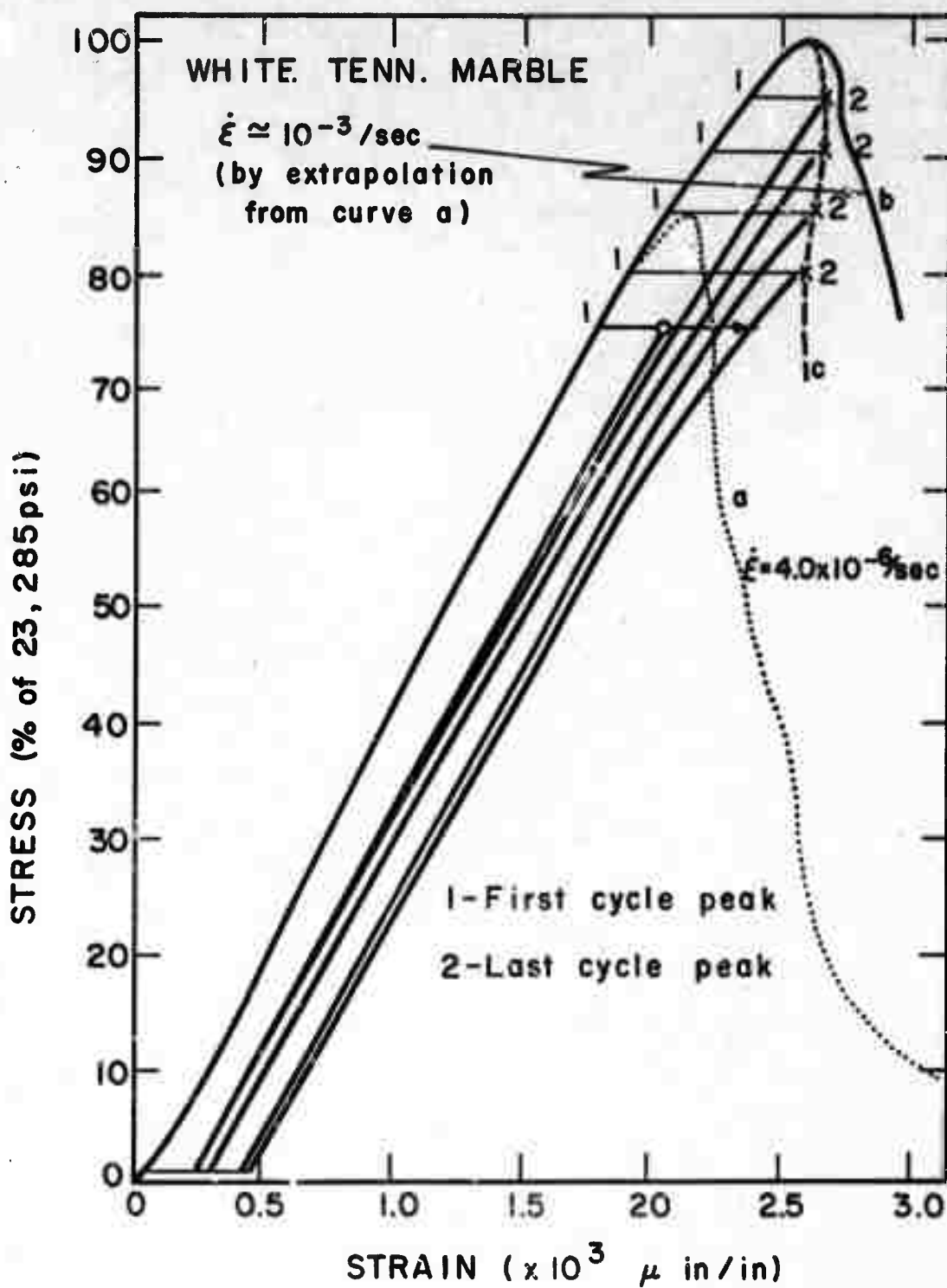


Figure 10. Strain difference between last and first stress-strain cycle peaks versus expected complete stress-strain curve - White Tennessee marble.

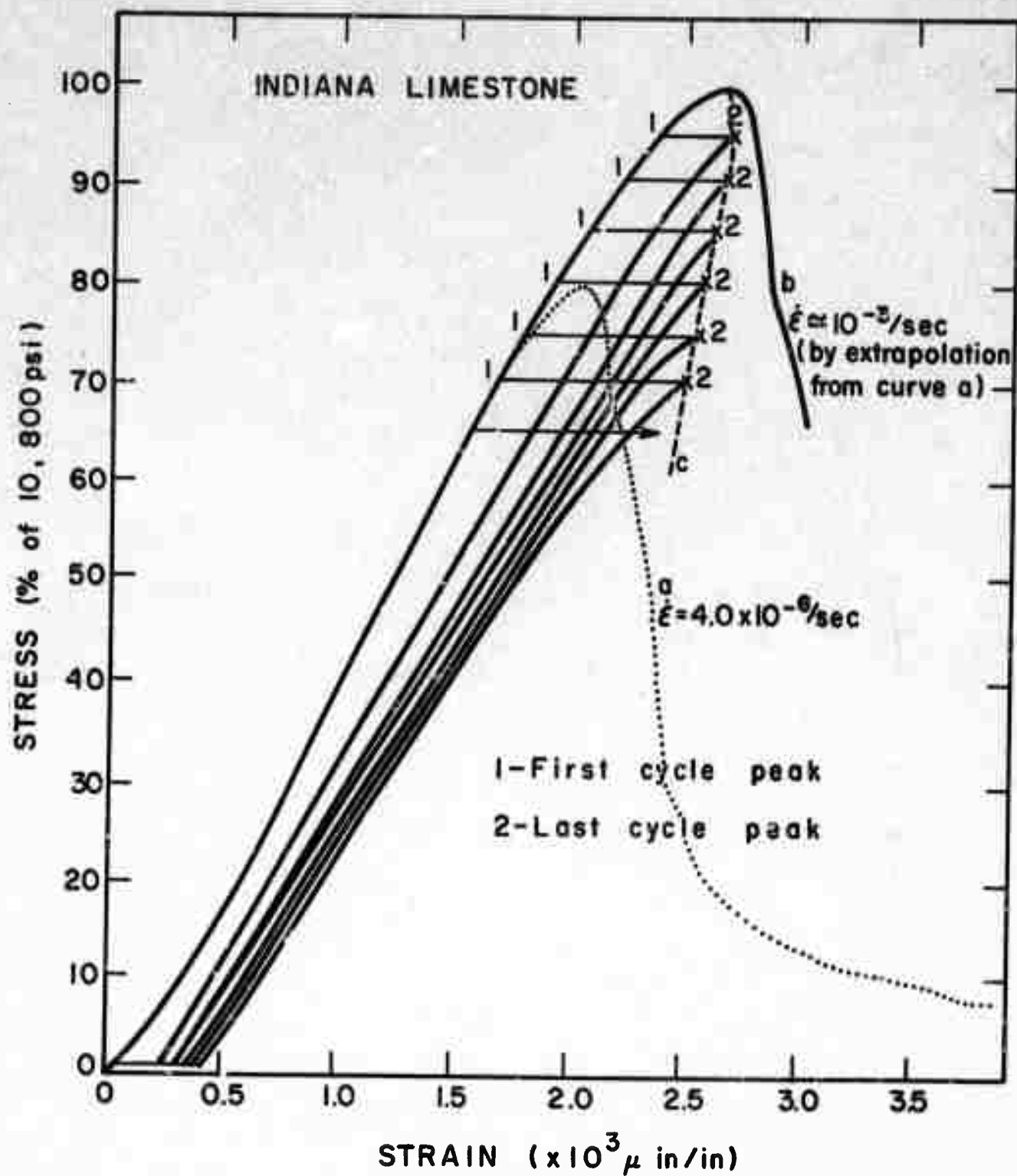


Figure 11. Strain difference between last and first stress-strain cycle peaks versus expected complete stress-strain curve - Indiana limestone.

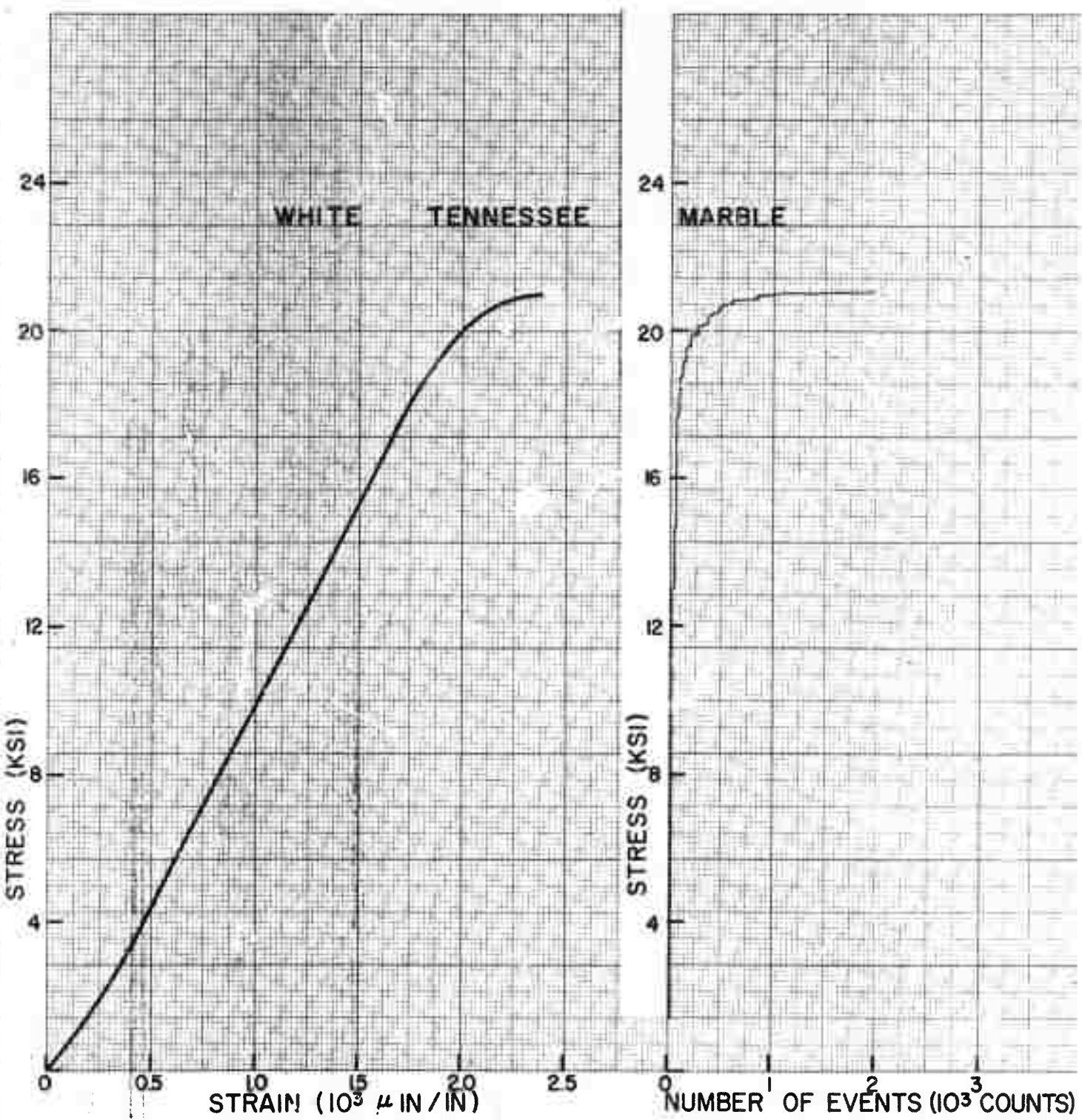


Figure 12 - Stress-strain curve and acoustic emission in monotonic compression (White Tennessee marble).

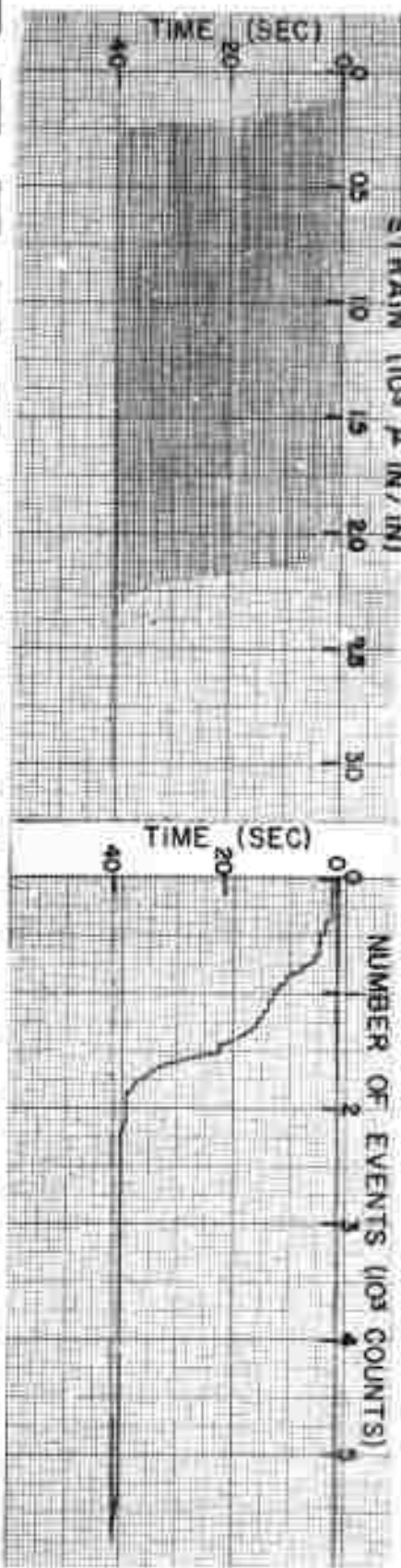
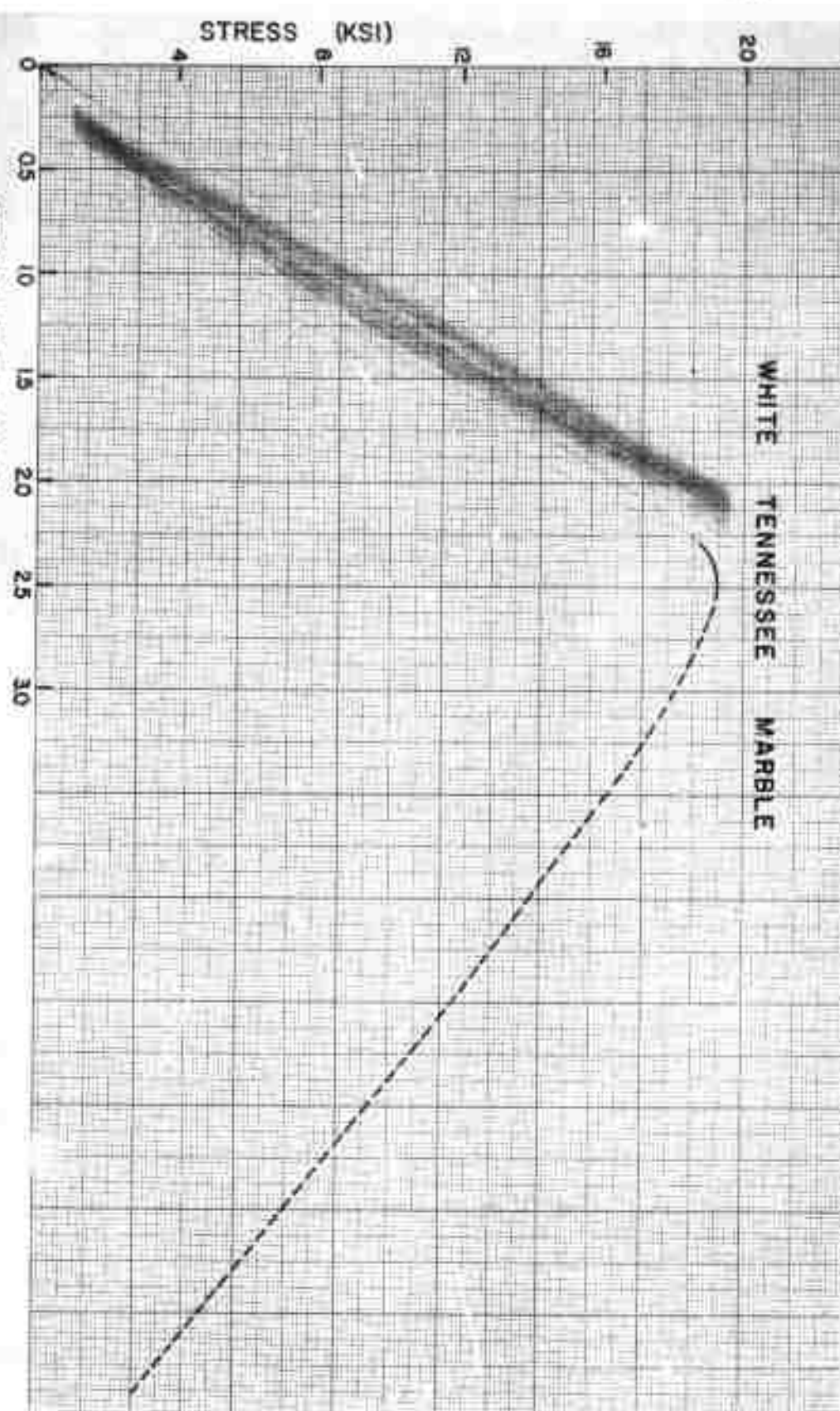
Figure 13 - Typical recording during cyclic loading of White Tennessee marble.

38

20

WHITE
TENNESSEE

MARBLE



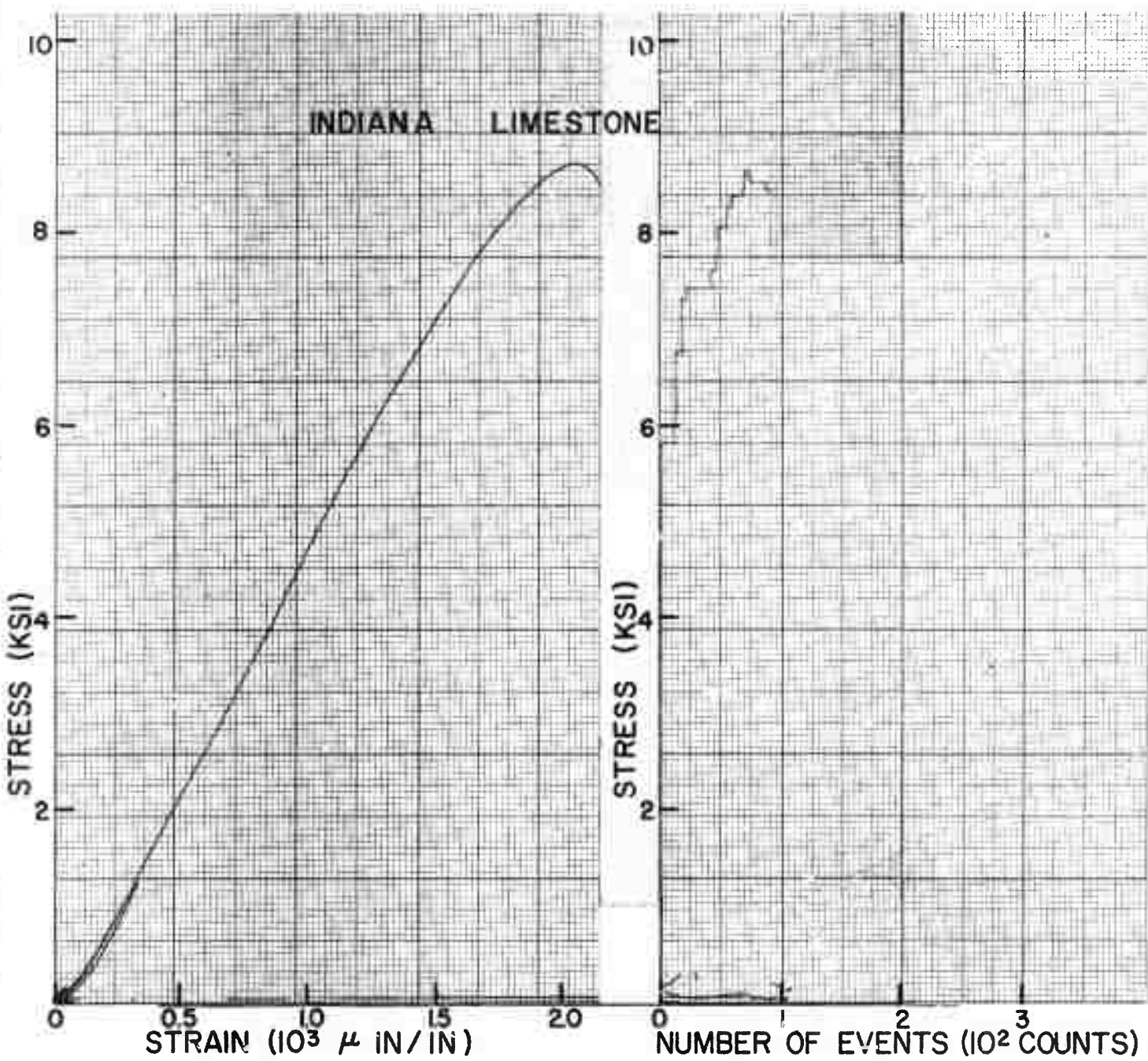


Figure 14 - Stress-strain and acoustic emission in monotonic compression Indiana limestone.

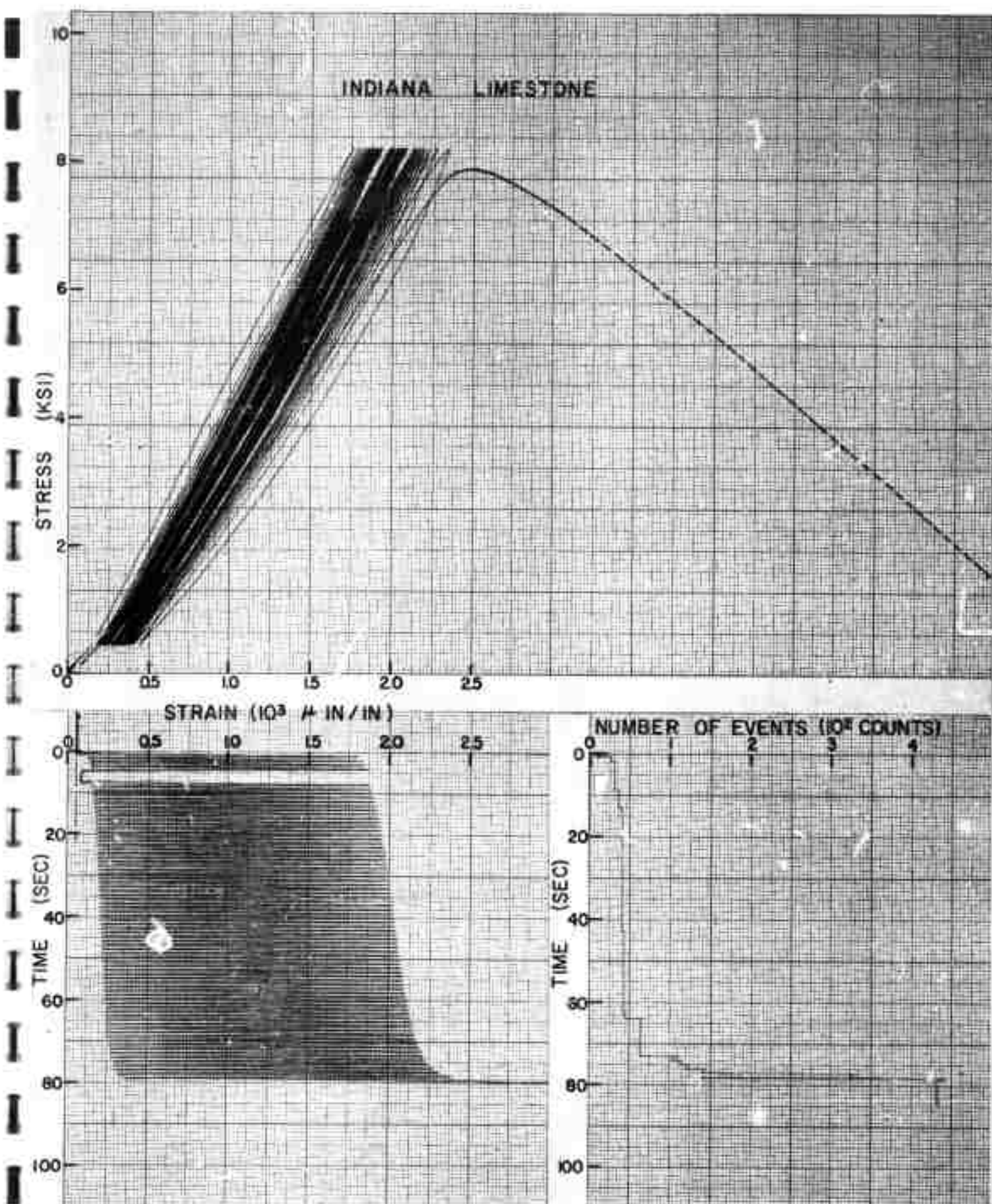


Figure 15 - Typical recordings during cyclic loading of Indiana limestone.

state stage in the form of a linear strain increase. The third and final stage is of accelerating upper peak strain ending in specimen failure (last 5-15 cycles). The three stages can be easily matched to those in the stress-strain plots. Figures 13 and 15 show that the lower peak strain points underwent a more reduced increase during the test. This implies, and Figure 9 verifies, that the average tangent modulus generally decreased with cycling. The results of this measurements are given in Table 2.

IV. Lateral Strain and Volumetric Changes

Lateral strain was measured in a number of specimens and samples of the recordings are shown in Figures 16 and 17. Both rocks exhibited large hysteresis loops in the first stress-lateral strain cycle, after which the hysteresis decreased during the next few cycles and narrowed to an almost constant size for the bulk of the testing time. The final stage, prior to failure was undistinguishable in the marble, but quite evident in the limestone, where the peaks of the cyclic stress-lateral strain curve crepted at an accelerated pace and the respective hysteresis loops opened again considerably. Table 3 presents the changes in the Poisson's Ratio values in the specimens analyzed in Figures 18 and 19. Although total axial strain and total lateral strain increased significantly in both rocks during cycling the change in the value of the Poisson's Ratio of the marble was negligible. The limestone lateral strain per cycle increased at a higher rate than its axial strain so that the final Poisson's Ratio was about double the initial value.

From the recorded stress-axial strain and stress-lateral strain curves the volumetric changes in fatigued specimen were calculated by using the relationship:

$$\text{Volume change/unit volume} = \text{axial strain} + \text{twice the lateral strain.}$$

In an elastic material subjected to uniaxial compressive loading, the volume is expected to decrease with an increase in the applied stress. In the marble (Figure 18) the volume change was indeed negative, although the tendency as the cyclic loading progressed was to approach the line of no volume change. In the limestone, the trend toward volume increase was clear from the very first cycles. The last stage prior to failure indeed yielded volumetric gains throughout the loading cycle (Figure 19). The tendency toward volume increase during cyclic loading is again indicative of permanent internal changes occurring in rock. These changes could be attributed to the phenomenon of microcracking, which has been found to occur in rocks under static loading. The developing microcracks could increase the lateral strain well beyond its elastic limit and in this way

TABLE 2
AVERAGE CHANGE IN TANGENT MODULUS WITH CYCLING

Rock	Tangent Modulus at 50% of the Upper Peak Stress First Cycle (psi)	Tangent Modulus at 50% of the Upper Peak Stress Last Cycle (psi)
White Tennessee Marble	11.1×10^6	9.9×10^6
Indiana Limestone	4.9×10^6	4.0×10^6

TABLE 3
CHANGE IN POISSON'S RATIO WITH CYCLING
(From Tangential Strains Measured at 50% of the Upper Peak Stress
for Specimens Analyzed in Figs. 18 and 19)

White Tennessee Marble		Indiana Limestone	
Cycle	Poisson's Ratio	Cycle	Poisson's Ratio
1	0.281	1	0.235
5	0.271	30	0.433
10	0.270	67	0.444
20	0.282	68	0.488

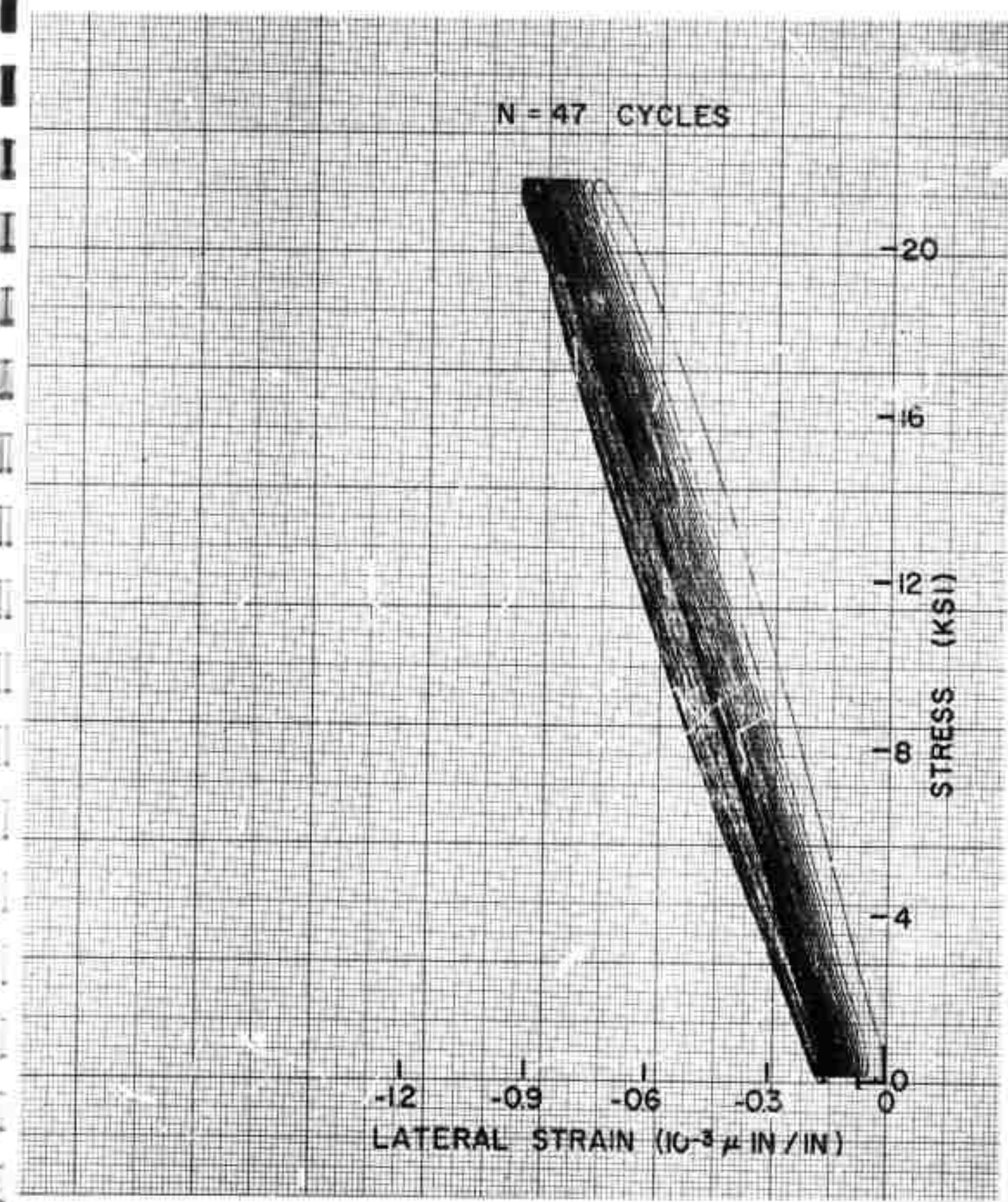


Figure 16 - Typical stress-lateral strain recording in cyclic loading of White Tennessee marble.

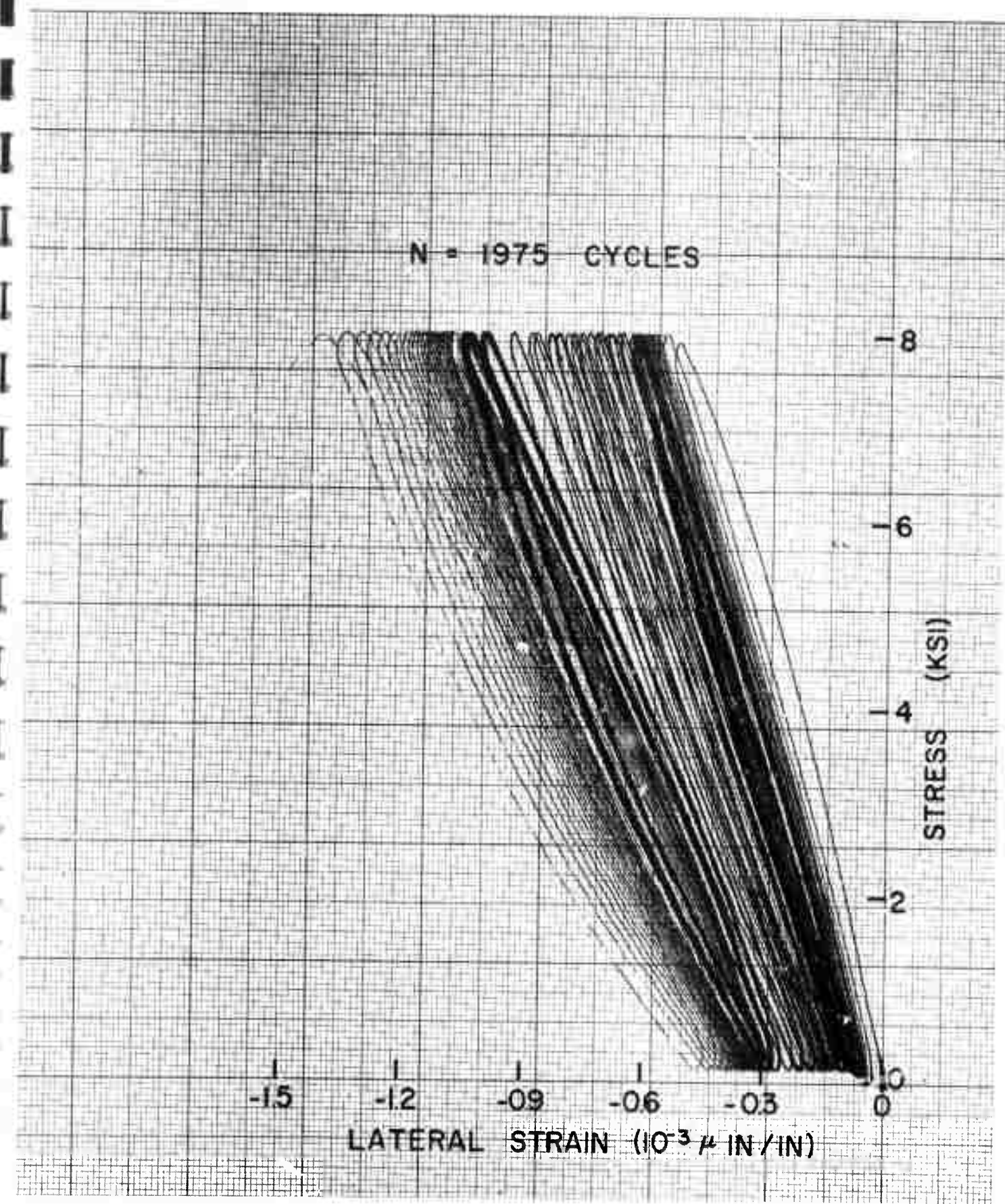


Figure 17 - Typical stress-lateral strain recording in cyclic loading of Indiana limestone.

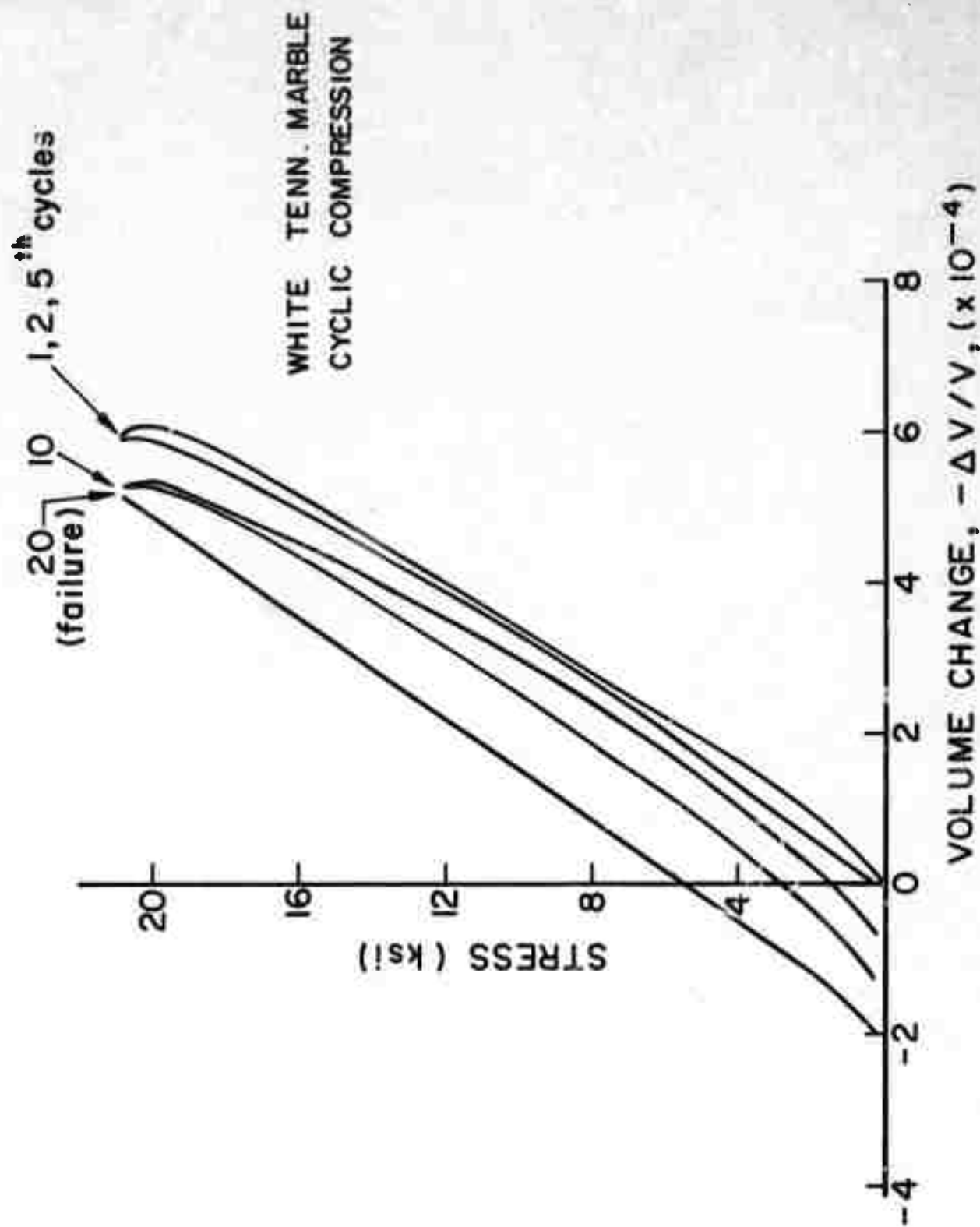


Figure 18. Calculated typical volumetric changes in cyclically loaded White Tennessee marble.

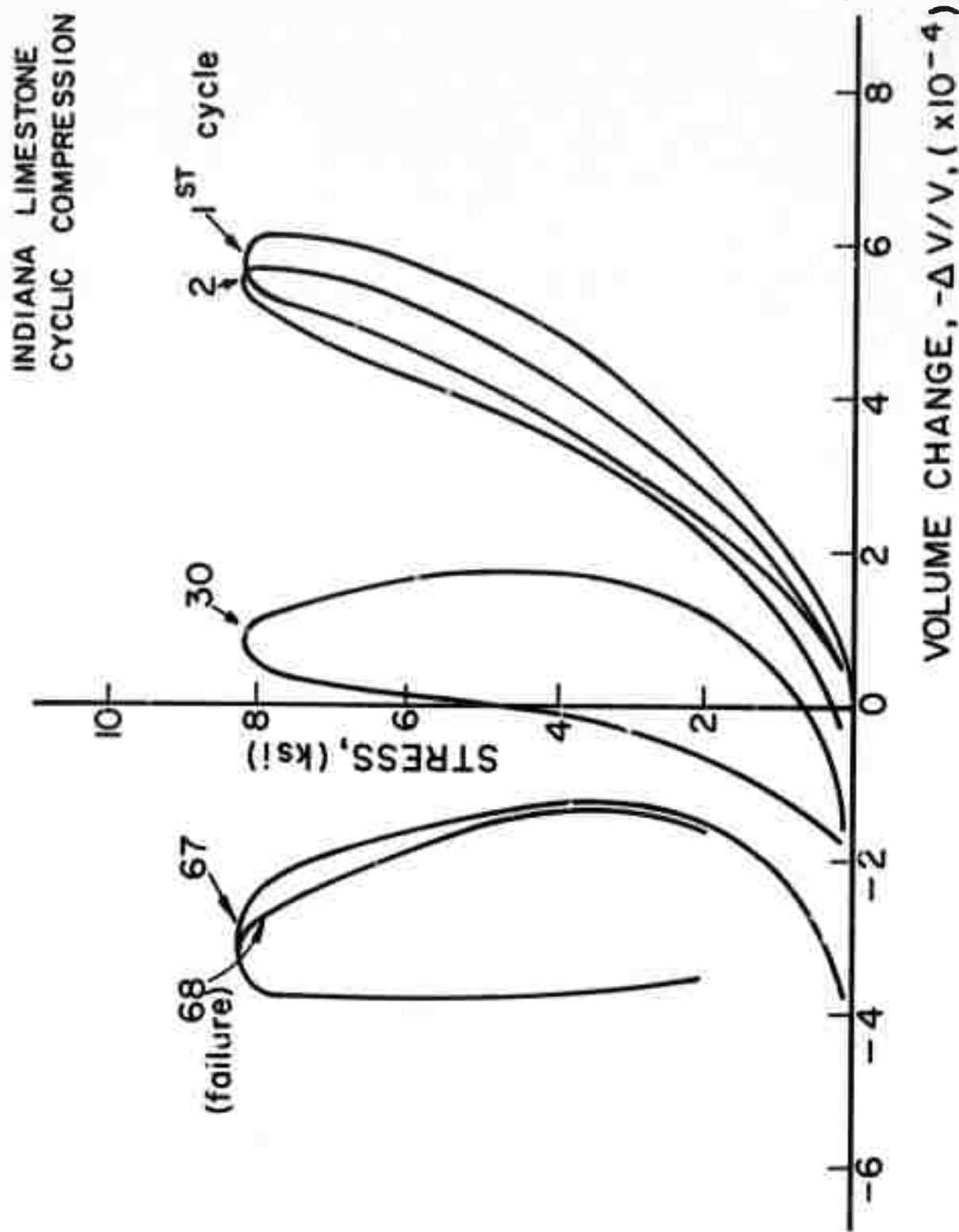


Figure 19. Calculated typical volumetric changes in cyclically loaded Indiana limestone.

affect the volumetric change. With each loading cycle more microcracks are possibly initiated, others are extended and the lateral strain is slightly (marble) or considerably (limestone) increased. The difference in lateral strain and volumetric increase between the two rocks may be a result of their initial structure. The marble has a very low initial porosity and the minute cracks that develop during loading do not appreciably increase its bulk volume. The limestone is a very porous rock and microcracks are bound to run into the existing voids until interconnections between pores are formed. These larger voids will more easily facilitate large permanent deformation in the lateral direction and will enhance permanent bulk volume changes as shown in Figure 19.

V. Microseismic Activity During Cycling

Previous experimental work (16, 17) has shown that processes related to brittle fracture initiation in rock, such as microcracking, intergranular slip, crack propagation, emanate elastic waves that can be detected by appropriate sensors on the surface of the specimen as microseismic (or acoustic) emission. To further the understanding of the internal mechanism that brings about fatigue failure selected specimen were appropriately instrumented enabling the acoustic emission to be detected and recorded during cycling. A number of monotonic compression tests were run first and the recorded emission in the form of total acoustic events were plotted as in Figures 12 and 14. The results were similar to previously published ones (18, 19). At about 60% of the compressive strength acoustic events strong enough to be counted were recorded, signalling the initiation of microcracking. It continued throughout the remainder of the test, accelerating considerably when the applied load approached the compressive strength. It is interesting to note that the number of events in the marble were an order of magnitude larger than in the limestone. One possible explanation is that the abundance of pores in the limestone eliminates the need for as large an amount of cracks as in the marble in order to bring about failure.

The second and most important phase of these tests was the counting of acoustic emission events from typical cyclically loaded specimen in both rocks (Figures 13 and 15). Not enough tests have been run so far; hence, the results reported are only qualitative, and to a certain extent speculative. It appears, however, that the mechanism of fatigue is indeed one of microcracking. Acoustic events were usually recorded from the very first cycle since the upper peak load was always well within the inelastic zone. Following the first cycle the acoustic emission continued to increase at an ever decreasing rate. During the steady-state stage (see strain-time behavior) almost no new events were recorded in the

Indiana limestone (Figure 15). As fatigue failure was approached the number of events increased considerably in both rocks. This accelerated stage started at about the same time or earlier than the corresponding stage in strain vs. time records. The total number of events recorded per test was larger than in monotonic loading but of the same order of magnitude.

A theory based on the acoustic emission results would be very similar to that based on stress-strain behavior, namely: a major amount of microcracking occurs in the very first cycle, followed by continuous microcracking at a reduced rate. During the latter stage the major mechanism is probably that of extension of existing cracks with the possible initiation of some additional microfractures. Finally, the new and extended cracks coalesce, propagate with increasing acceleration, and form the macroscopic fault planes upon which failure occurs.

VI. Photography, Optical Diffraction and Photomicrography

White Tennessee marble

The optical investigation of the marble specimens subjected to fatigue stresses was carried out in specimens that had been cyclically loaded to 85% of their compressive strength. Specimens were removed from the testing machine at different stages of the loading (Figure 20) and, thereafter, sectioned, polished, photographed for inspection and optical diffraction analysis, further polished, and photomicrographed. The results are shown in Figures 21-26.

The photographs (2.5X) of entire specimens removed at different stages of the loading show what the naked eye can observe on the sectioned rock: no visible fractures or other disturbances at zero stress (Figure 21a), very little noticeable change at 10 cycles (Figure 22a), clearly seen predominantly vertical cracks at 500 cycles (Figure 23a), much longer and more pronounced fractures at 3,000 cycles (Figure 24a), severely damaged section at 3,700 cycles just prior to failure (Figure 25a), and faulted rock after fatigue fracture (Figure 26).

The negatives of the described photographs were analyzed by optical diffraction analysis in the laboratories of the Department of Geological Sciences, University of Wisconsin, Milwaukee. The diffraction pattern is a two dimensional Fourier transform yielding information about orientation and frequency of diffracting elements. The higher the frequency of an element, the farther away from the center will its diffracted dot be. Figure 21b is the transform of an undeformed Tennessee marble specimen. Elements of low frequency are abundant. These elements represent the fabric of the

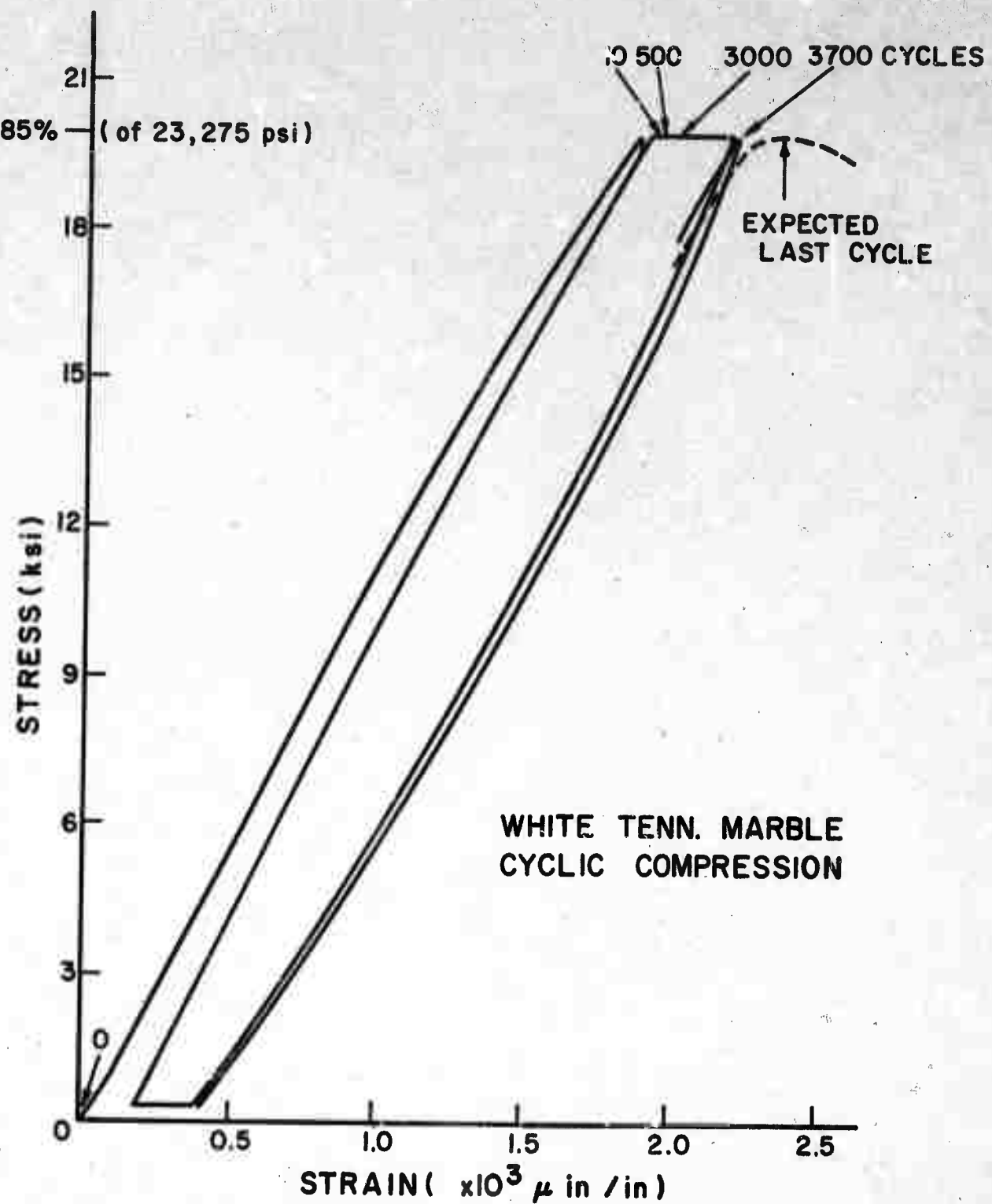


Figure 20. Typical stress-strain curve for cyclically loaded White Tennessee marble, (upper peak stress = 85%), showing the position of the specimens that were optically analyzed (Figures 21-26).

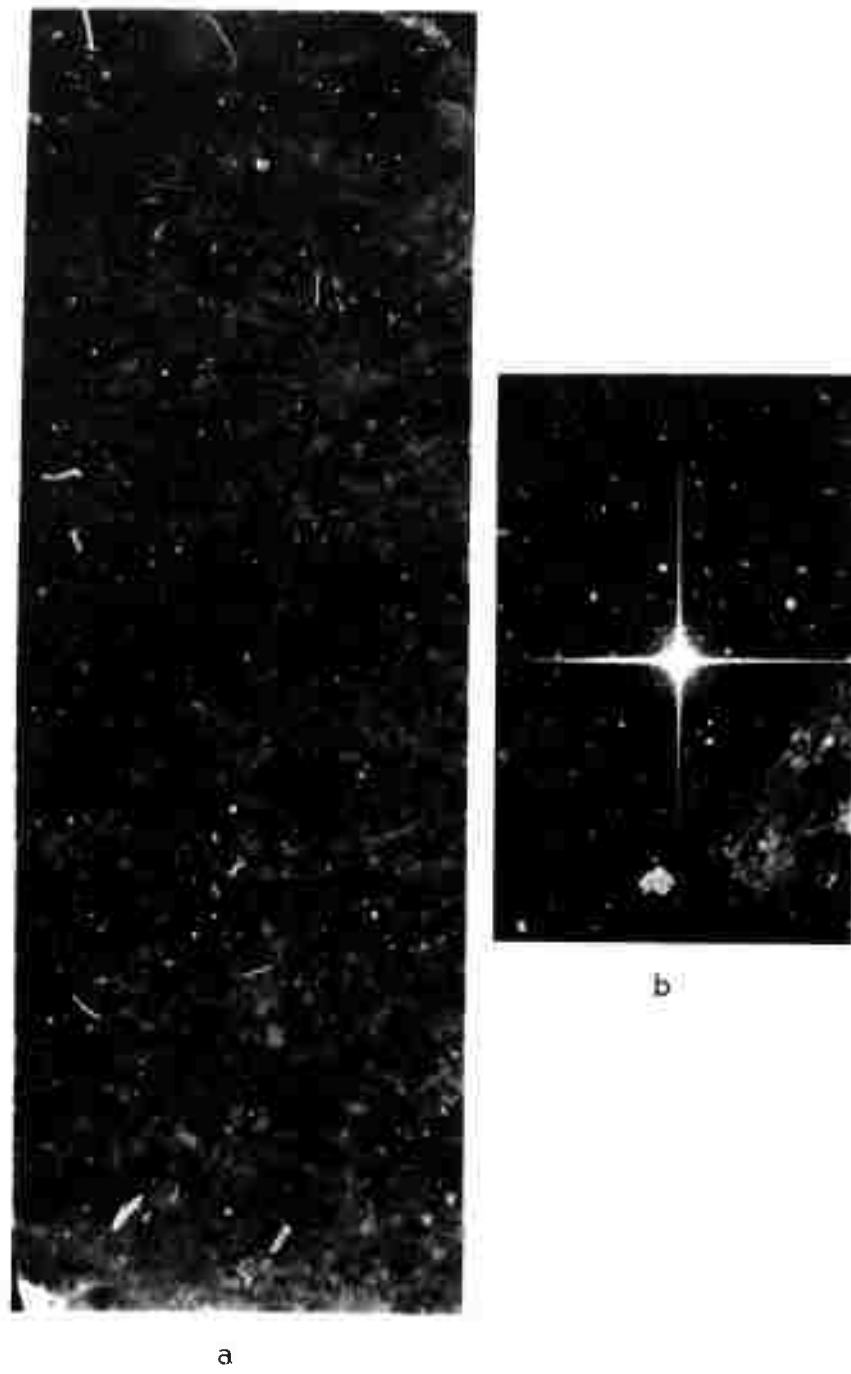


Figure 21 - White Tennessee marble - Optical analysis of a specimen prior to loading (See Figure 20).
a - Photograph of a vertical section (2.5 X)
b - Optical diffraction pattern of a.



Figure 21.

c
Reproduced from
best available copy.

c - Photomicrograph of a typical section in
a (40X)

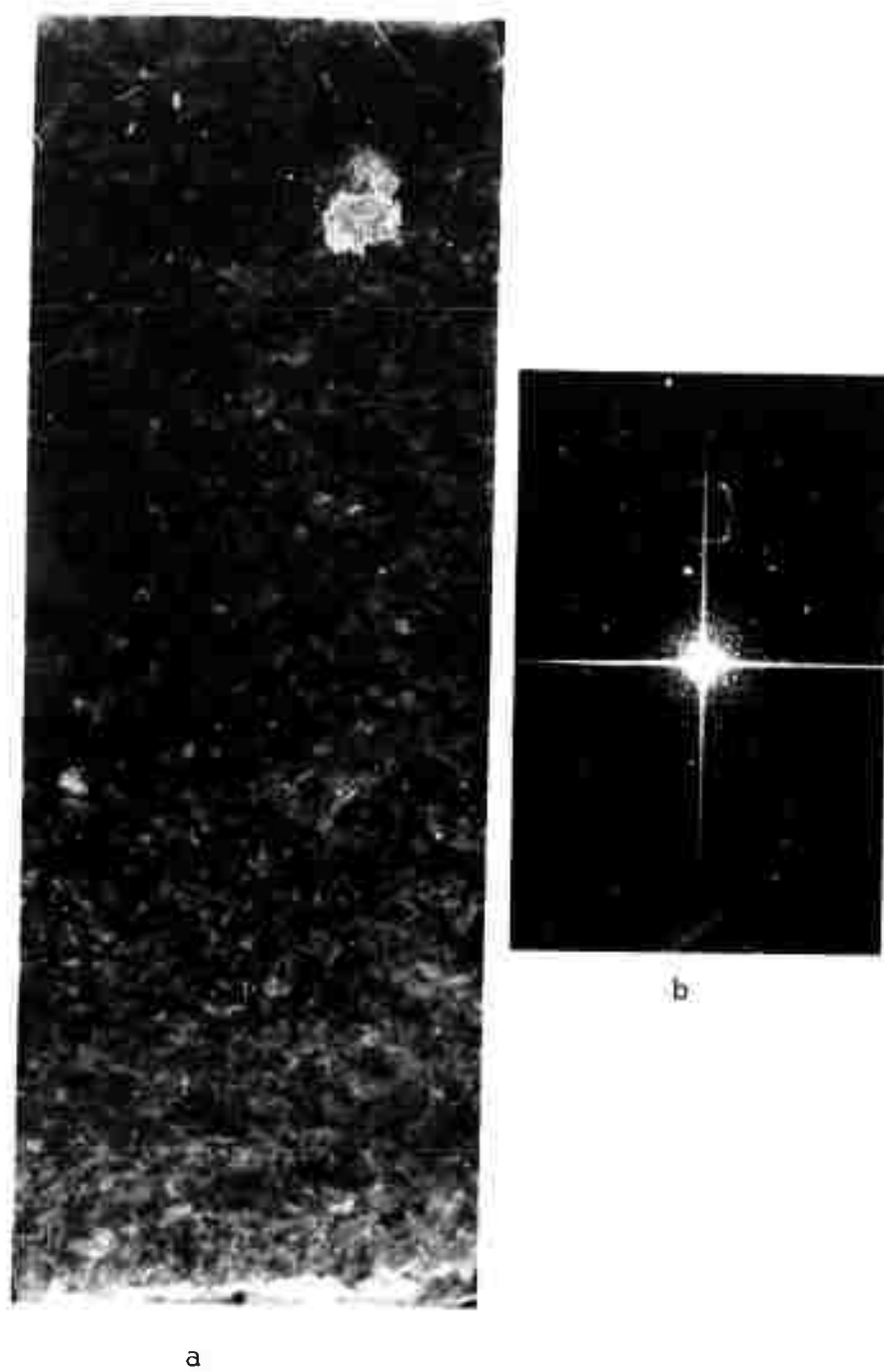


Figure 22 - White Tennessee marble - optical analysis
of a specimen after 10 cycles of loading
(See Figure 20)

a - Photograph of a vertical section (2.5 X)

b - Optical diffraction pattern of a.



c

Figure 22.

c - Photomicrograph of a typical section in
a (40 X).

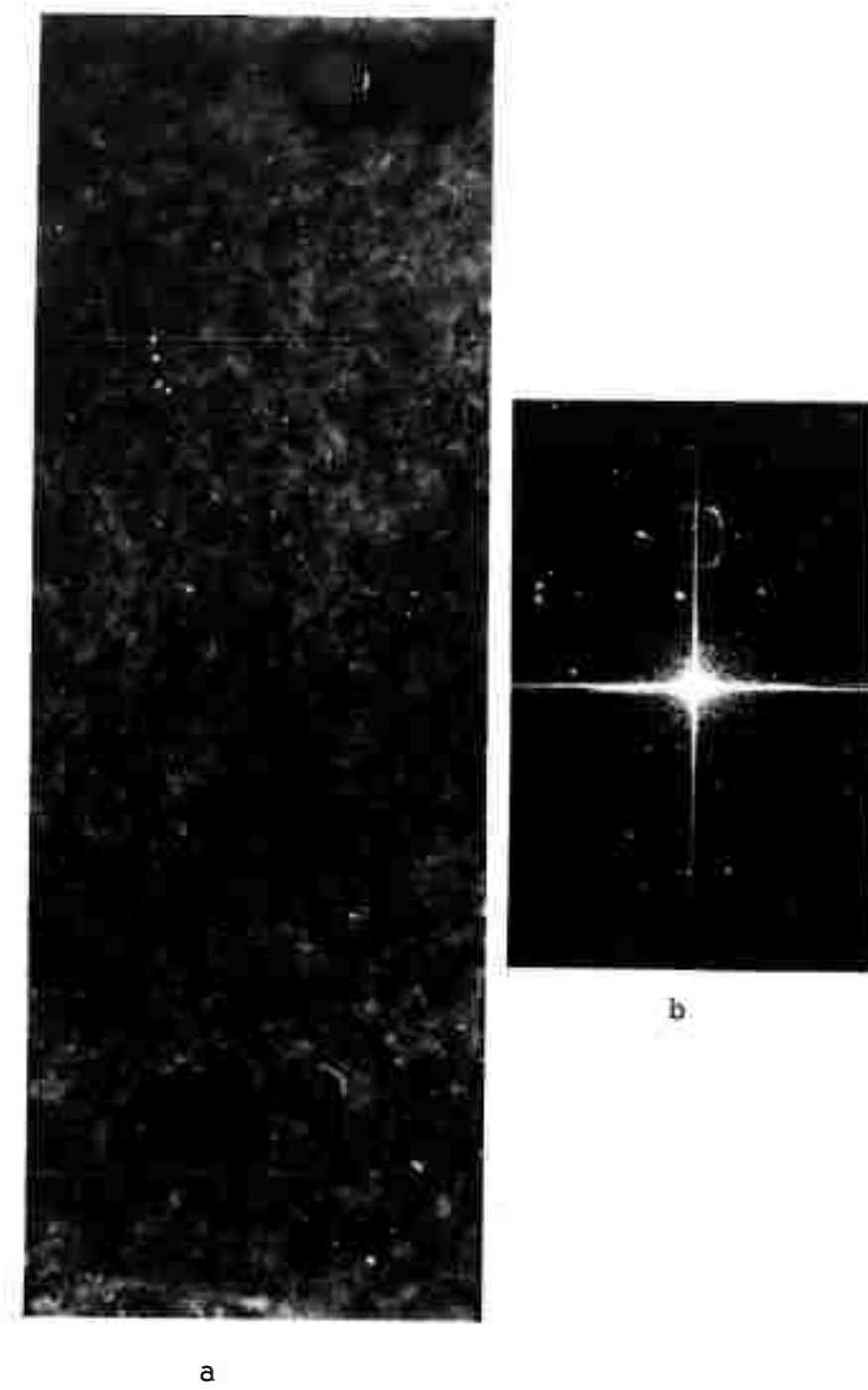
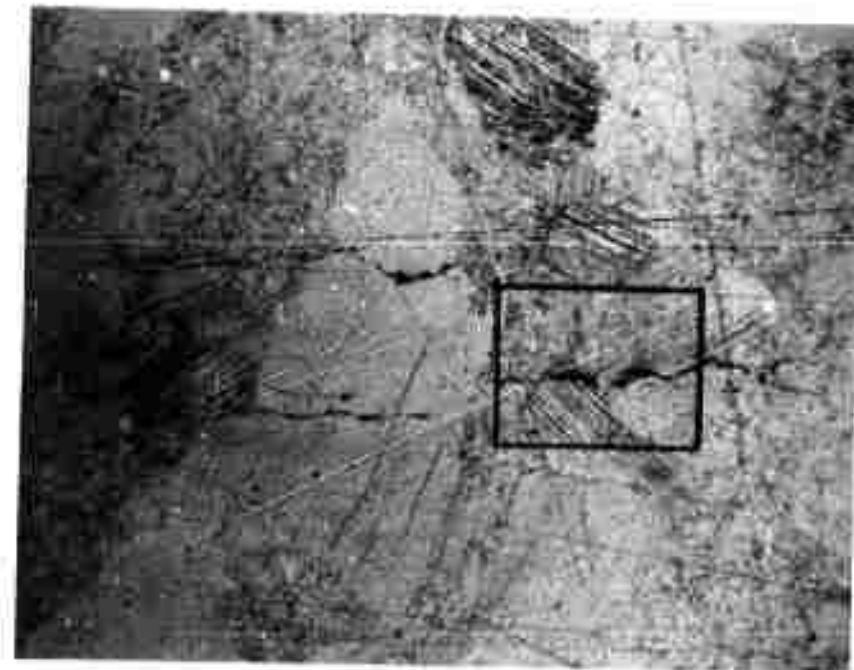


Figure 23 White Tennessee marble - Optical analysis of a specimen after 500 cycles of loading (See Figure 20).
a - Photograph of a vertical section (2.5 X)
b - Optical diffraction pattern of a.



d

Reproduced from
best available copy.



c

Figure 23.

c - Photomicrograph of a typical section in $\underline{\alpha}$ (40 X)d - Photomicrograph of a section of interest in $\underline{\alpha}$ (160 X)

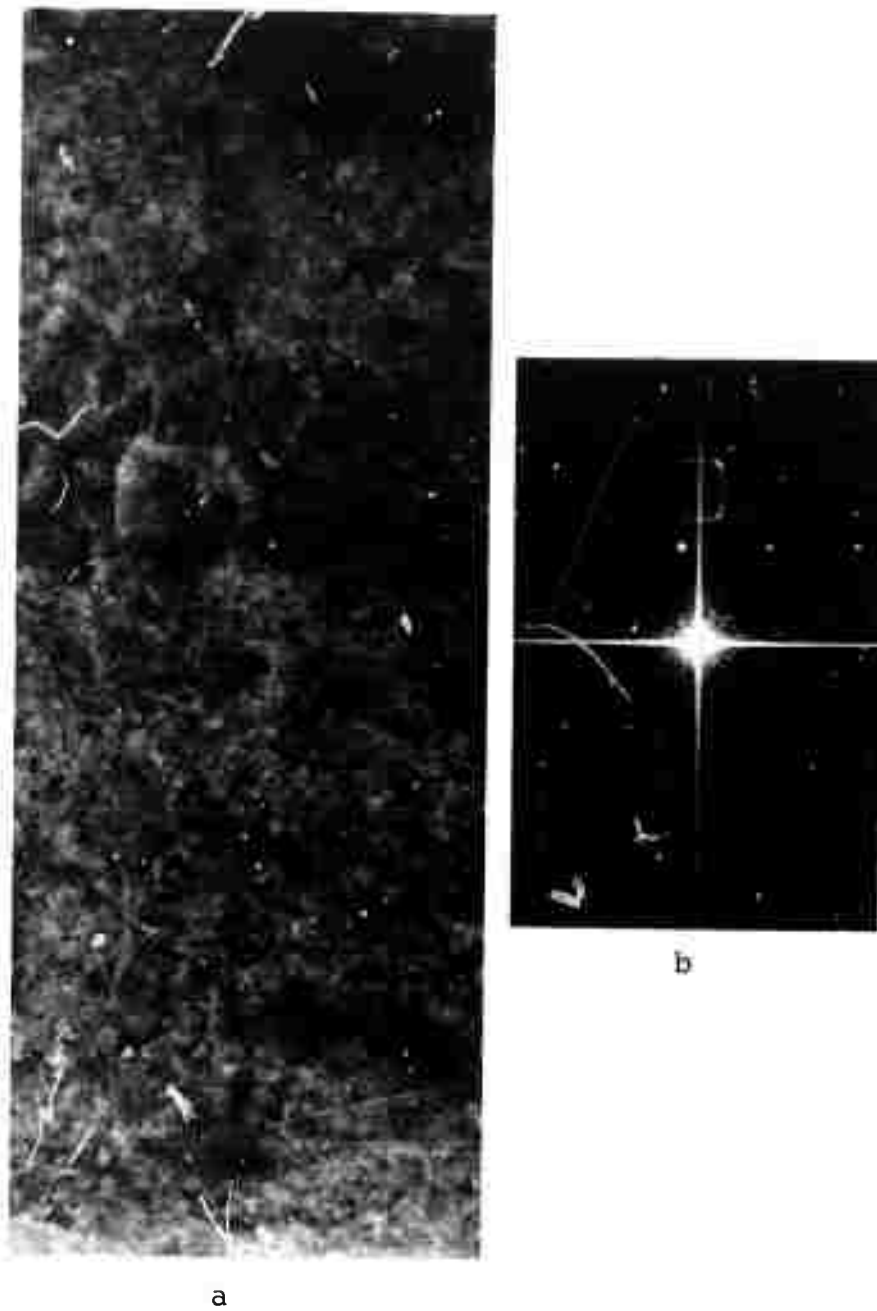
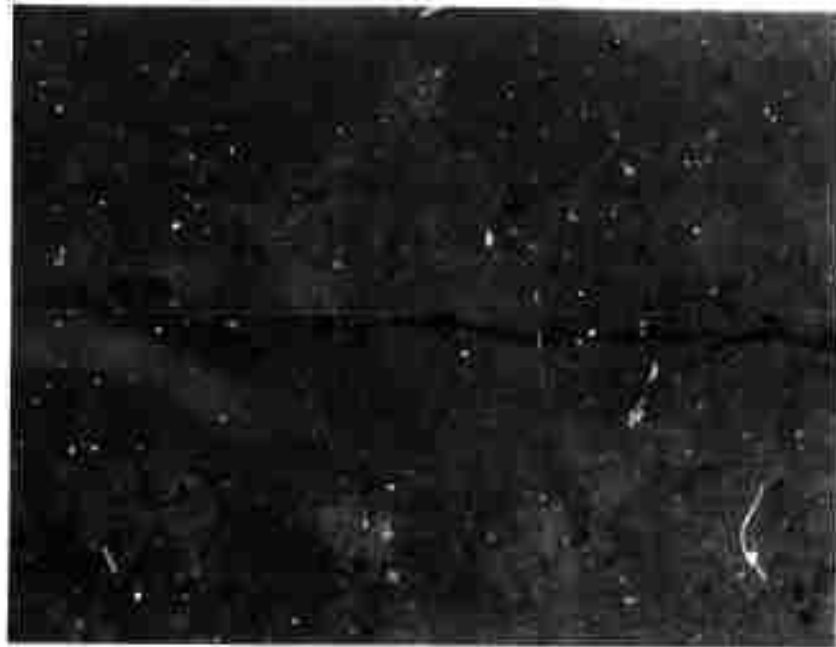


Figure 24. White Tennessee marble - optical analysis of a specimen after 3,000 cycles of loading (See Figure 20).
a - Photograph of a vertical section (2.5 X)
b - Optical diffraction pattern of a.



d

Reproduced from
best available copy.



c

Figure 24.

c - Photomicrograph of a typical section in a (40 X)d - Photomicrograph of a section of interest in c (400 X).



a



b

Figure 25 - White Tennessee marble - optical analysis of a specimen after 3,700 cycles of loading (See Figure 20).
a - Photograph of a vertical section (2.5 X)
b - Optical diffraction pattern of a.



c

Figure 25.

c - Photomicrograph of a section of interest in
a (40 X)



Reproduced from
best available copy. 

Figure 26. Photograph of a White Tennessee marble specimen (2.5 X), fatigued in cyclic loading (See Figure 20).

rock. An increase in the high frequency content of the transform is noted in the same rock after 10 cycles of compressive loading (Figure 22b). The increase continues as the number of cycles reaches 500 (Figure 23c). This is probably due to the development and growth of cracks in the specimen. At 3000 cycles the high frequency content appears reduced (Figure 24c), and can be attributed to the widening of the cracks. In the very last cycles prior to failure the high frequency content is again increased, suggesting new fractures.

A typical view of an undeformed section at a magnification of 40X is presented in Figure 21c. The grains appear well cemented to each other with no visible discontinuity of any kind. Ten loading cycles later (Figure 22c), the grain boundaries became more distinct. It appears that the cyclic stresses have caused definite damage to the cementing material, and slip might have occurred between grains. These grain boundary discontinuities are probably the initial microcracks. At 500 cycles (Figure 23c, d) nearly vertical cracks appear to have traversed grains and initial coalescence is indicated. At 3,000 cycles (Figure 24c, d) intragranular cracks reach considerable length and the process of coalescence continues. Finally, at the last cycle before failure (Figure 25c) the process of coalescence accelerates and vertical fractures considerably increase in width, signalling imminent failure. It should be noted that all the photomicrographs were taken from areas near the central part of the sections.

Indiana limestone

An identical optical analysis to that described above was carried out in Indiana limestone, except that the specimens tested were loaded to an upper peak cyclic load of 75% of the compressive strength. The results obtained were rather disappointing since changes observed due to fatigue were minimal.

Figures 27a, 28a, 29a are photographs of limestone sections in virgin condition, during the steady-state stage, and in one of the last cycles before failure, respectively. No visible difference can be observed between the sections. The reason can be at least partially found by studying the photomicrographs. As seen in Figure 27c the rock is highly porous and solid intact rock does not extend too far in a plane. Hence, when micro-fractures occur they have no long way to extend before reaching a neighboring void (Figures 28c, d). Thus, no extensive fracturing is necessary to bring about coalescence as this process is basically accomplished by the pores with the help of interconnecting cracks. Figures 29c, d for the last stage of the cyclic loading is almost identical to Figures 28c, d.

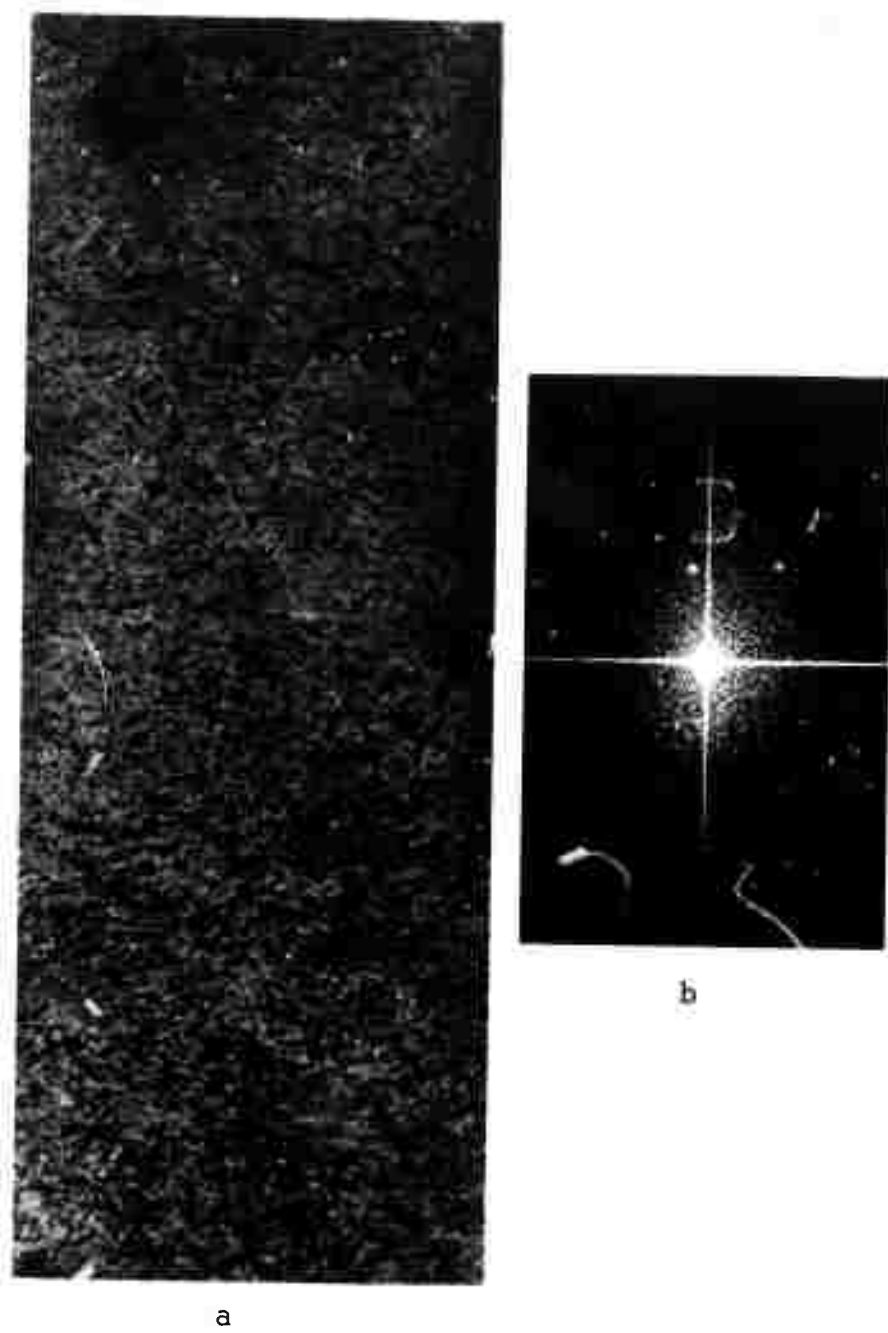


Figure 27. Optical analysis of a previously unloaded specimen of Indiana limestone.

a - Photograph of a vertical section (2.5 X).

b - Optical diffraction pattern of a.



C

Figure 27.

C -- Photomicrograph of a typical section in
a.

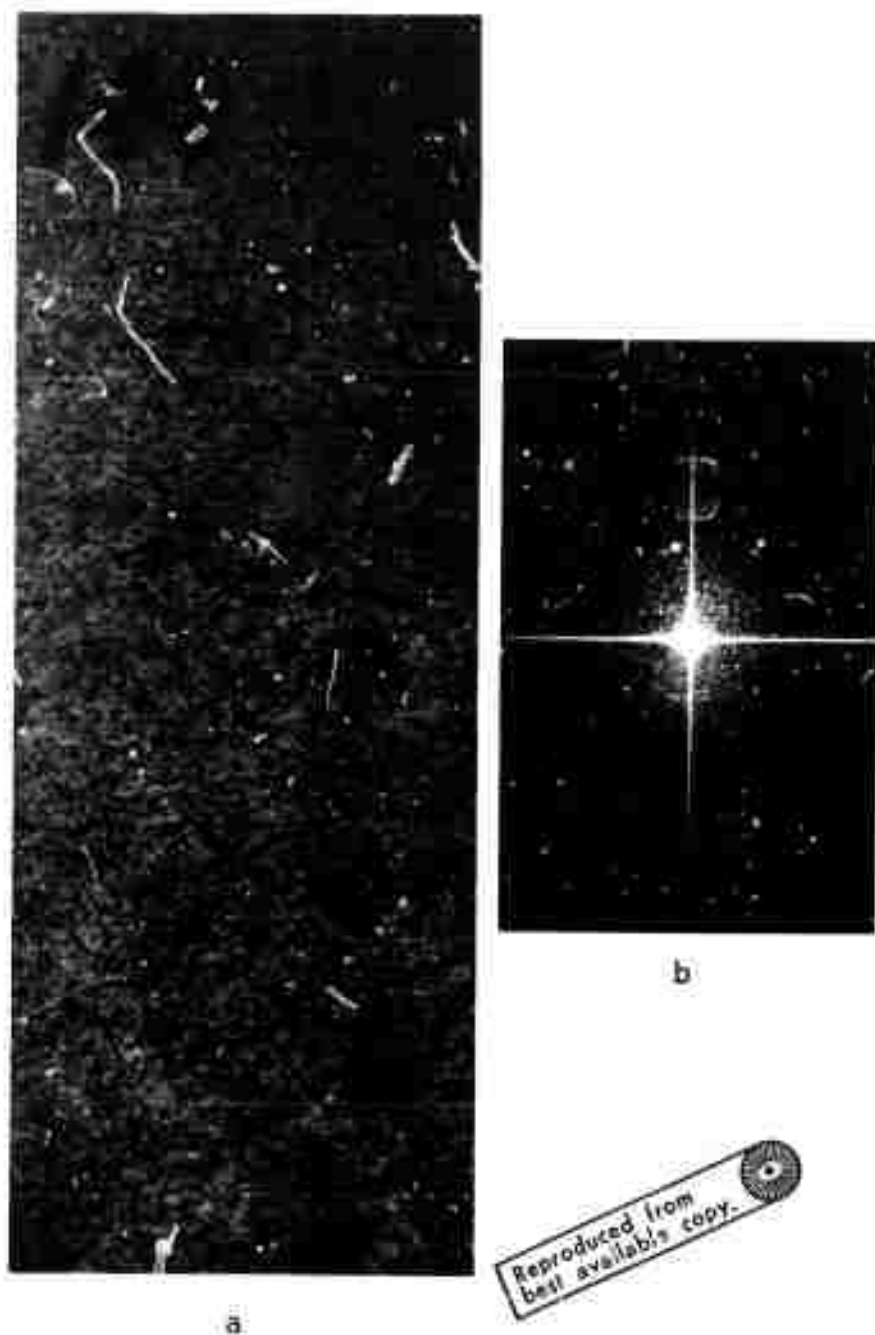
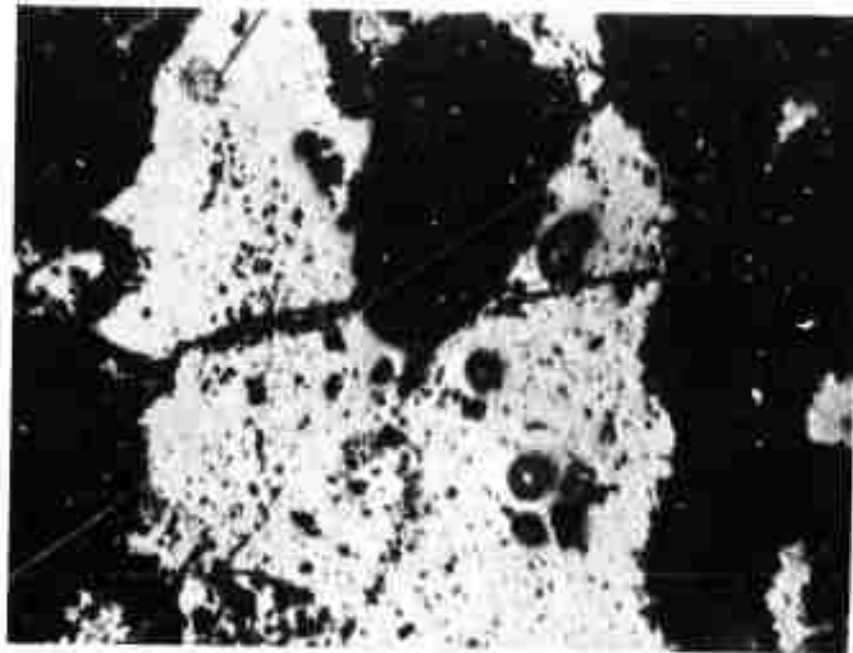


Figure 28. Indiana limestone - Optical analysis of a specimen after being cyclically loaded to well within the steady state stage (upper peak stress = 75%).

a - Photograph of a vertical section (2.5 X)

b - Optical diffraction pattern of a.

d



c

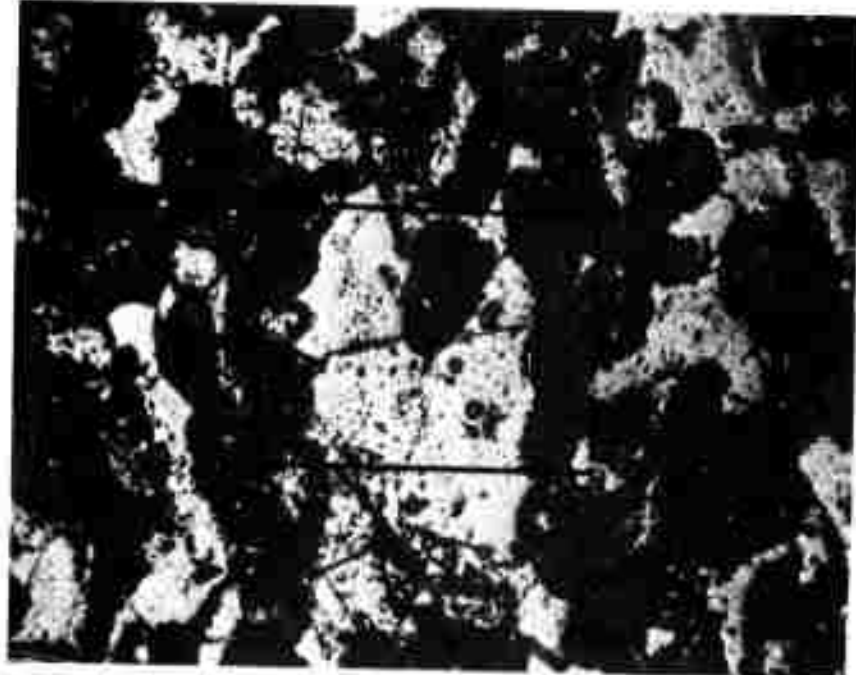


Figure 28.

c - Photomicrograph of a typical section in a (40 X)d - Photomicrograph of a section of interest in c (100 X)

Reproduced from
best available copy.

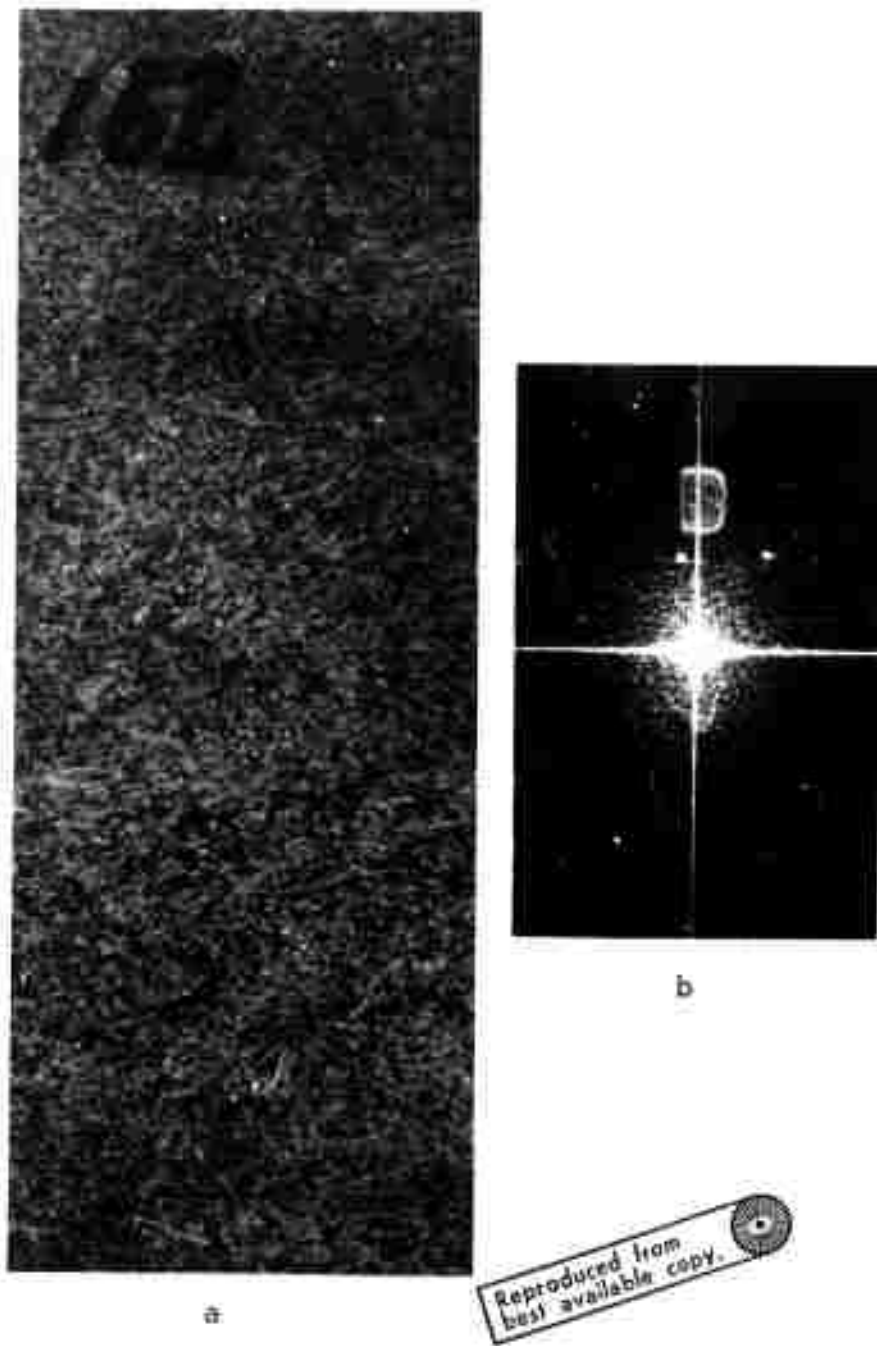


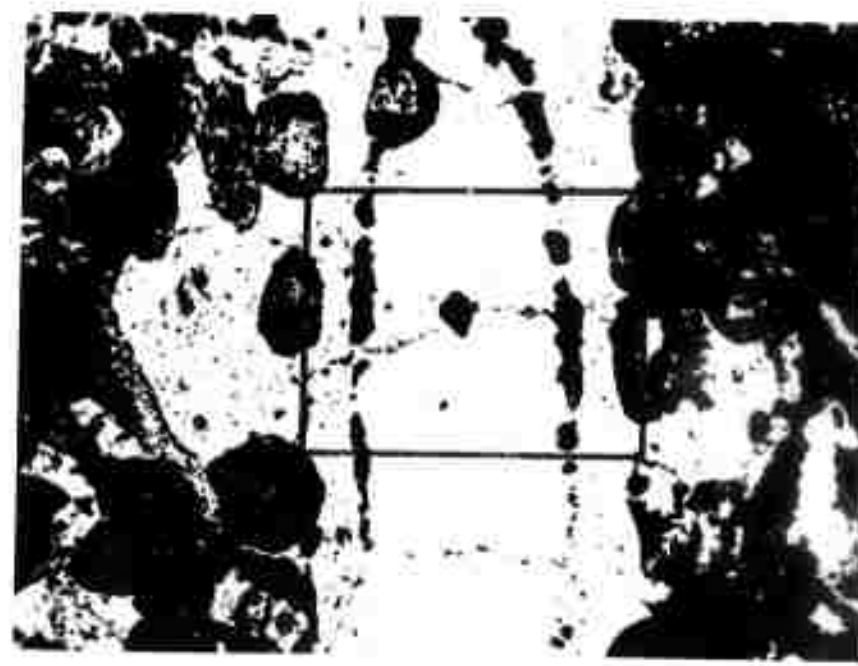
Figure 29. Indiana limestone - Optical analysis of a specimen after being cyclically loaded to the accelerated tertiary stage, just before failure (upper peak stress = 75%).

a - Photograph of a vertical section (2.5 X).

b - Optical diffraction pattern of a.



d



c

Figure 29.

c - Photomicrograph of a typical section in α (40 X)d - Photomicrograph of a section of interest in γ (100 X).



Figure 30 - Photograph of a fatigued Indiana limestone specimen.

These results seem to fit well with the reduced amount of acoustic emission observed in Indiana limestone as compared to White Tennessee marble.

Figure 30 shows a vertical section of a fatigue failed specimen of Indiana limestone. The general appearance of the faulting is quite similar to that in the marble.

The optical diffraction analysis of Indiana limestone shows similar trends to Tennessee marble as far as microcracking during the test but reveals the difference in the fabric between the two rocks. The undeformed specimen transform shown in Figure 27b has a greater high frequency content than the one for Tennessee marble (Figure 21b) due to the finer grained nature of the limestone and possibly the closer spacing of other fabric elements. The specimen taken well within the steady-state stage shows a decrease in high frequency content (Figure 28b), attributed to widening of the cracks at that phase of the cyclic loading. Finally, the specimen removed just before cyclic failure (Figure 29b) reveals a considerable high frequency content increase, probably due to the formation of new fractures.

b. Stress-Controlled Tests with Constant Mean Stress

The results described so far were all obtained in stress-controlled cyclic loading with a constant lower peak stress. In order to determine the effect of the lower peak stress on fatigue, a series of tests were run in White Tennessee marble in which the mean stress between the upper and lower peaks was kept constant throughout at 50% of the compressive strength. The results are presented in the form of an S-N curve in Figure 31. Comparison with Figure 7 reveals that for very high stress amplitudes there is negligible difference between constant mean-stress tests and constant lower peak stress tests. However, when the upper peak stress drops to 85% and below, the life of the specimen under constant mean-stress is prolonged almost 10 fold relative to that of constant lower-peak stress specimens. Thus, by lifting the lower peak of the loading cycle the resistance of the marble to fatigue is greatly improved. It is surprising in the least, to find that a seemingly insignificant variation of the test can bring such different results. These findings open the door to speculation regarding what would be the consequences of extending the lower peak load to the zero value and, beyond it, into tension. Such testing is planned for the forthcoming year.

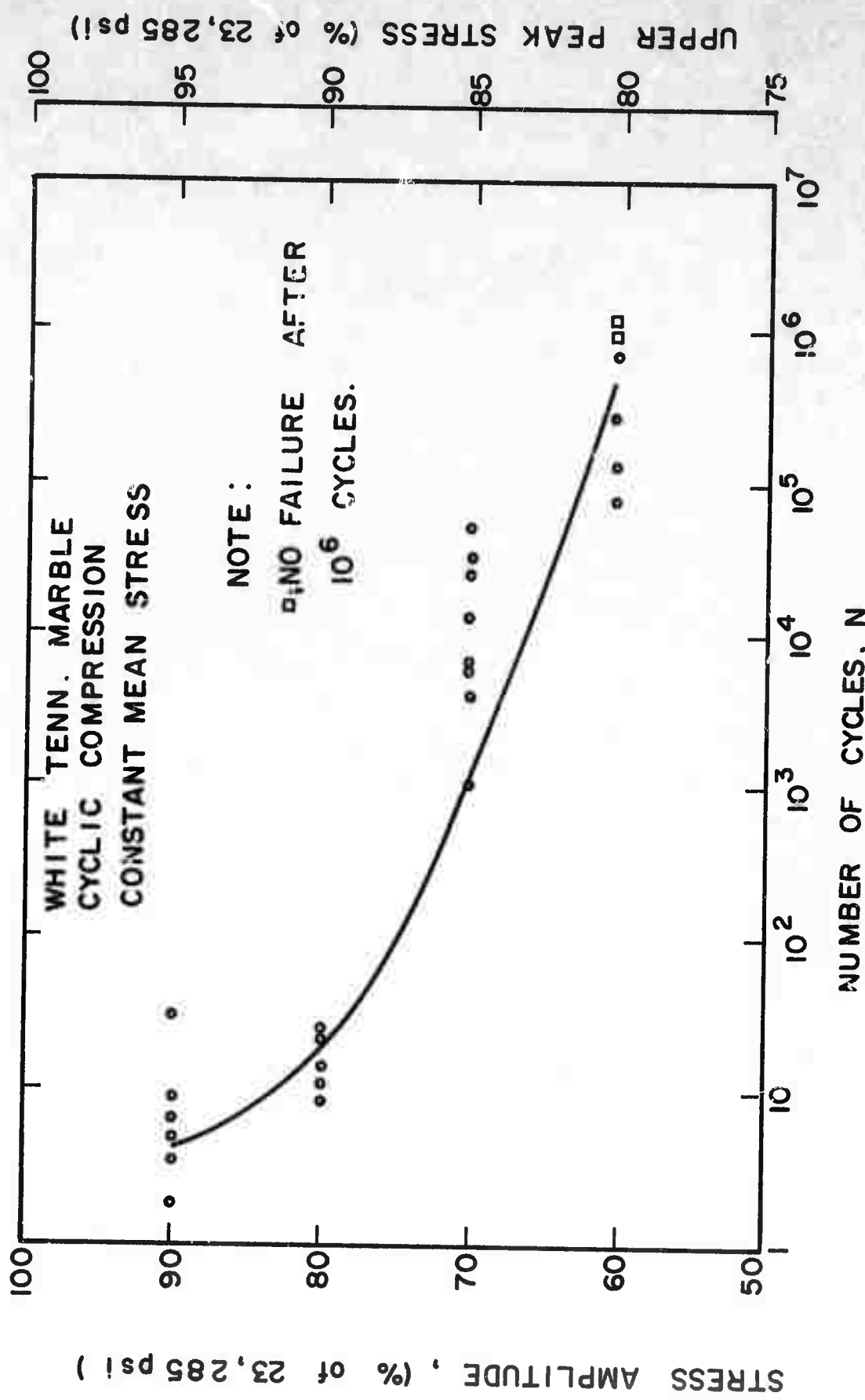


Figure 31. S-N curve for White Tennessee marble subjected to cyclic compression under constant mean stress (= 50% of compressive strength).

c. Strain-Controlled Tests with Constant Lower Peak Strain

A series of cyclic tests were run in both rocks under strain control (at 1 cps). The lower peak strain was kept constant and the upper peak strain was varied from test to test. No ϵ -N curves were obtained as these tests were only run to observe trends in rock behavior.

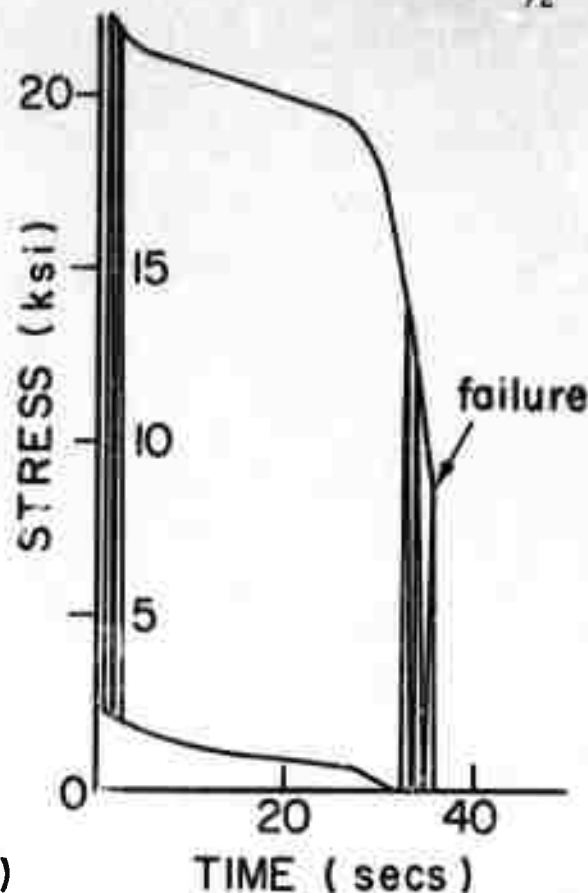
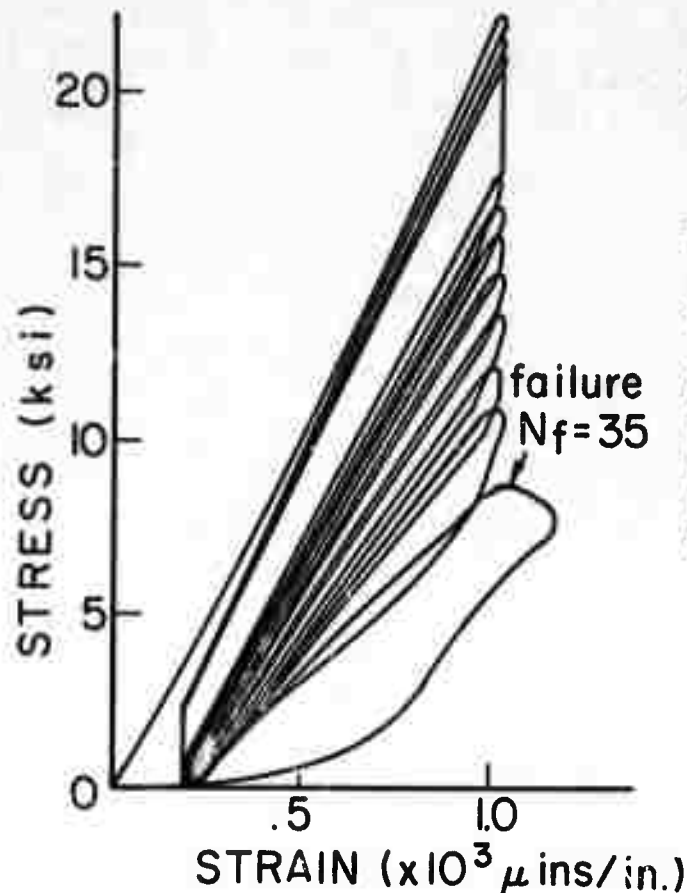
Two basically different reactions to cyclic strain loading were noticed. White Tennessee marble in most cases behaved as depicted in Figure 32. The stress-strain curve for the first cycle had a large hysteresis loop. It was followed by cycles of ever decreasing loops and peak stress relaxation, followed by a large number of cycles of no change except for continuous peak stress drop, and culminated by a sudden increase in hysteresis which accelerated from cycle to cycle until failure. In the particular case of Figure 32 the peak stress dropped at failure from 21,500 psi in the first cycle to 8,500 psi in the 35th and last cycle.

The stress-time behavior (Figure 32) showed a primary stage of decelerating peak stresses, a straight-line steady state stage for the bulk of the cycles, and a very sharp acceleration in the peak stress relaxation ending in failure. The acoustic emission counts revealed a continuous microcracking mechanism accelerated towards failure.

The behavior of Indiana limestone was different in that, instead of brittle fatigue, one observed a stress relaxation curve tending asymptotically to a constant value (Figure 6). Indeed specimens of limestone never broke in these tests and had to be removed from the loading machine because of experimental limitations when the lower peak cyclic stress reached zero.

d. Cyclic Loading of Failed Rock

The "discovery" of the complete stress-strain curve in recent years has changed the meaning of rock strength. The classical approach had been that rock subjected to loads equal or larger than its compressive strength would collapse violently and its load carrying ability eliminated. It has been demonstrated, however, (20) that under some conditions (like stiff machine loading, or strain-controlled loading) rock is capable of supporting substantial stresses even after it has reached its compressive strength. Such "failed" but active rock can be encountered in underground excavations, in pillars, sidewalls, etc. It was thus decided to test the ability of failed rock to support cyclic loading.



WHITE TENN. MARBLE
CYCLIC COMPRESSION

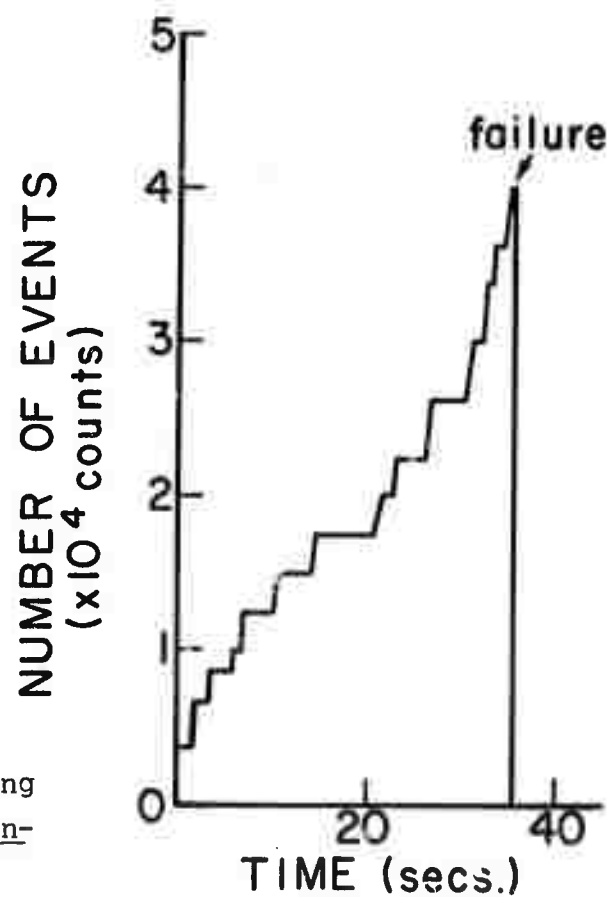


Figure 32. Typical recordings during cyclic compression under strain-control.

To begin with, a series of experiments were run in White Tennessee marble that had first been loaded in strain-control to its compressive stress carrying capacity limit (referred to as the compressive strength). A typical complete stress-strain curve obtained in this fashion is shown on top of Figure 33. As noted in the other four plots of Figure 33, specimens were loaded in strain-control to their compressive strength, unloaded, and then cyclically loaded in stress control keeping the lower peak stress constant throughout the testing. Figure 34 gives the S-N curve for the failed rock. Surprisingly it remained quite strong and although it weakened somewhat with respect to the intact rock (Figure 7), it could definitely perform useful work. Note that at loads reaching 67% of its compressive strength the rock could not be fatigued in 10^6 cycles!

Going back to Figure 33, note that the cyclic creep undergone by the upper peak stress was limited by the descending portion of the complete stress-strain curve. This point was raised earlier for intact rock (Figures 10 and 11).

An additional series of tests was contemplated well within the failed region characterized by the descending part of the complete stress-strain curve. Due to the very steep descending stress-strain curve in White Tennessee marble as obtained at any of the strain rates available with the existing equipment, a different rock, namely Cherokee Georgia marble, was chosen for these tests. As seen in Figure 35 the slope of the failed portion of the curve is very mild for the latter rock (strain rate of $10^{-6}/\text{sec}$). This enabled one not only to obtain repeatable complete stress-strain curves, but also to stop the loading at any point in the failed zone and unload without the danger of specimen collapse. Georgia marble specimens were loaded in strain control to their compressive strength and beyond to 70% of the load carrying capacity within the failed zone. They were then unloaded, and cyclically loaded in stress control to upper peak values of different magnitudes. The results are shown in Figure 35. A preliminary S-N curve based on these tests is shown in Figure 36. Again, one is surprised to note that failed rock can still show remarkable strength as far as cyclic loading carrying capacity. It is emphasized again, however, that for the same peak loads in the unfailed mode the number of cycles would be appreciably larger. Moreover, it is clear that in both Tennessee and Georgia rocks the fatigue limit is lowered in failed rock. It can be noted again from Figure 35 that the upper peak of the last cycle falls again in the close proximity of the expected descending complete stress-strain curve. The behavior of failed rock under cyclic loading is of particular

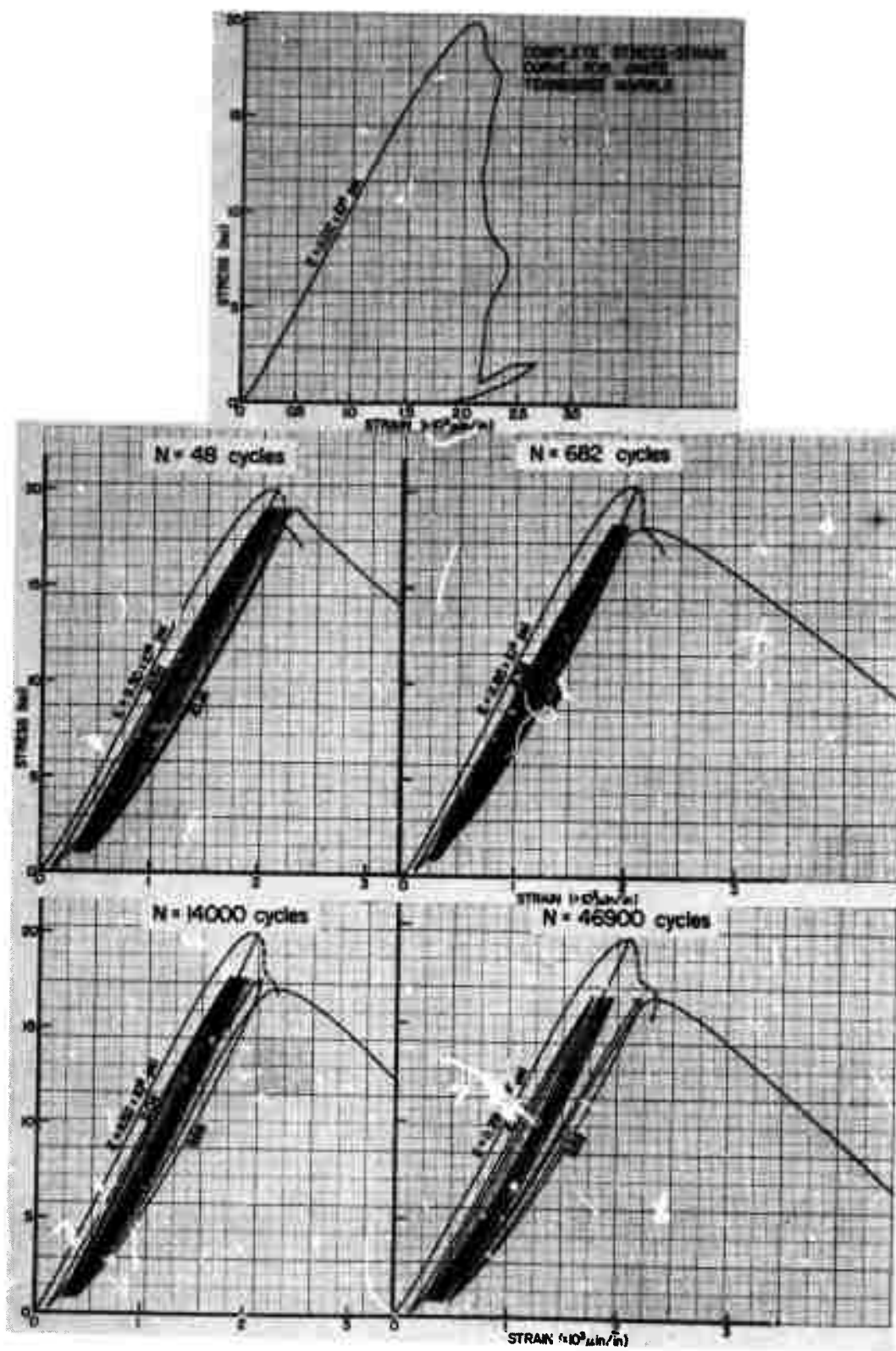


Figure 33 - Stress-strain curves for failed White Tennessee marble under cyclic loading (Broker line depicts the expected descending complete stress-strain curve).

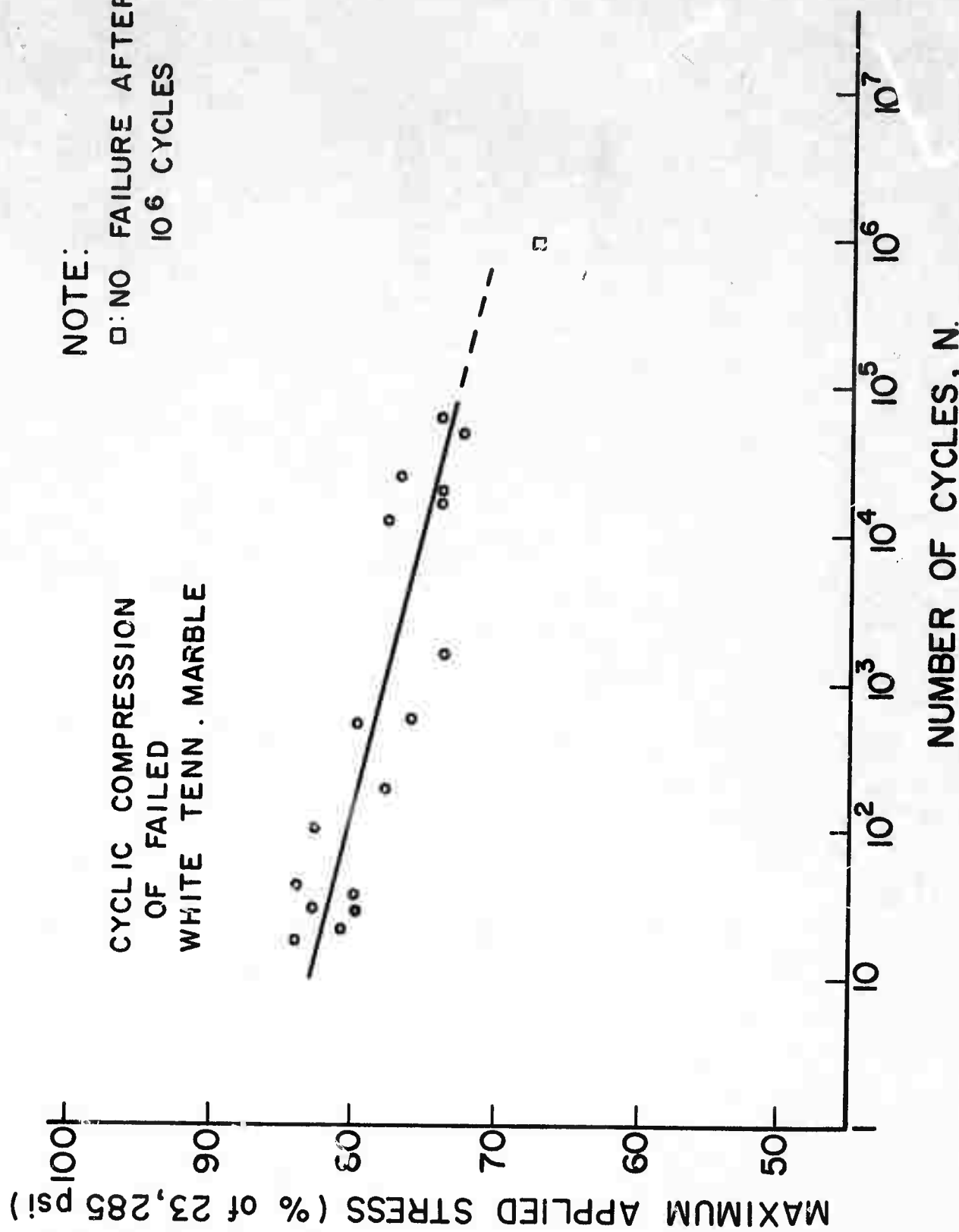


Figure 34. S-N curve for failed White Tennessee marble under stress-controlled cyclic compression.

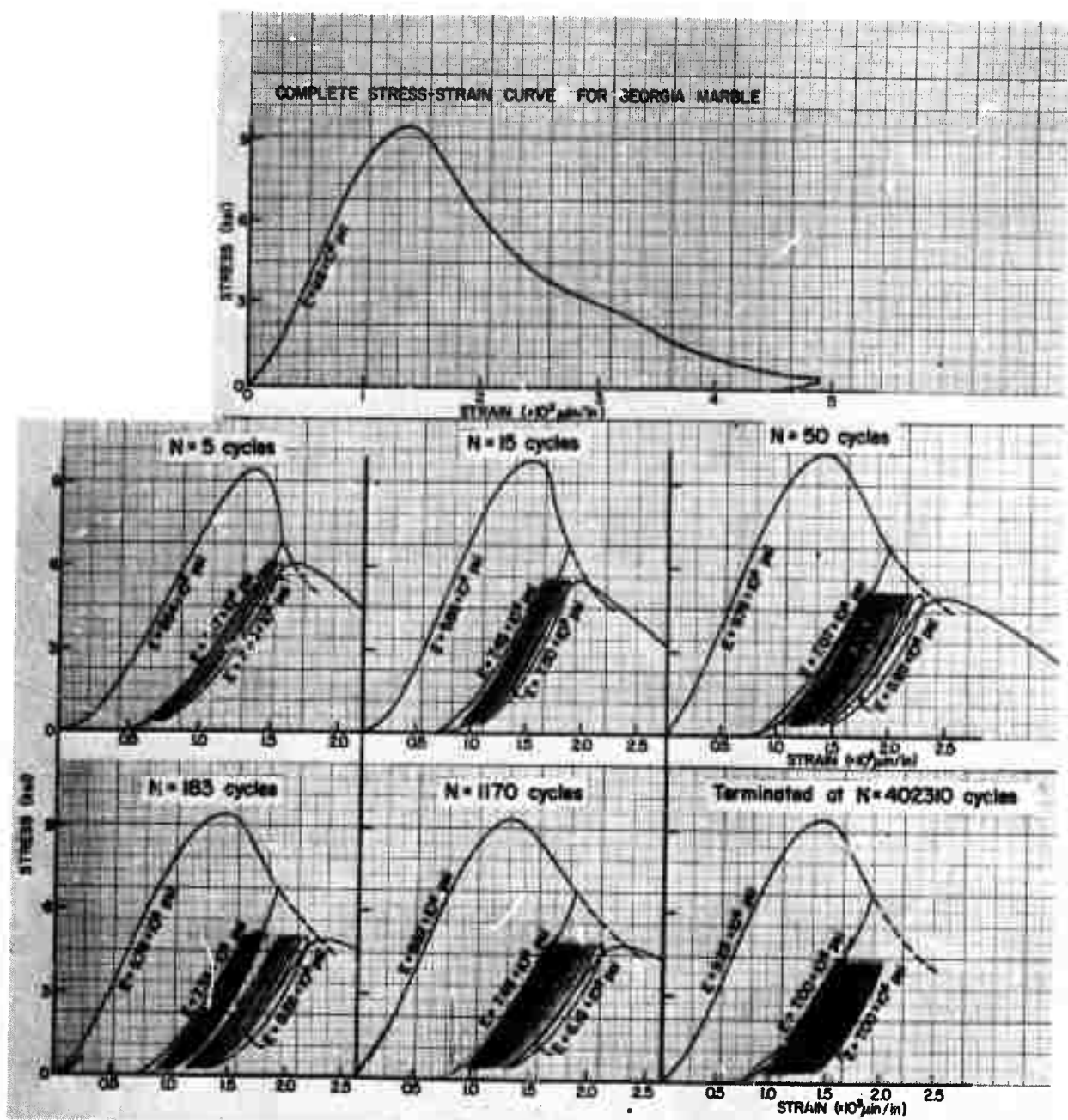


Figure 35 - Stress-strain curves for failed Cherokee Georgia marble under cyclic loading (Broken line depicts expected continuation of complete stress-strain curve).

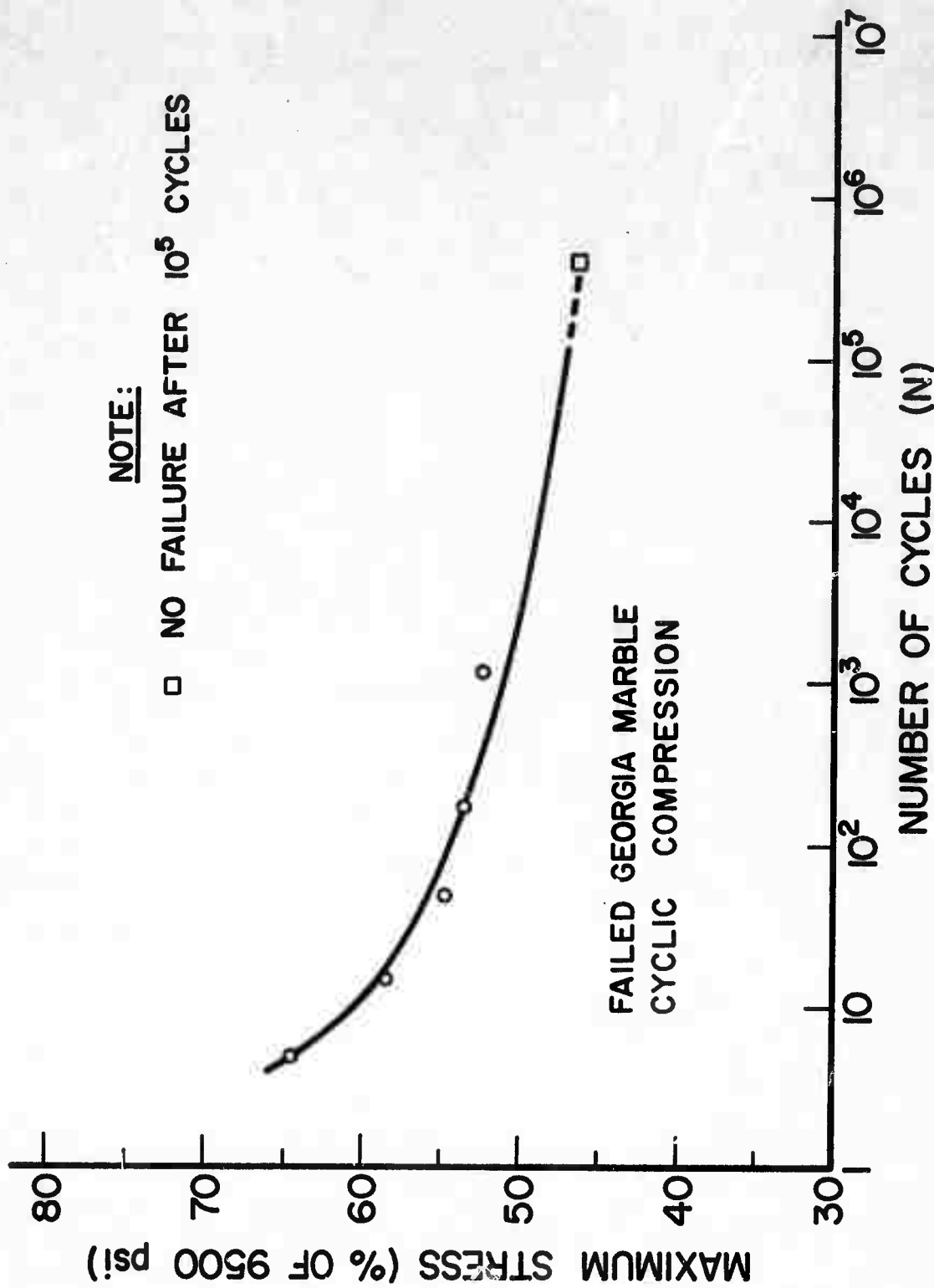


Figure 36. S-N curve for failed Cherokee Georgia marble under stress-controlled cyclic compression.

importance to the understanding of the reaction of failed underground pillars and walls subjected to fatigue type stresses. Because failed rock is internally fractured, the study may also be indicative of the behavior of jointed benches or slopes and faulted formations subjected to earthquake, blasting, or traffic loads.

B - TENSION

Monotonic Loading

It is a well known fact that tensile strength of rock is affected by the rate of loading. It was therefore imperative to determine the tensile strength for the rate of loading used during cycling. Table 4 gives the values obtained in both the indirect (Brazilian) and the direct tests. As expected the standard deviation in these tests was much higher percentage wise than in the compressive strength case (Table 1) since tensile strength is a more erratic property of rock.

Cyclic Loading

All cyclic tension tests were run in stress-control with a constant lower peak stress.

Quantitative results of the Brazilian indirect tests are given in Figures 37 and 38 in the form of suggested S-N curves for White and Pink Tennessee marble, respectively. As can be clearly noticed the scatter of experimental points is rather large, an expected characteristic of tension testing. The trends, however, in both rocks are very convincing: the tensile strength is weakened with repeated loading.

The cyclic uniaxial tension tests in Pink Tennessee marble yielded an S-N curve as shown in Figure 39. It is interesting to note from Figures 38 and 39 that the slopes of the suggested S-N curves for Pink Tennessee marble are almost identical and, hence, apparently independent of the type of tension loading. The major difference is in the values of the largest maximum peak stress applied (1700 psi in uniaxial tension, 1400 psi in Brazilian tests).

It should be emphasized that the scatter in experimental results of the uniaxial tension tests could not be attributed to the loading apparatus, but to the actual inconsistent rock behavior in tension. Evidence to that is the great majority of the specimens ruptured in tension in a plane normal to the applied load and away from the specimen ends (Figure 40). Common to all S-N curves obtained was the tendency of both rocks to be fatigue affected at lower relative levels of stress (taken as percentage of tensile strength) than in compression cyclic loading. These levels are not exactly comparable at this stage since tension tests were run only to a maximum of 150,000 cycles.

TABLE 4
TENSILE STRENGTHS AT DIFFERENT LOADING RATES OBTAINED BY TWO TESTING METHODS

Rock	Testing Method	Loading Rate (psi/sec)	Equivalent Cyclic Frequency (cps)	Specimen Tested	Mean Tensile Strength (psi)	Standard Deviation psi	Standard Deviation %
White Tennessee Marble	Brazilian	100	"static"	6	1350	88	6.5
	" "	3,000	1	5	1520	94	6.2
Pink Tennessee Marble	" "	100	"static"	5	1250	89	7.1
	" "	3,000	1	6	1410	188	13.3
" "	" "	100	"static"	7	1400	121	8.7
	" "	3,000	1	14	1700	232	13.6

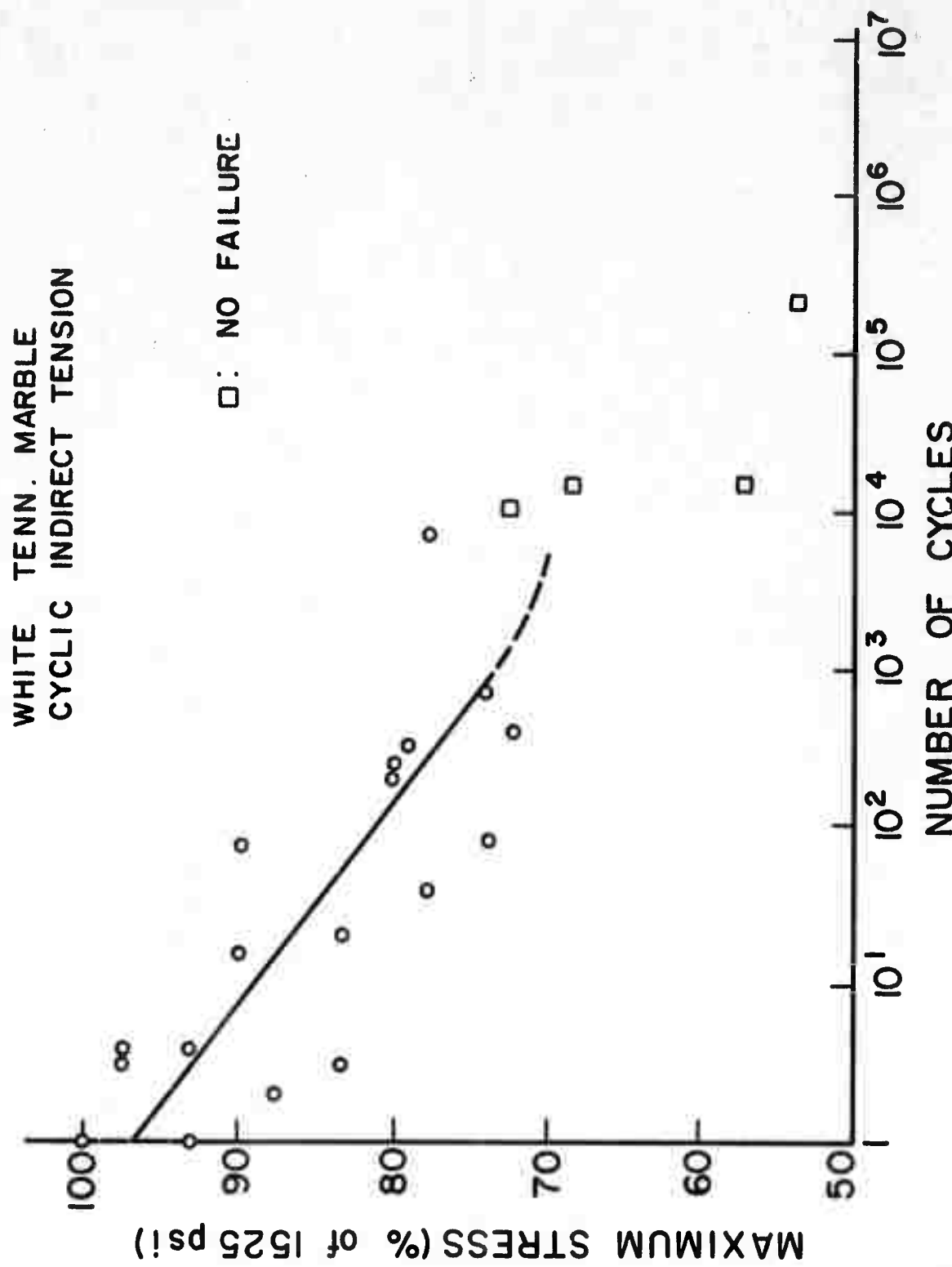


Figure 37. S-N curve for White Tennessee marble under Brazilian cyclic loading.

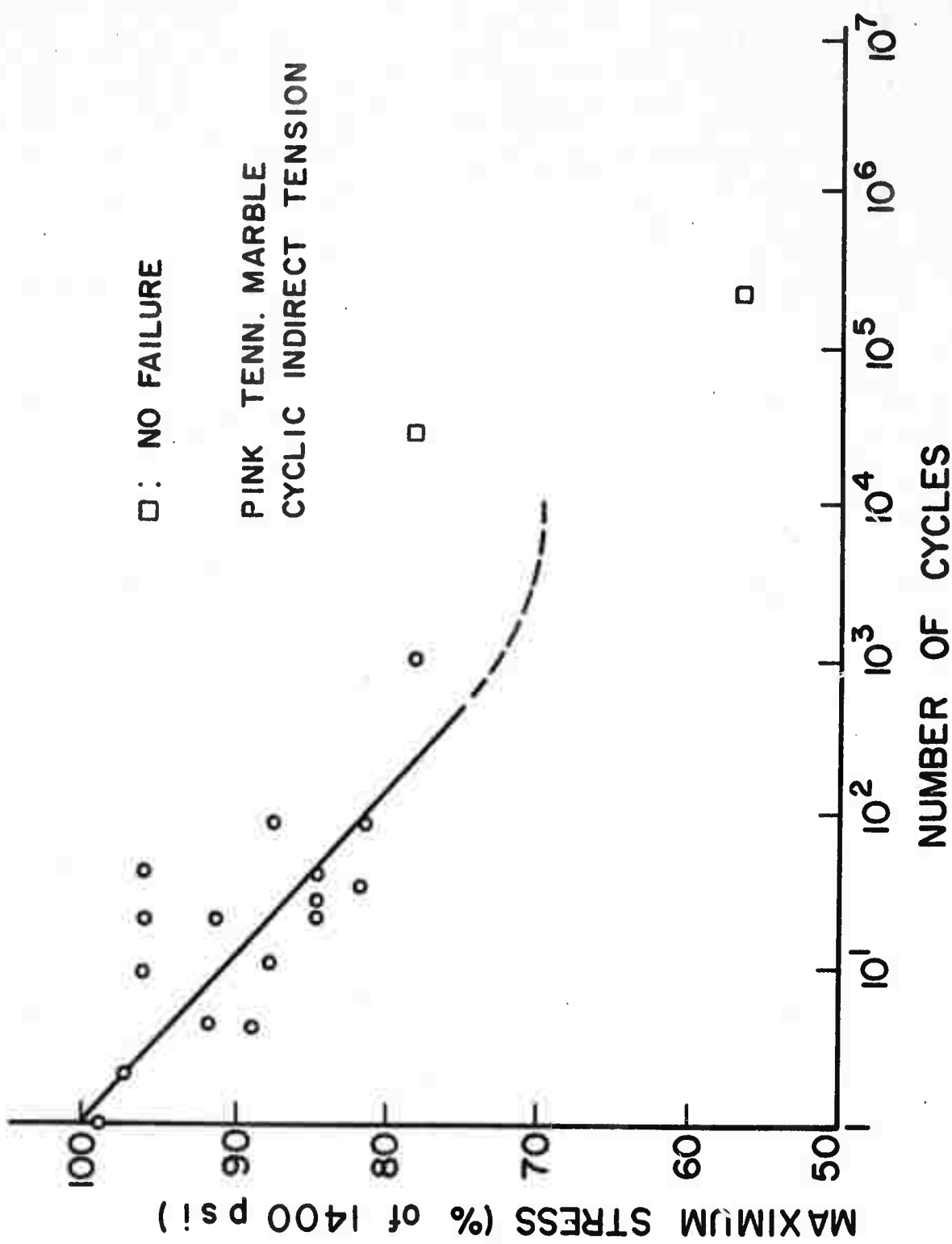


Figure 38. S-N curve for Pink Tennessee marble under Brazilian cyclic loading.

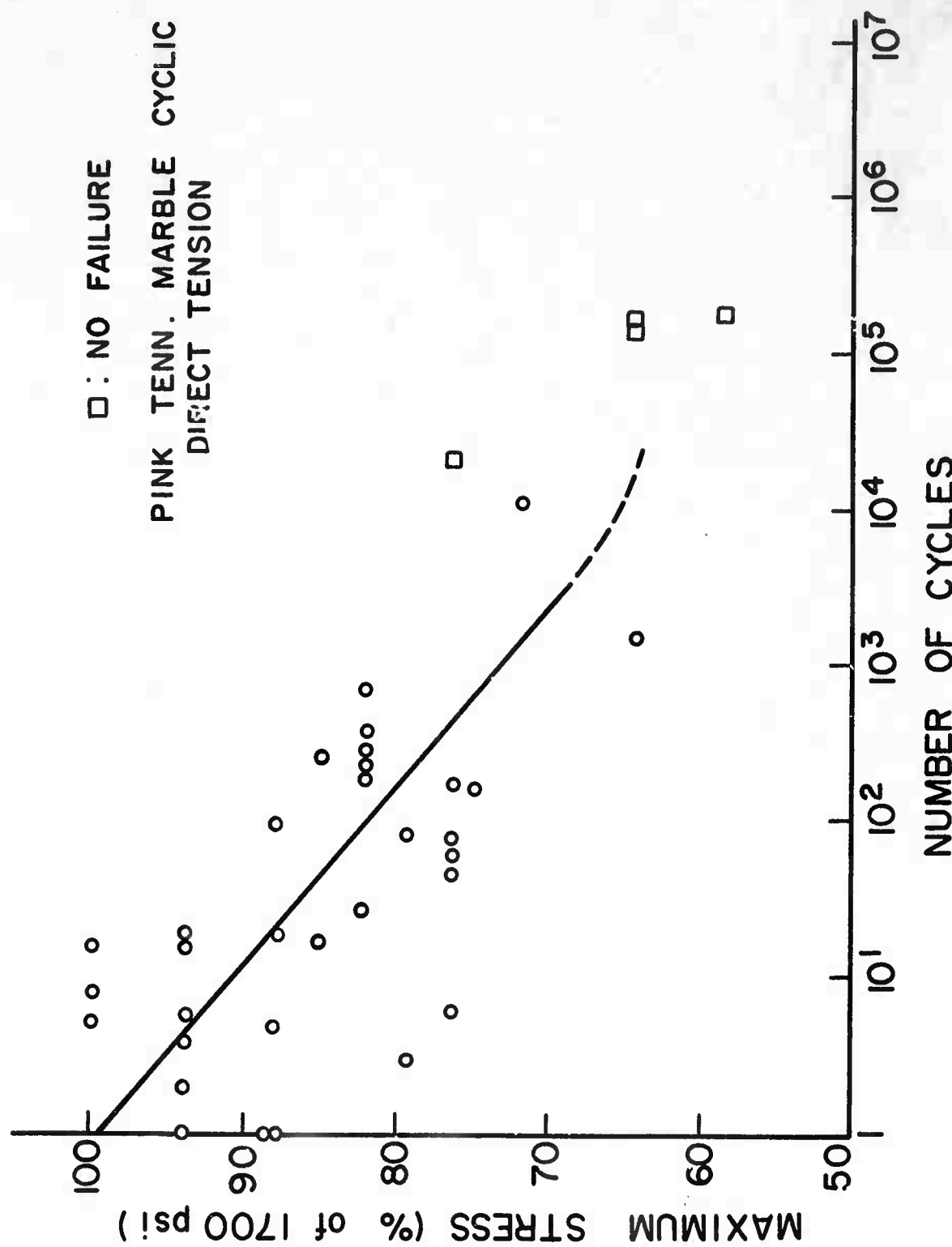


Figure 39. S-N curve for Pink Tennessee marble under uniaxial tension cyclic loading.

The fatigue behavior of the marble in tension was similar to that in compression as can be judged from the stress-strain and strain-time behavior (not reproduced here because of poor recordings). Total recorded strain was quite small so that noise and drift presented a problem but the trends were clearly observed. There are three stages similar to the compression case: primary, steady state and tertiary. The steady state stage is absent in short life tests but dominates the long life ones.

Acoustic emission was used advantageously in the tension tests. In a monotonic test microcracking, as sensed by the piezoelectric transducer, begins at about 60-70% of the tensile strength, continues at a slow rate and eventually accelerates to failure (Figure 41). Although the final failure type is completely different from compression, the recorder microseismic activity appears to be very similar. In cyclic tests, the major damage is observed in the first cycle with the rate of acoustic emission decaying, reaching a steady state, and finally accelerating just before failure (Figure 42). Again, a very comparable process to that of compressive fatigue.

An interesting observation was made when comparing the microseismic events emanated by Brazilian discs and by uniaxially pulled cylinders. The number of events recorded in the former was considerably higher than in the latter, indicating abundant crushing that occurs in the Brazilian specimens near the concentrated loading lines.

In the uniaxial tests there are questions still to be answered. Perhaps the most important is to determine the location of failure. Since strain gages directly bonded to specimens were used, the strain determined was limited to that under the 2 gages. In those cases where the failure surface was not at the center the measured strain in the last few cycles was less than when the failure was through the gages. This conclusion needs more checking but implies that the internal fracturing leading to tensile failure is rather localized. Three methods suggest themselves as possible means for checking the hypothesis:

(1) Sectioning rocks subjected to fatigue, both failed and unfailed and comparing these with sections of untested rocks to determine the degree and location of visible and microscopic damage due to cyclic loading, (2) Run more tests with strain gages to confirm more completely the above observations, (3) Reglue failed specimens and retest them either cyclicly or monotonically to failure to gauge the degree of damage outside the failure surface.

More tests also remain to be performed to test the acoustic emission characteristics at different stress (and hence different life levels).

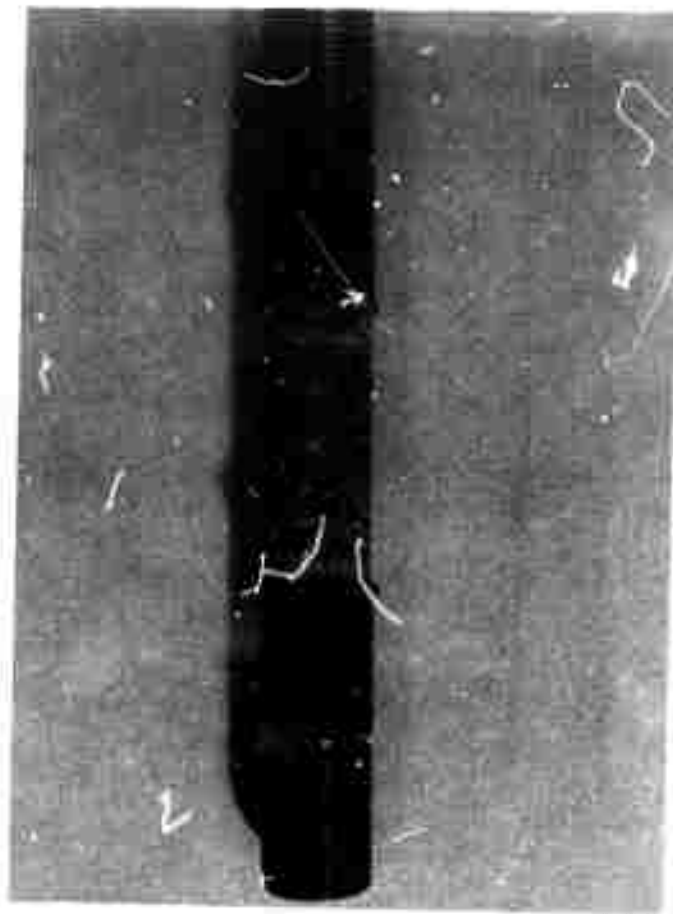


Figure 40 - Typical specimen of Pink Tennessee marble failed in uniaxial tension cyclic loading.

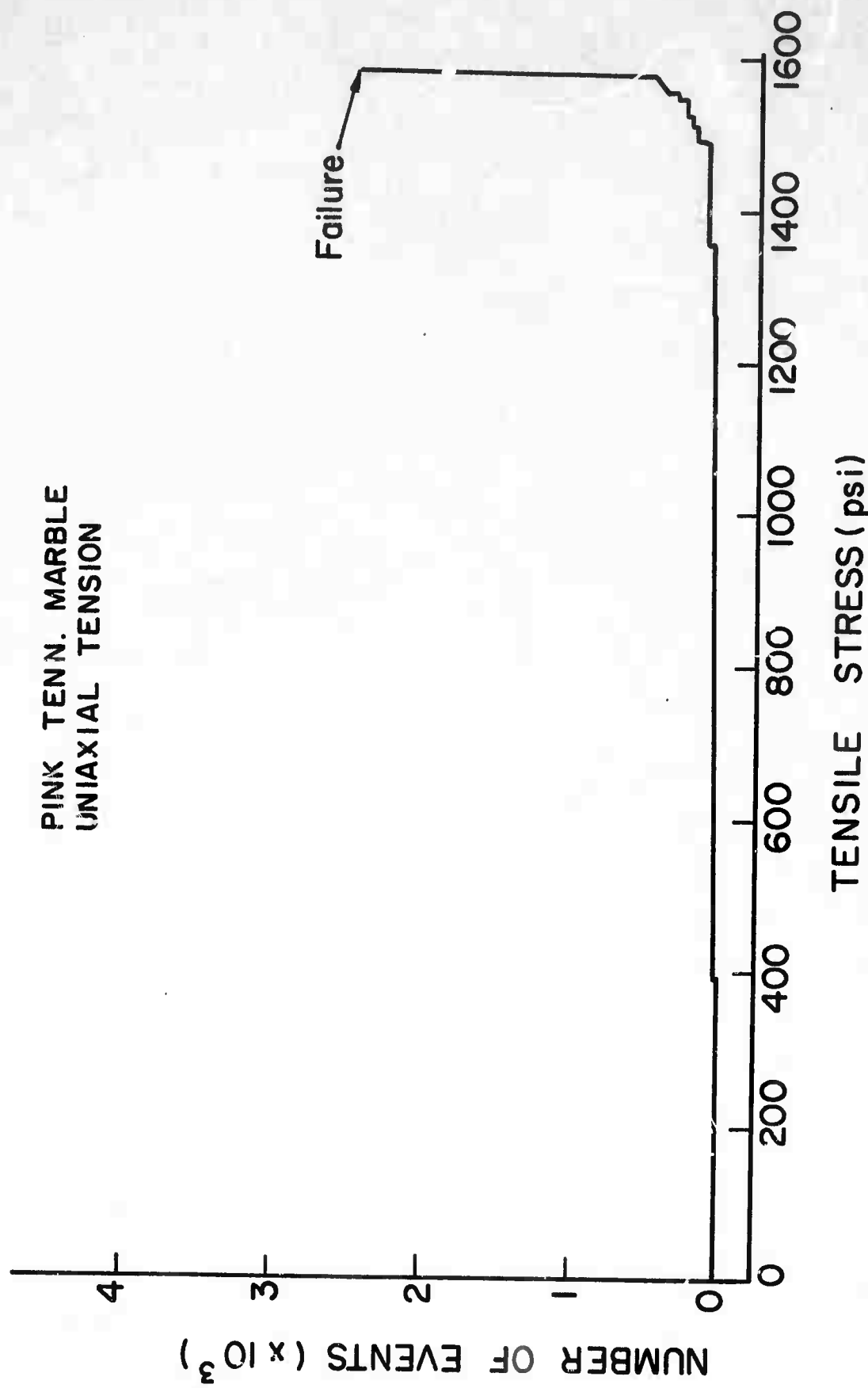


Figure 41. Acoustic emission in uniaxial tension monotonic loading -
Pink Tennessee marble.

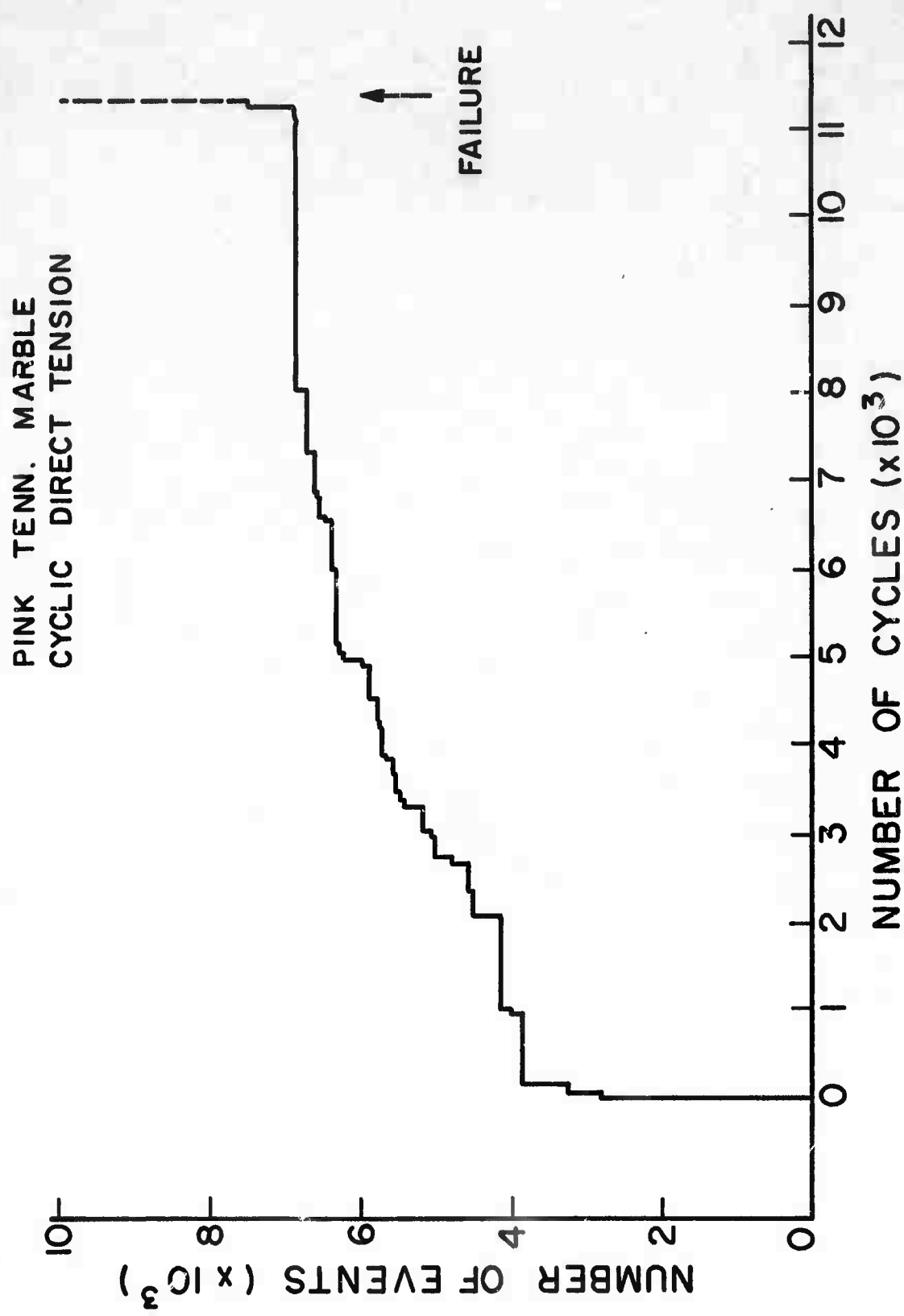


Figure 42. Acoustic emission in long life specimen of Pink Tennessee marble under uniaxial tension cyclic loading.

CONCLUSIONS AND PRACTICAL APPLICATIONS

The study of the mechanical behavior of two marbles and a limestone under cyclic loading suggests a number of important conclusions.

Mechanical Behavior

1. Brittle rock is weakened by cyclic loading, whether under compression or tension, if the upper peak load is above a certain threshold typical of the particular rock. The threshold appears to be within the inelastic range of the rock stress-strain characteristics. It is suggested that the fatigue strength at 10^6 cycles be used in design, instead of the commonly employed compressive strength or tensile strength values, in order to protect structures not only against static loads, but also against pulsating stress.
2. Failed rock exhibits a rather substantial strength under repetitive compressive loading. S-N curves for failed rock can be determined and used in the design of structures that may reach their peak load carrying capacity. As failed rock is usually broken, its S-N curve may be indicative of jointed and faulted rock behavior under cyclic loading.
3. Both the axial and the lateral strains undergo cyclic creep. The average tangential values of Young's Modulus and Poisson's Ratio vary with the cyclic loading. The former decreases; the latter tends to increase. This behavior can be construed as resulting from a weakening of the rock.
4. The volumetric strain undergoes what may be termed "cyclic compression dilatancy", i.e., the amount of volumetric strain decrease diminishes during cycling and may eventually turn into strain increase. The softer, more porous limestone accumulated a large permanent lateral strain and actually began gaining volume long before fatigue failure. The stiffer, less porous, marble never reached that stage prior to its brittle fracture.
5. It appears that the complete stress-strain curve defines the limit of the upper-peak-compressive-strain cyclic creep prior to failure. This important conclusion has two main consequences:

- a. The upper limit of the total deformation during cyclic loading may be predicted through knowledge of the quasi-static complete stress-strain curve. This has a very practical connotation since cyclic testing is tedious and extremely time consuming. If a relationship can be found between the number of cycles and the respective axial strain increase, the complete stress-strain curve may be utilized to also predict N to failure for any upper-peak-stress level.
- b. A class II rock, for which the descending complete stress-strain curve generally has a positive slope (e.g., Westerley granite, Solenhofen limestone) may be more fatigue prone than a class I rock since the material can only undergo a more limited permanent strain increase prior to failure.

Internal Structure Changes

Fabric analysis has so far been conducted only in cyclic compression specimens. The overall conclusions, emanating from the different approaches used, is that cyclic fatigue in rock is the result of a microfracturing process.

The stress-strain, strain-time curves were early indicators of structural damage that brought about large permanent deformation during cycling.

The microseismic detection device picked up signals from the very first cycle, suggesting microcracking. Further interpretation of the acoustic emission variation with cycling revealed a steady slow-down in crack initiation, in some cases coming to a complete halt. During the same period extension of existing cracks probably occurred. Cracks grew longer and closer to each other, propagation and coalescence followed and the emission accelerated signalling fatigue failure.

The optical diffraction technique also indicated an increase in fracture abundance in the first cycle, followed by a stage of near stagnation and widening of cracks, and a repeated increase in crack frequency in the last stage of specimen life.

The photomicrographic study clearly demonstrated grain boundary loosening in the first cycles, intragranular cracking in the following cycles, succeeded by crack extension, coalescence, widening of some fractures, and faulting.

Within the above frame of fatigue internal mechanism, differences were observed between the solid marble and the ultra porous limestone. The microseismic activity in the latter was much less extensive than in the marble, inferring a lesser degree of microcracking. The photographic results were consistent with the above, showing fewer cracks that had to extend far less and caused large volume increases and fatigue failure not through crack coalescence but rather through crack communication between existing voids.

In summary it is felt that the major consequences of fatigue loading in rock have been observed, detected, recorded and interpreted to the best of the reporter's ability. However, only the uniaxial case has been extensively studied and only two rock types have been comprehensively tested. Clearly, more work is needed and it is hoped to extend the study for at least two additional years.

FUTURE WORK

1. Extend the entire investigation to five different hard rock types.
2. Observe fabric changes in cyclic tension and combine them with acoustic emission to determine a possible mechanism of tensile fatigue failure.
3. Carry out an experimental investigation into the cyclic fatigue of rock under triaxial compression and tension-compression type loadings.
4. Study the reaction of failed and fractured rock to cyclic fatigue under different loading conditions.
5. Attempt to classify rocks according to their resistance to cyclic fatigue.

REFERENCES

1. Grover, H. J., Dehlinger, P., and McClure, G. M., "Investigation of Fatigue Characteristics of Rocks," report by Battelle Memorial Institute to Drilling Research, Inc., Nov. 30, 1950.
2. Burdine, N. T., "Rock Failure Under Dynamic Loading Conditions," Soc. of Petroleum Engineers Journal, March 1963, pp. 1-8.
3. Hardy, H. R., Jr., and Chugh, Y. P., "Failure of Geological Materials Under Low-Cycle Fatigue," Proc. of the Sixth Canadian Symposium on Rock Mechanics, Montreal, Canada, May 1970.
4. Haimson, B. C., Kim, C. M., "Mechanical Behavior of Rock under Cyclic Fatigue," Proceedings of the 13th Symposium on Rock Mechanics, Urbana, Illinois, Sept. 1970 (in press).
5. Nishimatsu, Y., and Heroesewojo, R., "The Effect of Mean Stress of the Stress Amplitude on the Rate Constants of Fatigue Failure of the Rock," J. of the Soc. of Material Sciences, Japan, Vol. 21, No. 209, 1971 (in Japanese with English abstract).
6. Saint-Leu, C., Sirieys, P., "La Fatigue des Roches," Proc. 1st Symp. on Rock Fracture, Nancy, France, 1971.
7. Shreiner, L. A., and Paslova, N. N., "Experimental Data on the Fatigue Breakdown of Rocks," Trudy lust. Wefti Akad. Nauk. SSSR, Vol. 11, 1958 (English translation).
8. Nordby, G. M., "Fatigue of Concrete--A Review of Research," Journal of the American Concrete Institute, Aug. 1958, pp. 191-219.
9. Hilsdorf, H. K., and Kesler, C. E., "Fatigue Strength of Concrete Under Varying Flexural Stresses," J. of Am. Concrete Inst., Vol. 63, No. 10, 1966.
10. Bennett, E. W., and St. T. Muir, S. E., "Some Fatigue Tests of High-Strength Concrete in Axial Compression," Mag. of Concrete Research, Vol. 19, No. 59, 1967.
11. Sedlacek, R., and Halden, F. A., Technical Report, Contract No. AF33(657)-10600, Wright-Patterson Air Force Base, Ohio.

12. Seed, H. B., "Soil Strength During Earthquakes," Proc. 2nd World Conf. on Earthquake Engineering, Tokyo, Japan, 1960.
13. Ellis, W., and Hartman, V. B., "Dynamic Soil Strength and Slope Stability," Journal of the Soil Mechanics and Foundations Division, ASCE, Vol. 93, No. SM4, July 1967, pp. 355-375.
14. Pincus, H. J., "Development of Capabilities of Optical Diffraction Analysis for Quantitatively Comparing and Correlating Rock Fabrics and Fabric Changes," Semiannual Technical Report, U. S. B. M. Contract No. H0210003, August 1971.
15. Hudson, J. A., Brown, E. T., and Rummel, F., "The Controlled Failure of Rock Discs and Rings Loaded in Diametral Compression," in Progress Report No. 24, Mineral Resources Res. Center, U. of Minn., 1971.
16. Scholz, C. H., "Microfracturing and the Inelastic Deformation in Compression," J. Geoph. Res., Vol. 73, No. 4, 1968.
17. Scholz, C. H., "Experimental Study of the Fracturing Process in Brittle Rock," J. Geoph. Res., Vol. 73, No. 4, 1968.
18. Suzuki, T., et al., "A New Approach to the Prediction of Failure by Rock Noise," Fourth Int'l. Conf. on Strata Control and Rock Mech., New York, 1964.
19. Scholz, C. H., "The Role of Microfracturing in Rock Deformation," 2nd Int'l. Congress on Rock Mechanics,
20. Wawersik, W. R., "Detailed Analysis of Rock Failure in Laboratory Compression Tests," thesis presented to the Univ. of Minnesota, Minneapolis in 1968 in partial fulfillment of the requirements for the degree of Doctor of Philosophy.